uOttawa

L'Université canadienne
Canada's university

FACULTÉ DES ÉTUDES SUPÉRIEURES ET POSTOCTORALES

uOttawa

L'Université canadienne
Canada's university

FACULTY OF GRADUATE AND POSDOCTORAL STUDIES

Stephanie L. Fowler
AUTEUR DE LA THÈSE / AUTHOR OF THESIS

M.Sc. (Biochemistry)
GRADE / DEGREE

Department of Biochemistry, Microbiology and Immunology
FACULTÉ, ÉCOLE, DÉPARTEMENT / FACULTY, SCHOOL, DEPARTMENT

Channel-Independent Function of Connexin 32 are Mediated by Protein-Protein Interactions: Discovery of Connexin 32 Binding Partners and Implication of Intracellular Connexins
TITRE DE LA THÈSE / TITLE OF THESIS

Steffany Bennett
DIRECTEUR (DIRECTRICE) DE LA THÈSE / THESIS SUPERVISOR

CO-DIRECTEUR (CO-DIRECTRICE) DE LA THÈSE / THESIS CO-SUPERVISOR

EXAMINATEURS (EXAMINATRICES) DE LA THÈSE / THESIS EXAMINERS

Heidi McBride

Jean-François Couture

Gary W. Slater
Le Doyen de la Faculté des études supérieures et postdoctorales / Dean of the Faculty of Graduate and Postdoctoral Studies

Channel-independent functions of connexin 32 are mediated by protein-protein interactions: Discovery of connexin 32 binding partners and implications of intracellular connexins

Stephanie L. Fowler

A thesis submitted to the Faculty of Graduate and Postdoctoral studies in partial fulfillment of the requirements for the degree of Masters of Science

Department of Biochemistry, Microbiology, and Immunology
University of Ottawa
Ottawa, ON, Canada

Your file Votre référence
ISBN: 978-0-494-61357-3
Our file Notre référence
ISBN: 978-0-494-61357-3

Abstract

Connexin proteins are the structural components of gap junctions and hemichannels, and are dynamically regulated in neural progenitor cells (NPCs) over the course of neurogenesis. While the classical role of connexins is to mediate juxtacrine and paracrine signalling through plasma membrane channels, new evidence suggests that a plethora of channel-independent signalling roles are initiated by protein-protein interactions. In this thesis, I provide evidence for a novel Connexin 32 (Cx32)-interactome (i.e., interacting proteins that may not be associated with plasma membrane channels) that can be subsequently tested for impact on NPC fate. Following rigorous testing of various Cx32 protein detection strategies designed to overcome a problem with brain-specific antibody cross-reactivity, I developed a new method to affinity-purify endogenous Cx32 combining sucrose gradient fractionation and immunoprecipitation (IP). Combined with high performance liquid chromatography and tandem mass spectrometry, nineteen Cx32 binding partners were identified. Surprisingly, many of these interacting proteins were predicted to localize to the mitochondrion. Interaction of Cx32 with sideroflexin-1 (SFXN-1), a putative mitochondrial protein, at both plasma and mitochondrial membranes was further verified by co-IP. Together, these results suggest that a small pool of Cx32 localizes to the mitochondrion and provides the first proof of principle that Cx32 interacts with mitochondrial protein complexes at both plasma membrane and mitochondrial locations.

Acknowledgements

First and foremost I would like to my supervisor, Dr. Steffany Bennett for her unrivaled patience and excitement for scientific discovery. I am deeply grateful for her caring mentorship, and constant support. I am also fortunate to have been excellently guided by my committee members, Drs. Daniel Figeys, Kristin Baetz, and Adam Rudner, whose scientific input has been exceedingly helpful. Also, this thesis would not be possible without the kindness and expertise of our academic administration officer, Carol Ann Kelly.

I am indebted to all of my colleagues in the lab, past and present, for making the lab environment as wonderful as it is. From impromptu dance parties and sing-alongs, to pretend fights over lab equipment tethered to its owner's desk with dental floss, to brilliant science revelations, it has been fantastic to work with all of you. Particularly, I would like to thank Ashleigh McLean and Leigh Anne Swayne, both for providing invaluable technical expertise, but also for being so encouraging throughout this process.

Most importantly, I wish to thank my family and close friends for their love and encouragement. To my parents, aunts, cousins, and to Nanna: I could not have done this without you. Thank you also Steve and Jennie for your incredible support and encouragement. Finally, to my bosom friend and fellow scientist, Catherine Sorbara: I am so glad I could share this journey with you, my Italian sister.

Table of Contents

List of Abbreviations

NPCs	Neural progenitor cells
Cx32	Connexin 32
IP	Immunoprecipitation
SFXN-1	Sideroflexin-1
CNS	Central nervous system
SVZ	Subventricular zone
SGZ	Subgranular zone
RMS	Rostral migratory stream
GFAP	Glial fibrillary acidic protein
DCX	Doublecortin
OPCs	Oligodengrocyte progenitor cells
IL	Intracellular loop
TM	Transmembrane
EL	Extracellular loop
CMT	Charcot-Marie-Tooth
PDGFαR	Platelet-derived growth factor alpha receptor
GPCRs	G protein coupled receptors
co-IF	Co-immunofluorescence
co-IP	Co-immunoprecipitation
ZO-1	Zona occludens-1
NT	N-terminus
CT	C-terminus
Y2H	Yeast two hybrid
AA	Antibody array
Dlgh-1	Discs large homolog-1
MAGUK	Membrane-associated guanylate kinase
Y/+, WT	Wildtype
Y/-, KO	Null-mutant
IB	Immunoblotting
IP	Immunoprecipitation
SDS	Sodium dodecyl sulfate
IF	Immunofluorescence
PCR	Polymerase chain reaction
PBS	Phosphate buffered saline
DTT	Dithiothreitol
BME	β-mercaptoethanol
RT	Room temperature
PVDF	Polyvinylidene fluoride
HRP	Horseradish peroxidase
Ab buffer	Antibody buffer
BSA	Bovine serum albumin
DMP	Dimethylpimelimidate
BARN	Blotting and removal of nitrocellulose
PVP-40	Poly(vinylpyrrolidone)

SDS-PAGE	Sodium dodecyl sulfate polyacrylamide gel electrophoresis
GrDG	Granule cell layer of the dentate gyrus
HEK	Human Embryonic Kidney
BiP	Binding protein
β-gal	β-galactosidase
DMEM	Dulbecco's modified Eagle medium
DMSO	Dimethylsulfoxide
EGTA	Ethylene glycol tetraacetic acid
UbA52	Ubiquitin A52 residue ribosomal fusion protein 1
RT-PCR	Reverse transcription polymerase chain reaction
MTC	Mitochondrial tricarboxylate carrier
ALAS2	Delta-aminolevulinate synthase 2
Tom	Translocase of the outer membrane
ROS	Reactive oxygen species
β-GA	18-β-glycyrrhetinic acid
TUNEL	Terminal UDP nick end labeling
O-2A	Oligodendrocyte-type-2-astrocyte progenitor
NT-3	Neurotrophin 3
$\Delta\Psi$	Mitochondrial inner membrane potential
TH	Thyroid hormone

List of Figures

List of Tables

Chapter 1: General Introduction

1.1 Neurodegenerative disease and our current strategies of brain repair

Neurodegenerative diseases affect more than 20 million people worldwide, and are a leading cause of death and social strain in our rapidly aging population (Yankner et al., 2008). Given this statistic, there is considerable need for advances in the field of brain repair, and the last few years have witnessed many exciting advances to interventions that halt the progression of disease or ameliorate the lives of afflicted patients.

Alzheimer disease is the most common neurodegenerative disorder and currently afflicts 238,000 Canadians over 65 (Ebly et al., 1994). This debilitating disease is characterized by a progressive decline in cognitive function leading to death in an average of 4.5 years following diagnosis (Xie et al., 2008). The histological hallmarks of Alzheimer disease include neurofibrillary tangles of aberrantly phosphorylated tau protein, β-amyloid plaque accumulation, and pyramidal neuron degeneration in the neocortex, hippocampus, and amygdala (Mann, 1996). Parkinson's disease is the second most common neurodegenerative disorder, yet is about 4 times less prevalent than Alzheimer disease. Parkinsonian symptomology includes tremor, rigidity, muscle stiffness, postural instability, and bradykinesia, which are attributed to a loss of dopamine neurons in the substantia nigra pas compacta (Olanow and Tatton, 1999).

In contrast to the neuronal loss associated with Alzheimer and Parkinson's diseases, multiple sclerosis, the third most prevalent disorder, is an autoimmune disorder that results in demyelination of axons due to the destruction of oligodendrocytes. Chronic immune system attacks to oligodendrocytes inhibit remyelination of axons, and produce variable symptoms including impaired vision and coordination, sensation, speech, cognitive function, and muscle weakness (Mitchell et al., 2005).

The treatments for such neurodegenerative diseases usually provide minimal amelioration of symptoms or only serve to slow the disease progression (Geldmacher et al., 2006), therefore, we are currently striving toward developing ways to regenerate or replace neurons and glia lost during injury or disease progression. This problem is being explored using two main strategies of central nervous system (CNS) cell replacement: (1) the introduction of exogenous human stem cells to the site of injury and (2) the activation of endogenous adult neural stem cells.

Human stem cells are derived from various sources, and can be stimulated to produce nearly all cell types of the body. Stem cells used for neural replacement or regeneration include those cultured from the inner cell mass of donated *in vitro* fertilization blastocysts or from fetal brain tissue (Ormerod et al., 2008). These multipotent stem cells are easily differentiated into neurons, astrocytes, or oligodendrocytes, however, there is a large risk of teratoma generation with the use of blastocyst-derived stem cells (Kiuru et al., 2009), and there are serious ethical and

logistical problems associated with the use of either cell type (Rouskova et al., 2008).

Adult stem cells are present and persist in several organs including the blood, intestine and the skin to support ongoing cellular turnover (Gage and Verma, 2003). Thus, while it was known that stem cells could be isolated from the brain and induced to differentiate to different CNS lineages, it was unclear whether they would represent a practical mechanism of cell replacement therapy given that the CNS does not significantly regenerate after injury. Not surprisingly, interest in adult neural stem cells has mounted quickly due to the numerous caveats involved in using embryonic and foetal stem cells (Mitchell et al., 2004; Emsley et al., 2005; Okano and Sawamoto, 2008). The current research pertaining to neural stem cells is aimed at understanding the molecular mechanisms that govern their proliferation, specification, and differentiation to different CNS cell types, with the hope of being able to activate and harness their endogenous regenerative capacity (Okano and Sawamoto, 2008).

1.2 Adult neurogenesis: neural progenitor cells are present along the lateral ventricle and within the dentate gyrus of the hippocampus

The two regions capable of significant neurogenesis in the adult brain are the subventricular zone (SVZ) of the lateral ventricle and the subgranular zone (SGZ) of the dentate gyrus of the hippocampus (Doetsch et al., 1999; Alvarez-Buylla and Lim, 2004; Fig 1.1). In the SVZ,

Figure 1.1: Schematic of neurogenesis from the two neurogenic niches of the adult brain.

Depicted is a representative saggital section (A) showing the two regions of the adult brain capable of significant neurogenesis, the SVZ of the lateral ventricle (B), and the SGZ of the dentate gyrus of the hippocampus (C). Panel A shows the progression of Type B GFAP/nestin+ NSCs capable of self-renewal and commitment to Type C cells that express only nestin. Type C cells have limited capacity for renewal, and differentiate to Type A DCX+ neuroblasts that fully differentiate into NeuN+ neurons following migration to the olfactory bulb. Panel B shows the progression of Type 1 nestin/GFAP+ NSCs towards increasingly committed neural progenitor cells (NPCs) with more limited self-renewal properties. Upon exit from the cell cycle (hatched black line in B and C), immature neurons migrate to the granule cell layer of the dentate gyrus. Abbreviations: SVZ: subventricular zone; SGZ: subgranular zone; GFAP: glial fibrillary acidic protein; NSCs: neural stem cells; DCX: doublecortin.

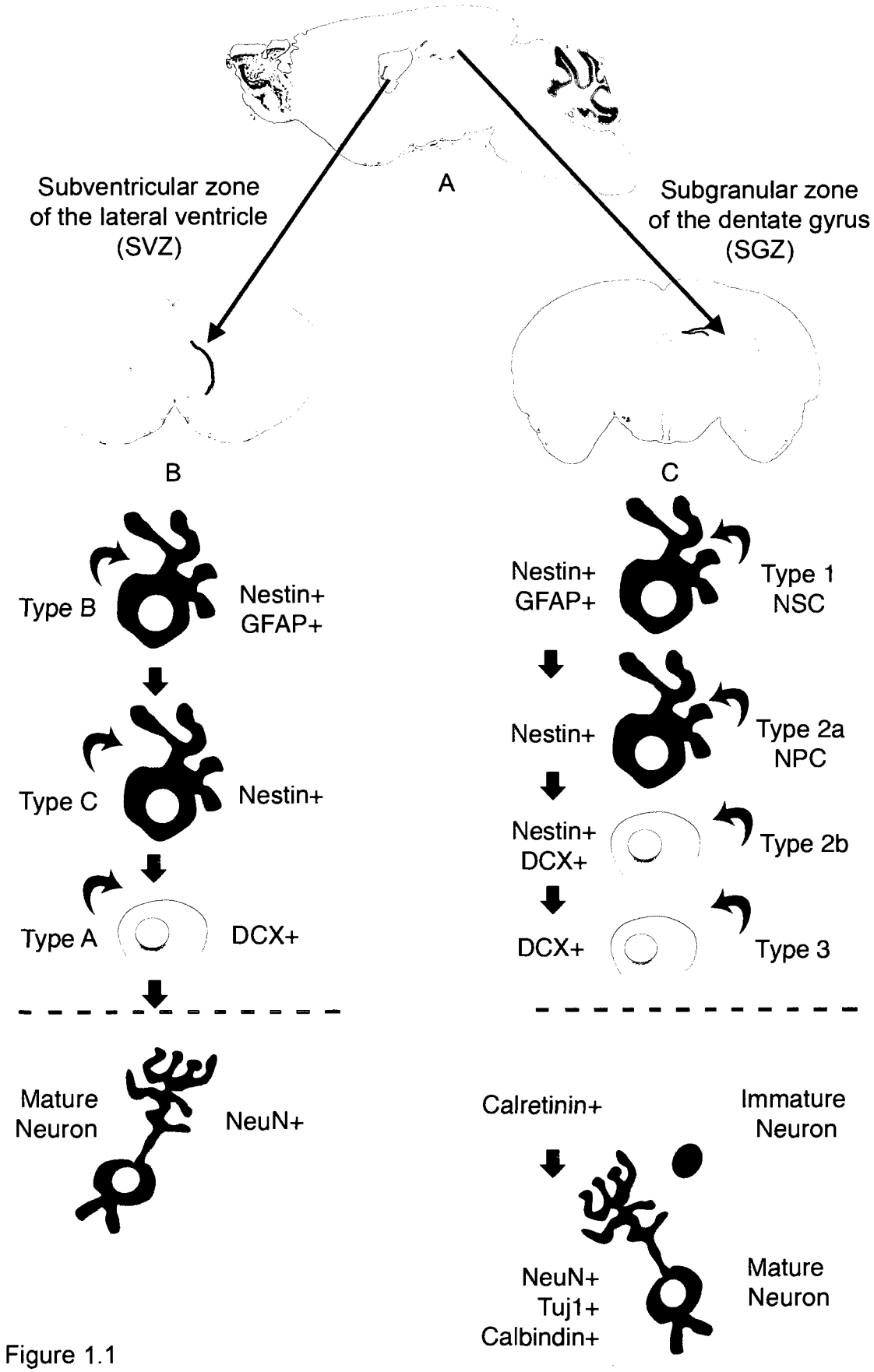
Subventricular zone
of the lateral ventricle
(SVZ)
A
Subgranular zone
of the dentate gyrus
(SGZ)
B
C
Type B
Nestin+
GFAP+
Type C
Nestin+
Type A
DCX+
Mature
Neuron
NeuN+
Nestin+
GFAP+
Type 1
NSC
Nestin+
Type 2a
NPC
Nestin+
DCX+
Type 2b
DCX+
Type 3
Calretinin+
Immature
Neuron
NeuN+
Tuj1+
Calbindin+
Mature
Neuron

Figure 1.1

(Lois and Alvarez-Buylla, 1993) have designated populations of slowly dividing astrocyte-like neural stem cells as type B cells. These type B cells give rise to actively proliferating type C cells that generate a pool of immature neuroblasts, or type A cells. Chains of neuroblasts ensheathed by the processes of type B cells migrate along the rostral migratory stream (RMS) to the olfactory bulb where they differentiate and incorporate as mature interneurons (Lois et al., 1996).

While SVZ neurogenesis is an important regenerative process, much of the work in our lab focuses on hippocampal neurogenesis due to its importance in learning and memory (Jarrard, 1993), as well as its ability to be specifically stimulated by the kainic acid seizure model (Aguado et al., 2007). Kempermann and colleagues (Kempermann et al., 2004) have described a model of hippocampal neurogenesis that characterizes the most identifiable milestones in the progression of stem cells to fully mature granule cell neurons. It begins with the Type 1 putative stem cell with supposed unlimited self-renewal capacities. Type 1 cells express the two intermediate filament proteins nestin and glial fibrillary acidic protein (GFAP), which are commonly used to define stem cells. Type 1 cells divide to produce Type 2a progenitor cells, which are most likely lineage determined, have limited capacity for self-renewal, and have lost the expression of GFAP. Type 2b cells arise from Type 2a cells and are characterized by their expression of doublecortin (DCX), a microtubule-associated protein expressed by immature neurons. Type 3 progenitor cells lose nestin expression and exit the cell cycle to become postmitotic

immature granule cells that are defined by their expression of a calcium binding protein calretinin (Brandt et al., 2003) and the DNA-binding, neuron-specific protein NeuN (Mullen et al., 1992). Finally, neurons expressing calbindin and NeuN are present in the granule cell layer of the hippocampus and over approximately 4-7 weeks of maturation, incorporate themselves into the hippocampal circuitry.

1.2.1 Early oligodendrocyte progenitor cells (OPCs) represent an untapped source of adult hippocampal neurogenesis

A second model of adult hippocampal neurogenesis has been proposed in which new neurons can be generated from either Type 1 or Type 2a progenitor cells without first generating Type 2b cells expressing DCX (Belachew et al., 2003; Aguirre and Gallo, 2004; Aguirre et al., 2004). This model of neurogenesis is thought to proceed through intermediary progenitor cells, which are characterized by their expression of the chondroitin sulfate proteoglycan NG2. NG2+ cells are traditionally known as OPCs, however, several authors report their ability to specify also to protoplasmic astrocytes in the grey matter (Zhu et al., 2008), and to functional GABAergic neurons in the hippocampus and SVZ (Belachew et al., 2003; Aguirre et al., 2004). While the neurogenic potential of $NG2^+$ polydendrocytes is highly debated at present (Komitova et al., 2009), this abundant source of progenitor cells may actually represent a novel source of adult neural progenitor cells.

1.3 Connexin-mediated communication: gap junction structure and function

The ability of a group of cells to properly function as a tissue is highly dependent upon their ability to communicate with each other. In higher and lower vetebrates, intercellular communication is, in part, mediated by proteinaceous channels called gap junctions (Goodenough, 1974; Beyer et al., 1990; Musil and Goodenough, 1990; White et al., 1995). Gap junction channels form inter-membrane conduits linking adjacent cells and are present in almost every cell type. The structural units of gap junction channels are the highly conserved connexin family of proteins. Connexins hexamerize to form half of the channel (a connexon) which docks with a connexon from an apposing cell membrane to form a continuous pore through which electrical signals and a variety of molecules less than 1 kDa can be shared amongst coupled cells (See Fig 1.3). Some important metabolites and signalling molecules permeable to gap junctions include Ca^{2+}, IP_3, cAMP, ATP, glycine, glucose, and various phosphorylated purine nucleotides (Alexander and Goldberg, 2003).

The connexin proteins are named according to their predicted molecular weights, and share several structural features including four alpha-helical trans-membrane domains, intracellular N and C-termini, two extracellular loops, and an intracellular loop (IL) bridging trans-membrane domains 2 and 3 (Fig 1.2). Connexon docking between adjacent cells is mediated by the highly conserved cysteine residues present on the

Figure 1.2: Connexins hexamerixe to connexons to form gap junction channels.

Connexin family members contain four highly conserved transmembrane domains, two extracellular and one intracellular loop, and intracellular N- and C-termini. Cx32 and Cx26 are presented to illustrate that most of the variation occurs in the length and sequence of the C-terminal domain (A). Six connexin proteins oligomerize to form connexons (B) which dock at non-junctional membranes to form hemichannels, or dock with connexons from adjacent cells to form gap junctions (C). Gap junction channels can be (I) homotypic; composed of 2 identical connexons and 12 identical connexins, (II) heteromeric; composed of two heterotypic connexons made up of different connexins, or (III) heterotypic; composed of two different, yet homotypic connexons.

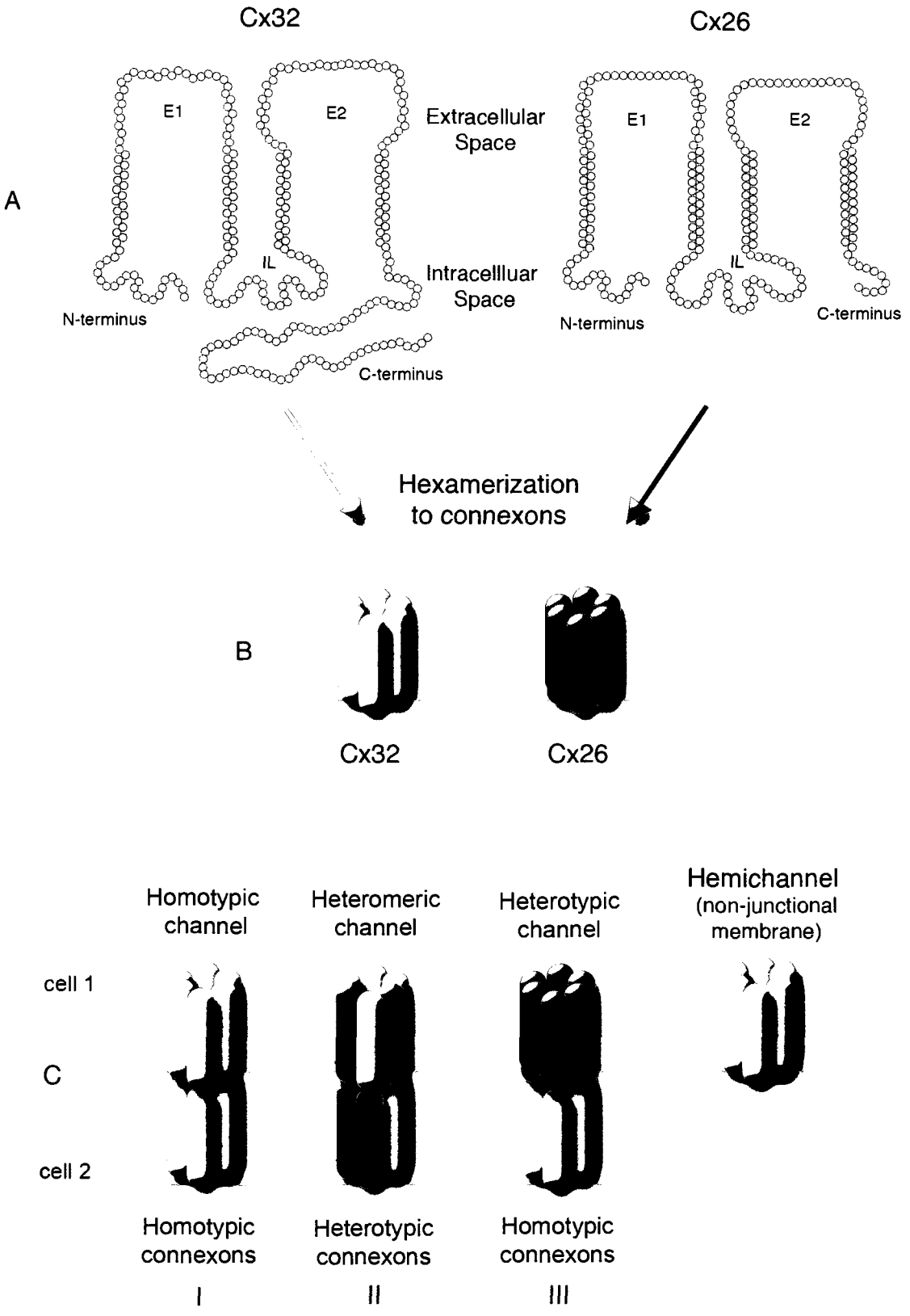
Cx32
Cx26
A
E1
E2
IL
Extracellular Space
Intracelllular Space
N-terminus
C-terminus
N-terminus
C-terminus
Hexamerization to connexons
B
Cx32
Cx26
Homotypic channel
Heteromeric channel
Heterotypic channel
Hemichannel (non-junctional membrane)
cell 1
C
cell 2
Homotypic connexons
I
Heterotypic connexons
II
Homotypic connexons
III

Figure 1.2

extracellular loops. There are twenty connexin family members present in the mouse genome (twenty-one in human), and most of the functional specificities between each of the homologs are conferred by variations in the length and sequence of the intracellular loop and C-terminal domains (Manthey et al., 2001). Furthermore, channel specificity is highly dependent upon which connexin family members are present in the channel. For example, connexons composed of the same connexin are homotypic, whereas connexons composed of different connexins are heterotypic. Similarly, gap junction channels composed of the same connexons are homomeric, and channels composed of different connexons are heteromeric (Fig. 1.2C). Given this level of complexity, there is a possibility of generating 196 different channels (Brink et al., 1997), however, not all combinations of connexin pairs are functional, and some arrangements are preferred over others (Bruzzone et al., 1996; Brink et al., 1997). In addition to channel regulation by connexin composition, gap junctional activity is highly sensitive to various gating mechanisms: the best studied being the modulation of connexin phosphorylation state (Herve and Sarrouilhe, 2006; Moreno and Lau, 2007).

The crystal structure of a Cx26 gap junction has recently been solved at 3.5 Å resolution (Maeda et al., 2009; Suga et al., 2009). While the intracellular loop and C-terminal residues were not successfully modeled, this structure provides important structural details with implications in permeability and gating of the channel. Furthermore, given

the highly conserved nature of the connexin transmembrane (TM) and extracellular loop (EL) domains (Hua et al., 2003), this structure is likely representative of those regions in the closely related Cx30 and Cx32 family members (Cruciani and Mikalsen, 2006).

Briefly, the Cx26 structure consists of an alpha helical N-terminus, four antiparallel alpha helical TM domains connected by ELs. The N-terminal end of EL1 contains a short stretch of the relatively rare 3_{10} helix (Rohl and Doig, 1996), while the C-terminal end contains a short alpha-helix. The N-terminal half of EL2 is predicted to be flexible, and the C-terminal half contains a 3_{10} turn followed by a conserved Pro-Cys-Pro motif resulting in reversal of its direction back to TM4. Both EL1 and EL2 contain short antiparallel β-sheets, with that of EL2 stretching over EL1 to form the outside wall of the connexon. Maeda and colleagues report that the height of the entire Cx26 gap junction channel (not including the relatively disordered intracellular loop and C-terminal residues) is ~155 Å, and the TM region of the channel is ~38 Å thick. The diameter of the connexon is largest at the cytoplasmic side of the membrane (~92 Å), and smallest at the extracellular side (~51 Å), with corresponding pore sizes of ~40 Å and ~25 Å. The channel pore is most narrow near the extracellular membrane surface (~14 Å). TM1 and TM2 face the interior of the channel, while TM3 and TM4 face the membrane environment, and the authors suggest from the relative arrangement of TM helices that the major pore-lining helix is TM1.

Most of the intra-protomer interactions are mediated by interactions between specific residues in the extracellular parts of the TM domains, and by hydrogen bonds between intracellular TM3 residues. Further, the four antiparallel helices are stabilized by dipole-dipole interactions. The inter-protomer interactions of hexameric Cx26 are mediated by different residues on the extracellular half of TM2 and TM4 and in the extracellular loops. Since most of the residues involved in both intra- and inter-protomer interactions are highly conserved amongst connexin family members, these details can likely be applied to the structure of Cx32.

Interestingly, crystallization of the Cx26 gap junction channel has revealed that the alpha helical N-termini of each of the protomers form a pore funnel at the intracellular opening of each connexon. The loop connecting the N-terminus to TM1 is very flexible, and the authors hypothesize that the six N-termini swing into the channel to create the ~14 Å funnel that is stabilized by a circular network of hydrogen bonds. It is suggested that the inside positive junctional membrane potential known to close Cx26 channels (Verselis et al., 1994) would cause a collapse of the funnel into a plug that physically blocks the pore. This observation is in accord with previous voltage gating and structural studies, however, the authors do not rule out the possibility that the IL and C-terminus contribute to the gating of Cx26 channels. It would be difficult to predict if such a pore funnel exists for Cx32, given that Cx32 channels are closed by an inside negative membrane potential instead of a positive potential (Verselis et al., 1994), and given that Cx32 has an Asn at position 2 in

place of the Asp at position 2 of Cx26. However, since most of the structural features of the TM and EL domains are well-conserved, the structure of Cx26 deduced by Maeda and colleagues can likely be used to infer which specific residues are important for Cx32 connexon and gap junction assembly and/or stabilization.

1.4 Connexin expression in the CNS

Of the twenty murine connexins, eleven are expressed in the CNS (Fig. 1.3). Mature neurons express mainly Cx45 and Cx36 (Sohl et al., 2005; Wellershaus et al., 2008), and as the excitable cells of the brain, rely heavily on gap junctional electrical conductance. Astrocytes express Cx43 and Cx30 (Nagy et al., 2003; Altevogt and Paul, 2004) and are involved in maintaining the brain homeostatic balance by recycling neurotransmitters and buffering extracellular potassium (Lemke, 2001; Freeman, 2006). Some authors report that Cx26 is also expressed by astrocytes (Nagy et al., 2001), however, others restrict detection to subpial and subependymal astrocytes (Mercier and Hatton, 2001), and its contribution to gap junction signalling is minimal (Mercier and Hatton, 2001; Nagy et al., 2001). Oligodendrocytes express Cx47, Cx32, and Cx29 (Altevogt and Paul, 2004; Kamasawa et al., 2005), and are responsible for ensheathing neuronal axons with myelin, the lipid-rich membrane sheets that enable rapid and efficient neurotransmission (Bunge, 1968). Cx29 does not form compatible gap junctions with any other connexin, yet is present in

Figure 1.3: Connexin expression in the CNS by mature cell types.
The CNS is composed of neurons and glia consisting mainly of astrocytes and oligodendrocytes. Neurons mediate electrical coupling by their expression of Cx36 and Cx45. Astrocytes mainly express Cx30 and Cx43, while oligodendrocytes express Cx47, Cx32, and Cx29. Astrocyte:astrocyte junctions are mediated by homotypic and heterotypic Cx30/Cx43 gap junctions, while astrocyte:oligodendrocyte junctions are mediated by heterotypic Cx43/Cx47 and Cx30/Cx32 channels. Cx29 does not gap with any other connexin, and likely forms hemichannels on the inner/adaxonal myelin membrane. These interactions between astrocytes and oligodendrocytes define, in part, the glial syncytium.

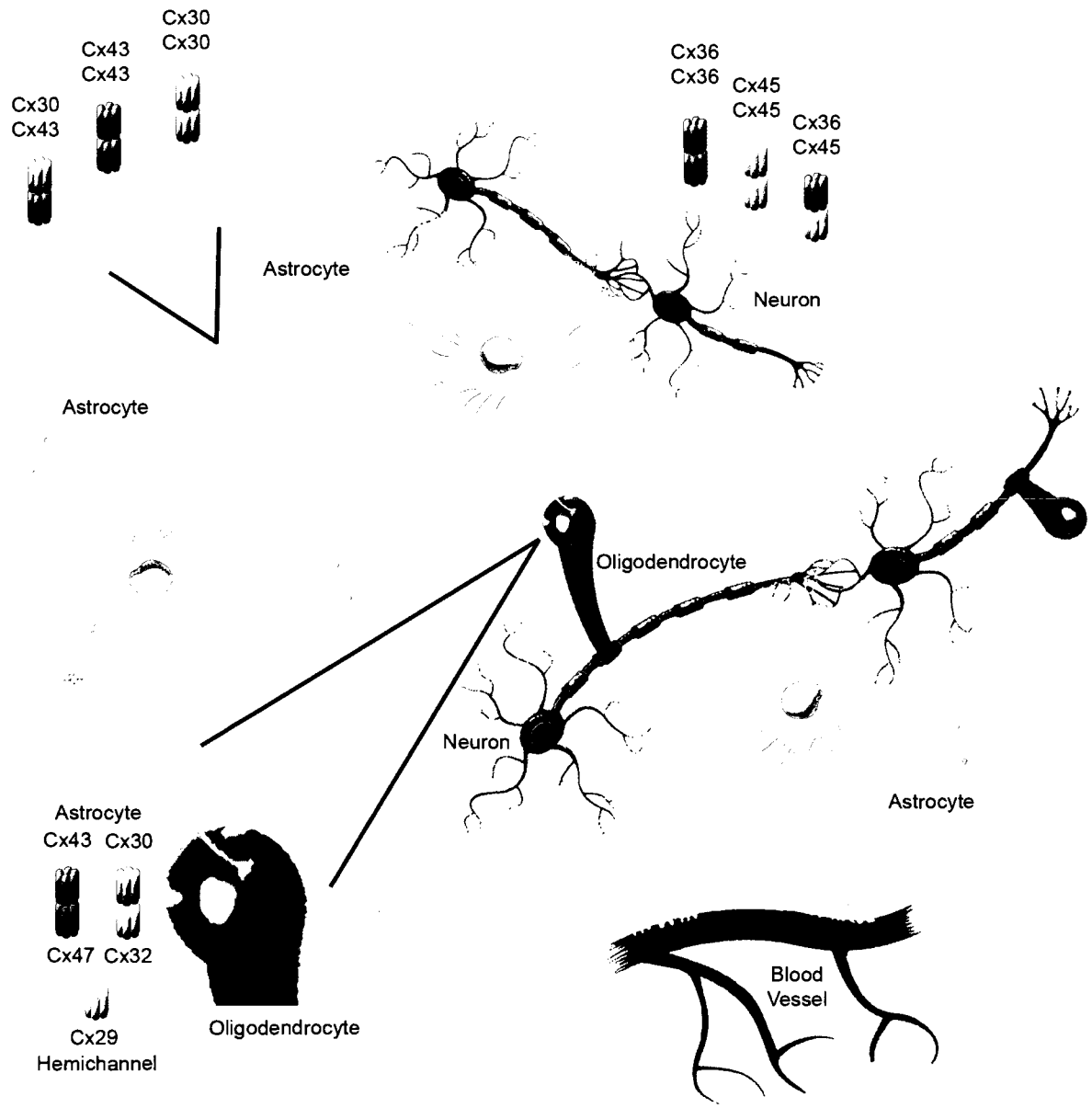
Cx30
Cx30
Cx43
Cx43
Cx30
Cx43
Astrocyte
Cx36
Cx36
Cx45
Cx45
Cx36
Cx45
Neuron
Astrocyte
Oligodendrocyte
Neuron
Astrocyte
Astrocyte
Cx43 Cx30
Cx47 Cx32
Cx29
Hemichannel
Oligodendrocyte
Blood
Vessel

Figure 1.3

hemichannel conformation on the inner/adaxonal myelin membrane (Goodenough and Paul, 2003; Theis et al., 2005; Orthmann-Murphy et al., 2008). Astrocytes are highly coupled to each other via Cx43/Cx43 and Cx30/Cx30 gap junctions, and are also coupled to oligodendrocytes via heterotypic Cx43/Cx47 and Cx30/Cx32 channels (Nagy et al., 2003; Altevogt and Paul, 2004; Theis et al., 2005; Orthmann-Murphy et al., 2008). While oligodendrocytes do not couple with each other (Rash et al., 2001), extensive astrocyte:astrocyte and astrocyte:oligodendrocyte gap junctions result in a pan-glial syncytium (Nagy and Rash, 2003). The functional significance of cytoplasmic continuity between astrocytes and oligodendrocytes has yet to be elucidated, however, it is likely important for specific neuronal functions (Fellin and Carmignoto, 2004; Halassa et al., 2007; Fields, 2008; Allen and Barres, 2009; Fellin, 2009), and may be involved in buffering of K^+ elaborated by neuronal activity, or in the propagation of Ca^{2+} waves (Menichella et al., 2006; Orthmann-Murphy et al., 2008).

Given the complexity and specificity of connexin expression in different neural cell types, it is clear that connexin-mediated communication is important. Indeed, the brain relies heavily on gap junction and hemichannel-mediated communication for the regulation of cortical development, and for normal functions including electrical and metabolic coupling, the establishment of complex neural circuits, and for the generation of oscillatory patterns in learning and memory (Sohl et al., 2005; Alldredge, 2008; Elias and Kriegstein, 2008). Ablation or mutation

of certain CNS connexin family members often has devastating effects. For example, any one of several mutations in the Cx32 gene results in a peripheral neuropathy called X-linked Charcot-Marie-Tooth (CMT) disease, which is characterized by demyelination of axons leading to a loss of muscle tissue and touch sensation (Bergoffen et al., 1993; Bruzzone et al., 1994). Alterations of connexin expression and/or function are also implicated in epileptogenesis, in the spread of both cytotoxic and neuroprotective signals during stroke, drug and alcohol addiction, and even in the efficacy of anaesthetics (Alldredge, 2008). Furthermore, Cx43 is altered in Alzheimer, Huntington, and Parkinson diseases (Nagy et al., 1996; Rufer et al., 1996; Vis et al., 1998).

1.4.1 Connexin-mediated communication is involved in directing NPC fate in the developing CNS, and in the adult SVZ and SGZ

In addition to the important role of connexins and gap junctions in the adult brain, we know that connexin-mediated communication is involved in fate determination of NPCs in the developing brain, as well as in both of the neurogenic niches of the adult brain (Elias and Kriegstein, 2008). Connexin-mediated communication has been implicated in NPC activation and specification (Yuste et al., 1995; Melanson-Drapeau et al., 2003), and more recently, it has been shown that the adhesive properties of gap junctions are necessary for NPC migration along radial glia in the neocortex (Elias et al., 2007). Furthermore, connexin-mediated

communication is required for proper axonal growth, guidance, and synaptogenesis of immature neurons during the establishment of the neural circuitry (Lo Turco and Kriegstein, 1991; Fulton, 1995).

In addition to being spatially distributed throughout the developing brain, connexin expression is also temporally regulated, which indicates distinct roles for connexin-mediated communication in different cell types, and a requirement for different connexins depending on the stage of development. For example, Cx43 and Cx26 are expressed by immature neurons and radial glia during development, but their expression is restricted to astrocytes in the adult. This decrease in Cx43 may be a signal for neuronal-specific differentiation, because Cx43 is decreased in neural-restricted teratocarcinoma cells when differentiated to neurons, but not when differentiated into glia (Bani-Yaghoub et al., 1997).

The temporal regulation of connexins is also evident upon examination of connexins in the developing cortex, wherein the overall expression of Cx43 increases, the expression of Cx26 initially increases and then decreases by post-natal week three, at which point the expression of Cx32 increases (Dermietzel et al., 1989; Nadarajah et al., 1997). This increase in Cx32 protein is concomitant with oligodendrocyte maturation (Parnavelas et al., 1983; Dermietzel et al., 1989; Belliveau et al., 1991) and reaches a maximum between postnatal week three and four (Nadarajah et al., 1997). Given that Cx32 is expressed only in oligodendrocytes in the brain, it is possible that the induction of Cx32 expression in OPCs enables them to respond to oligodendrocytic

maturation cues present in the environment, which supports the work from our laboratory wherein the induction of Cx32 was sufficient to restrict early OPCs to an oligodendrocyte lineage (Melanson-Drapeau et al., in preparation for re-submission; See Ch.1.6).

In addition to *in vivo* study, our laboratory uses the neurosphere model to study the repertoire of connexins expressed by hippocampal-derived postnatal NPCs and their effect on cell proliferation, specification, and survival. Lineage analysis of neurospheres cultured in suspension indicated that multipotential Type 1 progenitor cells express Cx26, Cx30, and Cx43 protein. Type 2a but not Type 2b and 3 progenitor cells committed to the neuronal lineage also express Cx37, Cx40, and Cx45 (Imbeault et al., 2009). Early OPCs positive for the lineage markers NG2 and platelet-derived growth factor alpha receptor (PDGFαR) express Cx29 (Menichella et al., 2003). Upon differentiation induced by engagement with laminin, the expression and subcellular localization of certain connexins was altered. Markedly, Cx32 and Cx36 protein was induced upon laminin plating in early oligodendrocytes and immature neurons, respectively (Worsdorfer et al., 2008; Imbeault et al., 2009). The induction of Cx32 protein in early OPCs expressing NG2, PDGFαR, and Cx29 may represent an important molecular switch function for Cx32 in the ability of OPCs to specify to oligodendrocytes, however the mechanism of this phenomenon is still under investigation. Overall, the changes in connexin expression following differentiation of NPCs indicate

dynamic regulation of connexins (Rozental et al., 1998), and highlight the importance of microenvironment-specific extracellular cues in NPC fate specification (Bratt-Leal et al., 2009; Imbeault et al., 2009).

1.5 Mechanisms of connexin-mediated communication

There are three main ways that connexins and gap junctions can be involved in both intercellular and intracellular signalling pathways. The first is by enabling cytoplasmic continuity amongst neighbouring cells through the formation of gap junction channels at the plasma membrane. The second form of communication is through hemichannels that result when connexons are present at the plasma membrane but do not dock with connexons from adjacent cells. As half of the gap junction channel, hemichannels allow cells to sample signalling molecules and metabolites from the extracellular environment (Goodenough and Paul, 2003). The third mechanism of connexin-mediated communication is channel-independent that can be accomplished in two main ways: 1.) connexins at the plasma membrane can act as adhesion molecules to aid in the migration/differentiation of progenitor cells (Elias et al., 2007), and 2.) connexins can interact with signalling proteins therein modulating intracellular signalling cascades (Giepmans, 2004; Herve et al., 2004; Herve et al., 2007). This thesis will focus on the channel-independent mechanisms of Cx32 communication mediated by protein interactions with intracellular connexin domains (Fig 1.4).

1.5.1 Channel-independent functions of connexin proteins

With the advent of advanced techniques in protein chromatography and mass spectrometric analyses, proteomic profiling of specific organelles and protein complexes has revealed a level of complexity in terms of protein interactions that had not been possible using conventional hypothesis-driven methodologies. We now recognize that many integral membrane receptors such as G protein coupled receptors (GPCRs), ligand gated ion channels, and receptor tyrosine kinase-linked receptors exist as large multi-protein assemblages composed of structural proteins, other receptors and ion channels, and most interestingly, a host of signalling molecules known to be effectors of important intracellular signalling cascades (Kabbani, 2008). Indeed, studies have shown that protein interactions with GPCRs actually mediate most aspects of the receptor life cycle including its synthesis, trafficking to the cell membrane, coupling to effecter targets, post-translational modifications, recycling, and degradation (Milligan and White, 2001; Bockaert et al., 2004).

Given the importance of regulatory membrane complexes, it is not surprising then that numerous proteins have been found to interact with connexins at gap junctional complexes (Giepmans, 2004; Herve et al., 2007). Indeed, gap junctions have been referred to as a type of "nexus" assembly, re-iterating the complexity of protein interactions at these sites (Duffy et al., 2002). The most well-studied connexin in terms of protein interactions, is the highly expressed Cx43 whose deletion is perinatal

Figure 1.4: Mechanisms of connexin-mediated communication.
Channel-dependent modes of connexin-mediated communication (A) are mediated by hemichannels and gap junction channels. Hemichannels mediate paracrine signalling with the microenvironment while gap junctions are responsible for electrical and metabolic coupling of adjacent cells (juxtacrine communication). Channel-independent connexin-mediated communication (B) is mediated by (I) adhesive contacts which aid in the migration of NPCs, and (II) intracellular protein-protein interactions that are involved in regulation of the connexin life cycle, stabilization or regulation of other membrane complexes, sequestration of signalling molecules, and/or in direct transcriptional regulation of target genes.

A Channel-dependent connexin-mediated communication

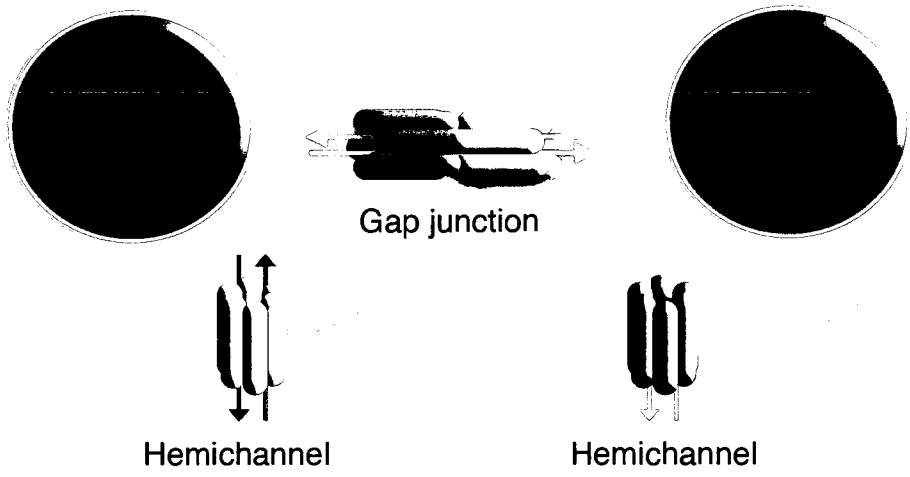

B Channel-independent connexin-mediated communication

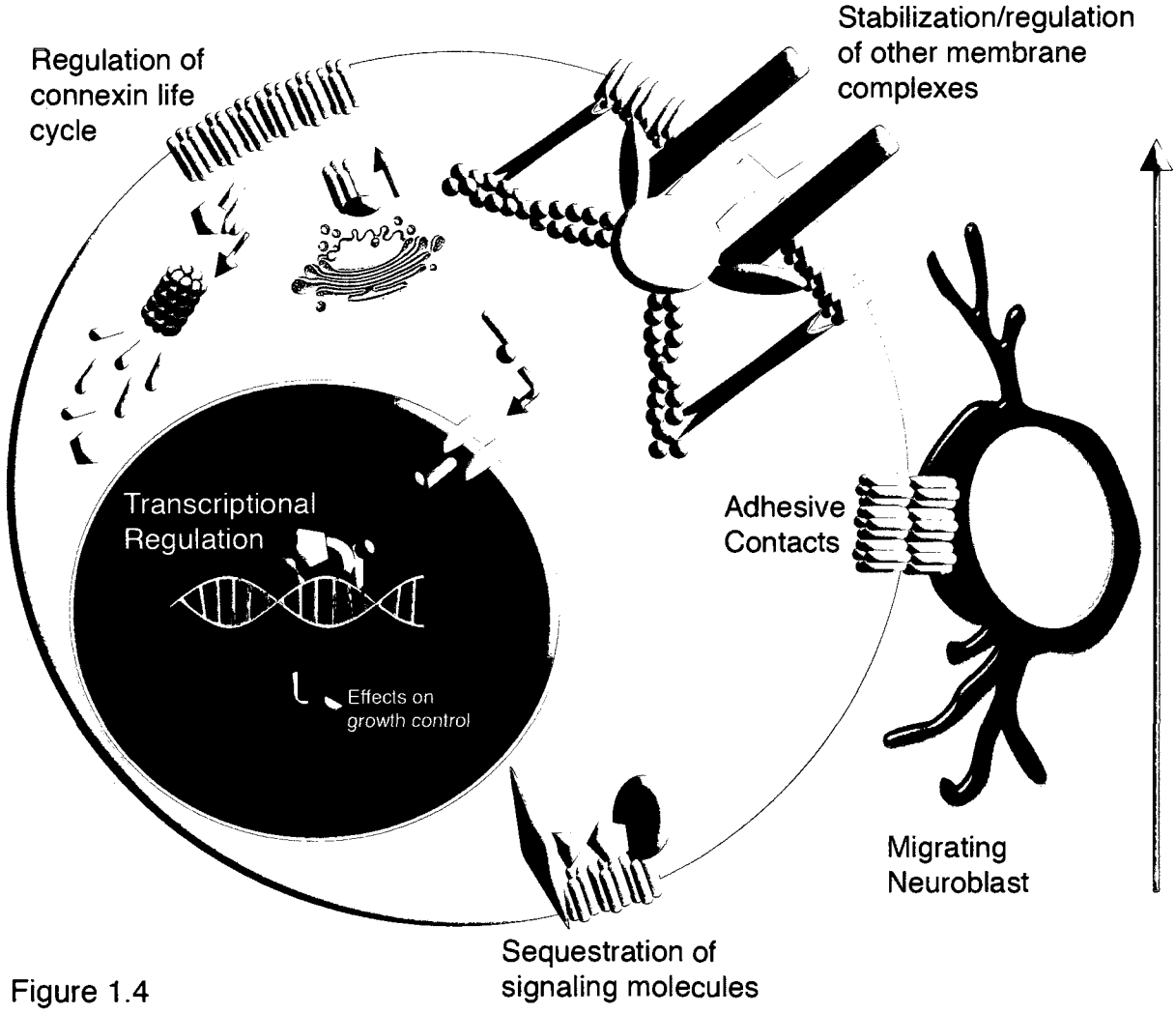

Figure 1.4

lethal due to cardiac malformation (Eckardt et al., 2004). In addition to a high level of expression in cardiac ventricle and atrium, Cx43 is also present in the brain, uterus, retina, lens, testes and spleen (Kadle et al., 1991). To date, there are approximately twenty known binding partners for Cx43 that include various kinases, transcription factors, and members of both the tight and adherens junctions (Giepmans, 2006). Based on the identities of the proteins associating with connexins, we can ascribe to them four possible functional categories: (1) Connexins may act as "regulatory sequesters" of signalling molecules by changing the equilibrium of bound and unbound signalling factors, thereby altering their availability to activate specific downstream targets (Ai et al., 2000; Duffy et al., 2007); (2) Connexins may bind to and help stabilize and/or regulate the function of other integral membrane junctional or receptor complexes (Giepmans and Moolenaar, 1998; Kojima et al., 1999; Schubert et al., 2002); (3) Proteins bound to connexins may alter the traffic, gating, stability, turnover etc., of gap junction plaques or 3.) Bound proteins may target individual connexins to the nucleus and affect transcription of target genes, or may act as accessory transcription factors once inside the nucleus (Moorby and Patel, 2001; Dang et al., 2003). While the datasets concerning the identity of connexin-interacting proteins are expanding, we understand very little about their functional significance, or what physiological effects could be modulated by altering the dynamics of connexin interactions.

1.6 Channel-independent protein-protein interactions dictate the intrinsic capacity of early OPCs to respond to extrinsic neurogenic stimuli

Work in our laboratory by Dr. Melanson-Drapeau has implicated Cx32 as a potent inhibitor of early OPC specification to neurons (Melanson-Drapeau et al., in preparation for re-submission; See Fig 1.5). Through a series of complementary loss and gain of function studies, she showed that hippocampal polydendrocytes actively proliferate and express Cx32 following kainic-acid induced seizure yet do not become neurons *in vivo* or *in vitro* (Melanson-Drapeau et al., 2003). Deletion of Cx32 enabled OPCs to regenerate lost hippocampal pyramidal neurons, and behavioural indices of hippocampal-dependent learning and memory were restored. Furthermore, ectopic expression of Cx32 in multipotential primary hippocampal progenitor cells and NT2/D1 cells prevented them from responding to extrinsic neurogenic stimuli, and their neurogenic capacity was greatly reduced. Interestingly, the inhibition of neurogenesis *in vitro* occurred even when cells were plated at such densities that cell-cell contacts were rarely observed, indicating that the effect of Cx32 was gap junction channel independent. It is possible that Cx32 hemichannels in $NG2^+$ OPCs mediate the transfer of signalling factors that favour oligodendrogenesis, however, given the results of this previous work, ***this thesis sought to establish the necessary methodologies and identify candidate interacting proteins required to test the hypothesis that***

Figure 1.5: OPCs hyperproliferate and may form functional neurons following excitotoxic injury.

The two main modes of adult hippocampal neurogenesis are depicted here. The first is as described in Fig. 1.1 wherein neurons are generated from DCX+ Type 3 NPCs. The pathway to the right describes an alternate mode of neurogenesis whereby NG2+ progenitor cells, classically known only as OPCs, can respond to neurogenic stimuli. Results from our laboratory show that following excitotoxic injury, this pool of OPCs hyperproliferates, and in WT animals are either apoptotically deleted, or can undergo oligodendrogenesis upon expression of Cx32. Some authors also report their ability to specify to certain astrocyte lineages. Our data indicate that genetic deletion of Cx32 may enable this pool of hyperproliferating OPCs to respond to neurogenic stimuli and generate functional neurons. Elucidating underlying mechanisms are, in part, the underlying rationale for this thesis. Abbreviations are as in Figure 1.1, including NG2+: chondroitin sulfate proteoglycan; OPCs: oligodendrocyte progenitor cells.

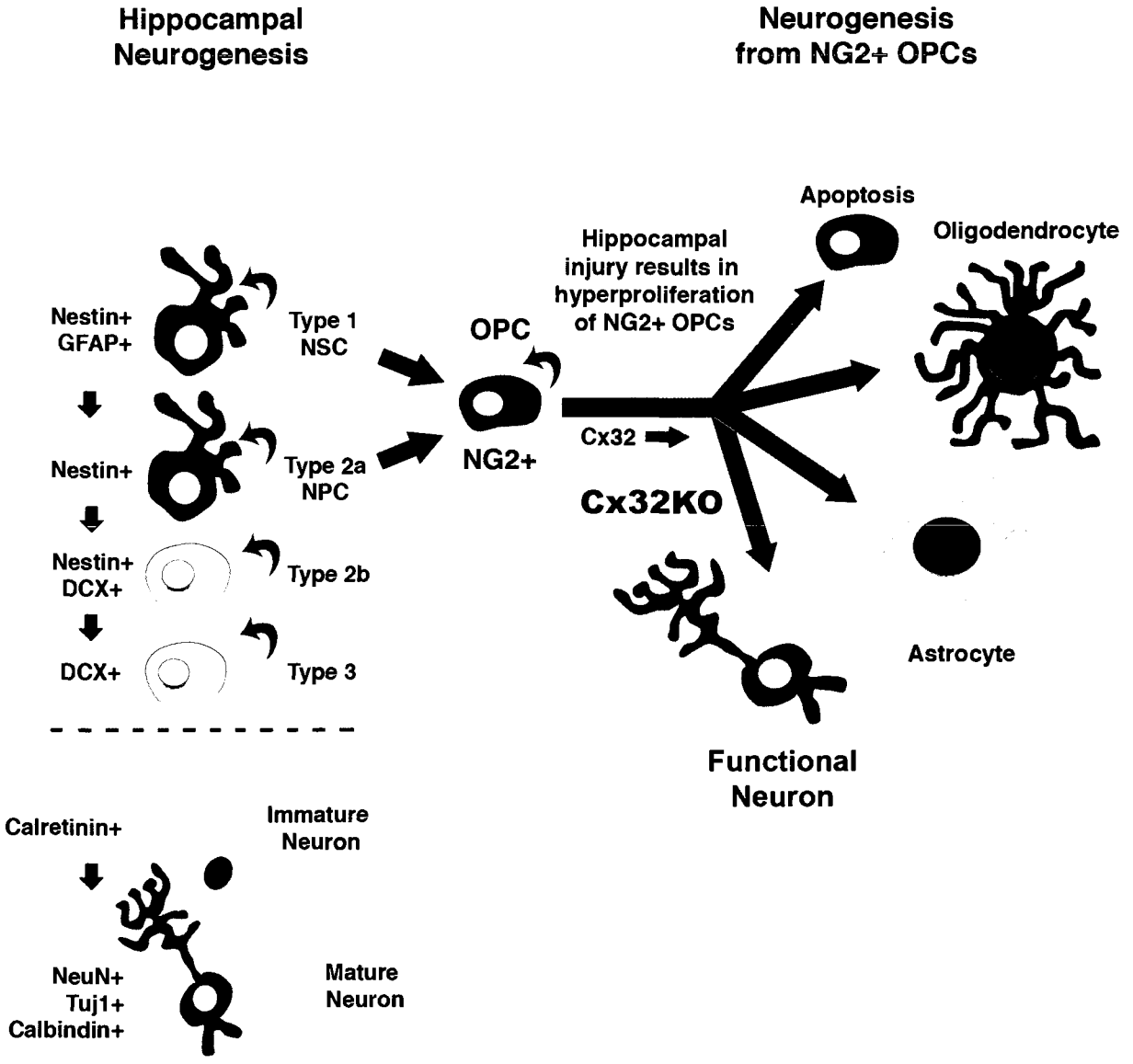
Hippocampal Neurogenesis
Neurogenesis from NG2+ OPCs
Nestin+ GFAP+
Type 1 NSC
Nestin+
Type 2a NPC
Nestin+ DCX+
Type 2b
DCX+
Type 3
OPC
NG2+
Hippocampal injury results in hyperproliferation of NG2+ OPCs
Cx32
Cx32KO
Apoptosis
Oligodendrocyte
Astrocyte
Functional Neuron
Calretinin+
Immature Neuron
NeuN+ Tuj1+ Calbindin+
Mature Neuron

Figure 1.5

protein interactions with Cx32 underlie the restriction of NG2$^+$ OPCs to an oligodendrocyte lineage in injured brain.

1.6.1 Our current knowledge of Cx32-interacting proteins

As stated above, we hypothesize that protein interactions with Cx32 mediate its ability to intrinsically regulate NG2$^+$ OPC fate, however, we know of few validated interactions with this connexin. Furthermore, most of these protein interactions identified to date have been determined in cultured hepatocytes often without proper null-mutant controls, and have not been confirmed as interacting partners of Cx32 in OPCs or mature oligodendrocytes. As such, I have summarized our current knowledge of Cx32 interacting proteins below, with the corresponding methodological information for each study located in Table 1.1.

Many of the known binding partners of Cx32 are members of other plasma membrane junctional complexes and lipid raft domains. As demonstrated by Kojima et al. (Kojima et al., 1999; Kojima et al., 2001) by co-immunofluorescence (co-IF) and co-immunoprecipitation (co-IP) assays, Cx32 interacts with the tight junction integral membrane proteins occludin and claudin-1, and the scaffolding protein zona occludens-1 (ZO-1) in cultured rat hepatocytes. This assemblage of proteins at tight junctions interacts with a large number of other proteins, and has been proposed as a sequestering site for transcription factors, protein kinases and phosphatases. It is thought that connexin association with tight

Table 1.1: Reported protein interactions with Cx32

Interacting Partner	Binding Site/Motif	Approaches	Cell/Tissue Type	Predicted Molecular Weight (kDa)	Reference
Occludin		CoIF; CoIP	Cultured rat hepatocytes	59.0	Kojima et al., 2001
Claudin-1		CoIF; CoIP	Cultured rat hepatocytes	22.9	Kojima et al., 2001
Calmodulin	NT (1-21); CT (216-230)	CoIF; Binding assay		16.8	Török et al., 1997
	NT (15-32)	CoIF;	Xenopus oocytes		Peracchia et al., 2000
ZO-1		CoIF; CoIP	Cultured rat hepatocytes	194.7	Kojima et al., 2001
ZONAB		CoIF	Mouse hippocampus and thalamus	31.8	Penes et al., 2005
Caveolin-1	aa 153-178	CoIP	NIH 3T3, HEK 293T, COS-7 cells	20.5	Schubert et al., 2002
Dlgh-1	SH3/Hook (CT and IL)	CoIF; CoIP*; Y2H; AA	Mouse liver, SKHep cels	103.0	Duffy et al., 2007
E-cadherin/α-catenin		CoIF	Cultured mouse hepatocytes	98.3/100.1	Kostin et al., 1999

NT: N-terminus; CT: C-terminus; IL: intracellular loop; Co-IF: Co-immunofluorescence; Co-IP: Co-immunoprecipitation, Y2H: yeast two hybrid; AA: antibody array. None of these studies employed Cx32-null controls except Duffy et al. wherein controls were not shown for co-IP data.

junctions aids in the organization and patterning of gap junctional plaques (Giepmans and Moolenaar, 1998; Toyofuku et al., 2001), in addition to placing connexins in close apposition to signalling factors with known roles in connexin regulation (Laing et al., 2001).

Cx32 also associates with the adherens junction proteins E-cadherin and α-catenin (Kostin et al., 1999). Adherens junctions are mechanical linkages between neighbouring cells and, through the α and ß-catenins, are linked to the actin cytoskeleton. Many of the adherens junction proteins are signal transduction molecules, and thus connexin association with these complexes is also likely to play an important role, particularly related to the status of cell-cell coupling (Yap et al., 1997; Herve et al., 2007). Cx32 is also reported to interact with Discs large homolog-1 (Dlgh-1), a membrane-associated guanylate kinase (MAGUK) family member with known tumor-suppressive properties. (Duffy et al., 2007) have shown that in the presence of Cx32, Dlgh-1 is sequestered at junctional complexes, however, acute removal of Cx32 causes nuclear translocation of Dlgh-1 where it activates target genes that restrict cell proliferation.

Numerous connexins including Cx32 are targeted to lipid rafts, the cholesterol-sphingolipid-rich microdomains that serve as regulators of membrane trafficking and signal transduction. Contained within lipid rafts are specialized caveolar domains composed of the caveolin family of proteins. Cx32, along with other connexins, have been shown to co-IP

and co-fractionate with caveolin-1 in numerous cell types, which could have important proximity implications for Cx32 interaction with the signalling complexes sequestered at these sites (Schubert et al., 2002).

Finally, Cx32 co-localizes with the ubiquitously expressed calcium binding protein, calmodulin, and possesses both N and C-terminal calmodulin binding motifs (Torok et al., 1997). Calmodulin inhibition studies show that calmodulin has an important role in the regulation of voltage and chemical gating of Cx32 channels (Peracchia et al., 2000), and appears to be necessary for proper Cx32 targeting to gap junctions (Ahmad et al., 2001). Calcium itself has long been known to regulate gap junction intercellular communication, so the interaction of Cx32 with calmodulin may also contribute to this process (Harris, 2001).

1.7 Rationale, Hypothesis and Objectives

Our laboratory has implicated Cx32 as an important molecular switch that directs $NG2^+$ OPCs to adopt an oligodendrocytic fate. Given that this effect is seen *in vitro* when no direct cell-cell contacts were made, I hypothesized that a channel-independent mechanism involving Cx32 was mediating the inhibition of OPC specification to neurons and restricting their fate to oligodendrocytes. More specifically, I hypothesized that protein-protein interactions with the intracellular domains of Cx32 were responsible for this effect. To test this hypothesis, I proposed to purify Cx32 from brain tissue and identify interacting proteins by liquid

chromatography tandem mass spectrometry (LC-MS/MS). However, I discovered that Cx32 antibodies were highly cross-reactive in brain tissue despite adequate specificity in liver. This obstacle was overcome, and further characterized by testing a battery of Cx32 antibodies for brain cross-reactivity, the results of which are presented in Chapter 2. As proof of principle, I developed and verified a method of endogenous Cx32 purification that specifically identified Cx32-interacting partners from liver tissue using null-mutant controls. Liver was used as a positive control tissue because it contains approximately ten-fold more Cx32 than brain tissue, does not exhibit cross-reactivity with Cx32 antibodies, and thus the methodology could be optimized while issues of brain-specific cross-reactivity were being overcome. The verification of our method and the validation of Cx32-interacting proteins in liver are presented in Chapter 3. Chapter 4 describes results validating the interaction between Cx32 and some of the proteins discovered by LC-MS/MS in brain tissue, which will be the focus of my PhD work. This thesis lays the technical groundwork for my PhD research and identifies novel interacting proteins of Cx32 that will be tested for their involvement in directing OPC specification. To achieve these objectives, three specific aims were addressed:

1.) Characterize available Cx32 antibodies in murine male brain and liver (both wildtype (Y/+) and null-mutant (Y/-)) to determine the most appropriate reagents for immunoblotting (IB) and immunoprecipitation (IP).

2.) Determine binding partners of Cx32 in murine liver by endogenous purification followed by protein identification by LC-MS/MS.

3.) Validate positive Cx32 interacting proteins by co-IP and co-IF.

Taken together, these results describe the resolution of a confounding technical obstacle in the connexin field that has repeatedly challenged studies of connexin function in the CNS and identify 18 novel Cx32 interacting proteins. One of these proteins is SFXN-1, a protein with homology to the rat mitochondrial tricarboxylate carrier. The interaction between Cx32 and SFXN-1 suggests a novel subcellular localization and function for Cx32 in the mitochondrion, and may be implicated in the regulation of mitochondrial dynamics, which could have important implications for NPC fate specification. Together, these data represent the first step towards discovering how we can promote specification of NPC and/or OPCs to neurons following brain injury or disease through modulation of connexin protein-protein interactions.

1.8 References

Aguado T, Romero E, Monory K, Palazuelos J, Sendtner M, Marsicano G, Lutz B, Guzman M, Galve-Roperh I (2007) The CB1 cannabinoid receptor mediates excitotoxicity-induced neural progenitor proliferation and neurogenesis. J Biol Chem 282:23892-23898.

Aguirre A, Gallo V (2004) Postnatal neurogenesis and gliogenesis in the olfactory bulb from NG2-expressing progenitors of the subventricular zone. J Neurosci 24:10530-10541.

Aguirre AA, Chittajallu R, Belachew S, Gallo V (2004) NG2-expressing cells in the subventricular zone are type C-like cells and contribute to interneuron generation in the postnatal hippocampus. J Cell Biol 165:575-589.

Ahmad S, Martin PE, Evans WH (2001) Assembly of gap junction channels: mechanism, effects of calmodulin antagonists and identification of connexin oligomerization determinants. Eur J Biochem 268:4544-4552.

Ai Z, Fischer A, Spray DC, Brown AM, Fishman GI (2000) Wnt-1 regulation of connexin43 in cardiac myocytes. J Clin Invest 105:161-171.

Alexander DB, Goldberg GS (2003) Transfer of biologically important molecules between cells through gap junction channels. Curr Med Chem 10:2045-2058.

Alldredge B (2008) Clinical connexions. J Clin Pathol 61:885-890.

Allen NJ, Barres BA (2009) Neuroscience: Glia - more than just brain glue. Nature 457:675-677.

Altevogt BM, Paul DL (2004) Four classes of intercellular channels between glial cells in the CNS. J Neurosci 24:4313-4323.

Alvarez-Buylla A, Lim DA (2004) For the long run: maintaining germinal niches in the adult brain. Neuron 41:683-686.

Bani-Yaghoub M, Bechberger JF, Naus CC (1997) Reduction of connexin43 expression and dye-coupling during neuronal differentiation of human NTera2/clone D1 cells. J Neurosci Res 49:19-31.

Belachew S, Chittajallu R, Aguirre AA, Yuan X, Kirby M, Anderson S, Gallo V (2003) Postnatal NG2 proteoglycan-expressing progenitor cells are intrinsically multipotent and generate functional neurons. J Cell Biol 161:169-186.

Belliveau DJ, Kidder GM, Naus CC (1991) Expression of gap junction genes during postnatal neural development. Dev Genet 12:308-317.

Bergoffen J, Scherer SS, Wang S, Scott MO, Bone LJ, Paul DL, Chen K, Lensch MW, Chance PF, Fischbeck KH (1993) Connexin mutations in X-linked Charcot-Marie-Tooth disease. Science 262:2039-2042.

Beyer EC, Paul DL, Goodenough DA (1990) Connexin family of gap junction proteins. J Membr Biol 116:187-194.

Bockaert J, Roussignol G, Becamel C, Gavarini S, Joubert L, Dumuis A, Fagni L, Marin P (2004) GPCR-interacting proteins (GIPs): nature and functions. Biochem Soc Trans 32:851-855.

Brandt MD, Jessberger S, Steiner B, Kronenberg G, Reuter K, Bick-Sander A, von der Behrens W, Kempermann G (2003) Transient calretinin expression defines early postmitotic step of neuronal differentiation in adult hippocampal neurogenesis of mice. Mol Cell Neurosci 24:603-613.

Bratt-Leal AM, Carpenedo RL, McDevitt TC (2009) Engineering the embryoid body microenvironment to direct embryonic stem cell differentiation. Biotechnol Prog 25:43-51.

Brink PR, Cronin K, Banach K, Peterson E, Westphale EM, Seul KH, Ramanan SV, Beyer EC (1997) Evidence for heteromeric gap junction channels formed from rat connexin43 and human connexin37. Am J Physiol 273:C1386-1396.

Bruzzone R, White TW, Paul DL (1996) Connections with connexins: the molecular basis of direct intercellular signalling. Eur J Biochem 238:1-27.

Bruzzone R, White TW, Scherer SS, Fischbeck KH, Paul DL (1994) Null mutations of connexin32 in patients with X-linked Charcot-Marie-Tooth disease. Neuron 13:1253-1260.

Bunge RP (1968) Glial cells and the central myelin sheath. Physiol Rev 48:197-251.

Cruciani V, Mikalsen SO (2006) The vertebrate connexin family. Cell Mol Life Sci 63:1125-1140.

Dang X, Doble BW, Kardami E (2003) The carboxy-tail of connexin-43 localizes to the nucleus and inhibits cell growth. Mol Cell Biochem 242:35-38.

Dermietzel R, Traub O, Hwang TK, Beyer E, Bennett MV, Spray DC, Willecke K (1989) Differential expression of three gap junction proteins in developing and mature brain tissues. Proc Natl Acad Sci U S A 86:10148-10152.

Doetsch F, Caille I, Lim DA, Garcia-Verdugo JM, Alvarez-Buylla A (1999) Subventricular zone astrocytes are neural stem cells in the adult mammalian brain. Cell 97:703-716.

Duffy HS, Delmar M, Spray DC (2002) Formation of the gap junction nexus: binding partners for connexins. J Physiol Paris 96:243-249.

Duffy HS, Iacobas I, Hotchkiss K, Hirst-Jensen BJ, Bosco A, Dandachi N, Dermietzel R, Sorgen PL, Spray DC (2007) The gap junction protein connexin32 interacts with the Src homology 3/hook domain of discs large homolog 1. J Biol Chem 282:9789-9796.

Ebly EM, Parhad IM, Hogan DB, Fung TS (1994) Prevalence and types of dementia in the very old: results from the Canadian Study of Health and Aging. Neurology 44:1593-1600.

Eckardt D, Theis M, Degen J, Ott T, van Rijen HV, Kirchhoff S, Kim JS, de Bakker JM, Willecke K (2004) Functional role of connexin43 gap

junction channels in adult mouse heart assessed by inducible gene deletion. J Mol Cell Cardiol 36:101-110.

Elias LA, Kriegstein AR (2008) Gap junctions: multifaceted regulators of embryonic cortical development. Trends Neurosci 31:243-250.

Elias LA, Wang DD, Kriegstein AR (2007) Gap junction adhesion is necessary for radial migration in the neocortex. Nature 448:901-907.

Emsley JG, Mitchell BD, Kempermann G, Macklis JD (2005) Adult neurogenesis and repair of the adult CNS with neural progenitors, precursors, and stem cells. Prog Neurobiol 75:321-341.

Fellin T (2009) Communication between neurons and astrocytes: relevance to the modulation of synaptic and network activity. J Neurochem 108:533-544.

Fellin T, Carmignoto G (2004) Neurone-to-astrocyte signalling in the brain represents a distinct multifunctional unit. J Physiol 559:3-15.

Fields RD (2008) Oligodendrocytes changing the rules: action potentials in glia and oligodendrocytes controlling action potentials. Neuroscientist 14:540-543.

Freeman MR (2006) Sculpting the nervous system: glial control of neuronal development. Curr Opin Neurobiol 16:119-125.

Fulton BP (1995) Gap junctions in the developing nervous system. Perspect Dev Neurobiol 2:327-334.

Gage FH, Verma IM (2003) Stem cells at the dawn of the 21st century. Proc Natl Acad Sci U S A 100 Suppl 1:11817-11818.

Geldmacher DS, Frolich L, Doody RS, Erkinjuntti T, Vellas B, Jones RW, Banerjee S, Lin P, Sano M (2006) Realistic expectations for treatment success in Alzheimer's disease. J Nutr Health Aging 10:417-429.

Giepmans BN (2004) Gap junctions and connexin-interacting proteins. Cardiovasc Res 62:233-245.

Giepmans BN (2006) Role of connexin43-interacting proteins at gap junctions. Adv Cardiol 42:41-56.

Giepmans BN, Moolenaar WH (1998) The gap junction protein connexin43 interacts with the second PDZ domain of the zona occludens-1 protein. Curr Biol 8:931-934.

Goodenough DA (1974) Bulk isolation of mouse hepatocyte gap junctions. Characterization of the principal protein, connexin. J Cell Biol 61:557-563.

Goodenough DA, Paul DL (2003) Beyond the gap: functions of unpaired connexon channels. Nat Rev Mol Cell Biol 4:285-294.

Halassa MM, Fellin T, Takano H, Dong JH, Haydon PG (2007) Synaptic islands defined by the territory of a single astrocyte. J Neurosci 27:6473-6477.

Harris AL (2001) Emerging issues of connexin channels: biophysics fills the gap. Q Rev Biophys 34:325-472.

Herve JC, Sarrouilhe D (2006) Protein phosphatase modulation of the intercellular junctional communication: importance in cardiac myocytes. Prog Biophys Mol Biol 90:225-248.

Herve JC, Bourmeyster N, Sarrouilhe D (2004) Diversity in protein-protein interactions of connexins: emerging roles. Biochim Biophys Acta 1662:22-41.

Herve JC, Bourmeyster N, Sarrouilhe D, Duffy HS (2007) Gap junctional complexes: from partners to functions. Prog Biophys Mol Biol 94:29-65.

Hua VB, Chang AB, Tchieu JH, Kumar NM, Nielsen PA, Saier MH, Jr. (2003) Sequence and phylogenetic analyses of 4 TMS junctional proteins of animals: connexins, innexins, claudins and occludins. J Membr Biol 194:59-76.

Imbeault S, Gauvin LG, Toeg HD, Pettit A, Sorbara CD, Migahed L, DesRoches R, Menzies AS, Nishii K, Paul DL, Simon AM, Bennett SA (2009) The extracellular matrix controls gap junction protein expression and function in postnatal hippocampal neural progenitor cells. BMC Neurosci 10:13.

Jarrard LE (1993) On the role of the hippocampus in learning and memory in the rat. Behav Neural Biol 60:9-26.

Kabbani N (2008) Proteomics of membrane receptors and signalling. Proteomics 8:4146-4155.

Kadle R, Zhang JT, Nicholson BJ (1991) Tissue-specific distribution of differentially phosphorylated forms of Cx43. Mol Cell Biol 11:363-369.

Kamasawa N, Sik A, Morita M, Yasumura T, Davidson KG, Nagy JI, Rash JE (2005) Connexin-47 and connexin-32 in gap junctions of

oligodendrocyte somata, myelin sheaths, paranodal loops and Schmidt-Lanterman incisures: implications for ionic homeostasis and potassium siphoning. Neuroscience 136:65-86.

Kempermann G, Jessberger S, Steiner B, Kronenberg G (2004) Milestones of neuronal development in the adult hippocampus. Trends Neurosci 27:447-452.

Kiuru M, Boyer JL, O'Connor TP, Crystal RG (2009) Genetic control of wayward pluripotent stem cells and their progeny after transplantation. Cell Stem Cell 4:289-300.

Kojima T, Kokai Y, Chiba H, Yamamoto M, Mochizuki Y, Sawada N (2001) Cx32 but not Cx26 is associated with tight junctions in primary cultures of rat hepatocytes. Exp Cell Res 263:193-201.

Kojima T, Sawada N, Chiba H, Kokai Y, Yamamoto M, Urban M, Lee GH, Hertzberg EL, Mochizuki Y, Spray DC (1999) Induction of tight junctions in human connexin 32 (hCx32)-transfected mouse hepatocytes: connexin 32 interacts with occludin. Biochem Biophys Res Commun 266:222-229.

Komitova M, Zhu X, Serwanski DR, Nishiyama A (2009) NG2 cells are distinct from neurogenic cells in the postnatal mouse subventricular zone. J Comp Neurol 512:702-716.

Kostin S, Hein S, Bauer EP, Schaper J (1999) Spatiotemporal development and distribution of intercellular junctions in adult rat cardiomyocytes in culture. Circ Res 85:154-167.

Laing JG, Manley-Markowski RN, Koval M, Civitelli R, Steinberg TH (2001) Connexin45 interacts with zonula occludens-1 and connexin43 in osteoblastic cells. J Biol Chem 276:23051-23055.

Lemke G (2001) Glial control of neuronal development. Annu Rev Neurosci 24:87-105.

Lo Turco JJ, Kriegstein AR (1991) Clusters of coupled neuroblasts in embryonic neocortex. Science 252:563-566.

Lois C, Alvarez-Buylla A (1993) Proliferating subventricular zone cells in the adult mammalian forebrain can differentiate into neurons and glia. Proc Natl Acad Sci U S A 90:2074-2077.

Lois C, Garcia-Verdugo JM, Alvarez-Buylla A (1996) Chain migration of neuronal precursors. Science 271:978-981.

Maeda S, Nakagawa S, Suga M, Yamashita E, Oshima A, Fujiyoshi Y, Tsukihara T (2009) Structure of the connexin 26 gap junction channel at 3.5 A resolution. Nature 458:597-602.

Mann DM (1996) Pyramidal nerve cell loss in Alzheimer's disease. Neurodegeneration 5:423-427.

Manthey D, Banach K, Desplantez T, Lee CG, Kozak CA, Traub O, Weingart R, Willecke K (2001) Intracellular domains of mouse connexin26 and -30 affect diffusional and electrical properties of gap junction channels. J Membr Biol 181:137-148.

Melanson-Drapeau L, Beyko S, Dave S, Hebb AL, Franks DJ, Sellitto C, Paul DL, Bennett SA (2003) Oligodendrocyte progenitor enrichment in the connexin32 null-mutant mouse. J Neurosci 23:1759-1768.

Menichella DM, Goodenough DA, Sirkowski E, Scherer SS, Paul DL (2003) Connexins are critical for normal myelination in the CNS. J Neurosci 23:5963-5973.

Menichella DM, Majdan M, Awatramani R, Goodenough DA, Sirkowski E, Scherer SS, Paul DL (2006) Genetic and physiological evidence that oligodendrocyte gap junctions contribute to spatial buffering of potassium released during neuronal activity. J Neurosci 26:10984-10991.

Mercier F, Hatton GI (2001) Connexin 26 and basic fibroblast growth factor are expressed primarily in the subpial and subependymal layers in adult brain parenchyma: roles in stem cell proliferation and morphological plasticity? J Comp Neurol 431:88-104.

Milligan G, White JH (2001) Protein-protein interactions at G-protein-coupled receptors. Trends Pharmacol Sci 22:513-518.

Mitchell AJ, Benito-Leon J, Gonzalez JM, Rivera-Navarro J (2005) Quality of life and its assessment in multiple sclerosis: integrating physical and psychological components of wellbeing. Lancet Neurol 4:556-566.

Mitchell BD, Emsley JG, Magavi SS, Arlotta P, Macklis JD (2004) Constitutive and induced neurogenesis in the adult mammalian brain: manipulation of endogenous precursors toward CNS repair. Dev Neurosci 26:101-117.

Moorby C, Patel M (2001) Dual functions for connexins: Cx43 regulates growth independently of gap junction formation. Exp Cell Res 271:238-248.

Moreno AP, Lau AF (2007) Gap junction channel gating modulated through protein phosphorylation. Prog Biophys Mol Biol 94:107-119.

Mullen RJ, Buck CR, Smith AM (1992) NeuN, a neuronal specific nuclear protein in vertebrates. Development 116:201-211.

Musil LS, Goodenough DA (1990) Gap junctional intercellular communication and the regulation of connexin expression and function. Curr Opin Cell Biol 2:875-880.

Nadarajah B, Jones AM, Evans WH, Parnavelas JG (1997) Differential expression of connexins during neocortical development and neuronal circuit formation. J Neurosci 17:3096-3111.

Nagy JI, Rash JE (2003) Astrocyte and oligodendrocyte connexins of the glial syncytium in relation to astrocyte anatomical domains and spatial buffering. Cell Commun Adhes 10:401-406.

Nagy JI, Li W, Hertzberg EL, Marotta CA (1996) Elevated connexin43 immunoreactivity at sites of amyloid plaques in Alzheimer's disease. Brain Res 717:173-178.

Nagy JI, Ionescu AV, Lynn BD, Rash JE (2003) Coupling of astrocyte connexins Cx26, Cx30, Cx43 to oligodendrocyte Cx29, Cx32, Cx47: Implications from normal and connexin32 knockout mice. Glia 44:205-218.

Nagy JI, Li X, Rempel J, Stelmack G, Patel D, Staines WA, Yasumura T, Rash JE (2001) Connexin26 in adult rodent central nervous system: demonstration at astrocytic gap junctions and colocalization with connexin30 and connexin43. J Comp Neurol 441:302-323.

Okano H, Sawamoto K (2008) Neural stem cells: involvement in adult neurogenesis and CNS repair. Philos Trans R Soc Lond B Biol Sci 363:2111-2122.

Olanow CW, Tatton WG (1999) Etiology and pathogenesis of Parkinson's disease. Annu Rev Neurosci 22:123-144.

Ormerod BK, Palmer TD, Caldwell MA (2008) Neurodegeneration and cell replacement. Philos Trans R Soc Lond B Biol Sci 363:153-170.

Orthmann-Murphy JL, Abrams CK, Scherer SS (2008) Gap junctions couple astrocytes and oligodendrocytes. J Mol Neurosci 35:101-116.

Parnavelas JG, Luder R, Pollard SG, Sullivan K, Lieberman AR (1983) A qualitative and quantitative ultrastructural study of glial cells in the developing visual cortex of the rat. Philos Trans R Soc Lond B Biol Sci 301:55-84.

Peracchia C, Sotkis A, Wang XG, Peracchia LL, Persechini A (2000) Calmodulin directly gates gap junction channels. J Biol Chem 275:26220-26224.

Rash JE, Yasumura T, Dudek FE, Nagy JI (2001) Cell-specific expression of connexins and evidence of restricted gap junctional coupling between glial cells and between neurons. J Neurosci 21:1983-2000.

Rohl CA, Doig AJ (1996) Models for the 3(10)-helix/coil, pi-helix/coil, and alpha-helix/3(10)-helix/coil transitions in isolated peptides. Protein Sci 5:1687-1696.

Rouskova L, Hruska I, Filip S (2008) Issues and ethical problems of stem cell therapy--where is Hippocrates? Acta Medica (Hradec Kralove) 51:121-126.

Rozental R, Morales M, Mehler MF, Urban M, Kremer M, Dermietzel R, Kessler JA, Spray DC (1998) Changes in the properties of gap junctions during neuronal differentiation of hippocampal progenitor cells. J Neurosci 18:1753-1762.

Rufer M, Wirth SB, Hofer A, Dermietzel R, Pastor A, Kettenmann H, Unsicker K (1996) Regulation of connexin-43, GFAP, and FGF-2 is not accompanied by changes in astroglial coupling in MPTP-lesioned, FGF-2-treated parkinsonian mice. J Neurosci Res 46:606-617.

Schubert AL, Schubert W, Spray DC, Lisanti MP (2002) Connexin family members target to lipid raft domains and interact with caveolin-1. Biochemistry 41:5754-5764.

Sohl G, Maxeiner S, Willecke K (2005) Expression and functions of neuronal gap junctions. Nat Rev Neurosci 6:191-200.

Suga M, Maeda S, Nakagawa S, Yamashita E, Tsukihara T (2009) A description of the structural determination procedures of a gap junction channel at 3.5 A resolution. Acta Crystallogr D Biol Crystallogr 65:758-766.

Theis M, Sohl G, Eiberger J, Willecke K (2005) Emerging complexities in identity and function of glial connexins. Trends Neurosci 28:188-195.

Torok K, Stauffer K, Evans WH (1997) Connexin 32 of gap junctions contains two cytoplasmic calmodulin-binding domains. Biochem J 326 (Pt 2):479-483.

Toyofuku T, Akamatsu Y, Zhang H, Kuzuya T, Tada M, Hori M (2001) c-Src regulates the interaction between connexin-43 and ZO-1 in cardiac myocytes. J Biol Chem 276:1780-1788.

Verselis VK, Ginter CS, Bargiello TA (1994) Opposite voltage gating polarities of two closely related connexins. Nature 368:348-351.

Vis JC, Nicholson LF, Faull RL, Evans WH, Severs NJ, Green CR (1998) Connexin expression in Huntington's diseased human brain. Cell Biol Int 22:837-847.

Wellershaus K, Degen J, Deuchars J, Theis M, Charollais A, Caille D, Gauthier B, Janssen-Bienhold U, Sonntag S, Herrera P, Meda P, Willecke K (2008) A new conditional mouse mutant reveals specific expression and functions of connexin36 in neurons and pancreatic beta-cells. Exp Cell Res 314:997-1012.

White TW, Bruzzone R, Paul DL (1995) The connexin family of intercellular channel forming proteins. Kidney Int 48:1148-1157.

Worsdorfer P, Maxeiner S, Markopoulos C, Kirfel G, Wulf V, Auth T, Urschel S, von Maltzahn J, Willecke K (2008) Connexin expression

and functional analysis of gap junctional communication in mouse embryonic stem cells. Stem Cells 26:431-439.

Xie J, Brayne C, Matthews FE (2008) Survival times in people with dementia: analysis from population based cohort study with 14 year follow-up. BMJ 336:258-262.

Yankner BA, Lu T, Loerch P (2008) The aging brain. Annu Rev Pathol 3:41-66.

Yap AS, Brieher WM, Gumbiner BM (1997) Molecular and functional analysis of cadherin-based adherens junctions. Annu Rev Cell Dev Biol 13:119-146.

Yuste R, Nelson DA, Rubin WW, Katz LC (1995) Neuronal domains in developing neocortex: mechanisms of coactivation. Neuron 14:7-17.

Zhu X, Hill RA, Nishiyama A (2008) NG2 cells generate oligodendrocytes and gray matter astrocytes in the spinal cord. Neuron Glia Biol 4:19-26.

Chapter 2: Tissue-specific cross-reactivity of connexin32 antibodies: Problems and solutions unique to the central nervous system

2.1: Objectives

The overarching goals of this study were to overcome the technical issues plaguing Cx32 detection in the brain, and to establish the capacity to specifically immunopurify Cx32 from tissues with abundant Cx32 protein expression but limited expression of other connexin family members (i.e., liver), as well as from tissues with restricted Cx32 protein expression but a wide profile of related connexin family members (i.e., brain). In both cases, specificity was verified using null-mutant controls.

2.2: Statement of author contributions

This chapter, in its entirety, represents a paper accepted for publication in August 2009 to the journal of Cell Communication and Adhesion by SF and ACM as joint first authors under the supervision of SB[1]. SF performed the IB, IP, and fractionation experiments, and ACM performed the animal dissections, genotyping, and immunofluorescent analyses. Jean-Phillipe Lambert of the Ottawa Institute of Systems Biology provided expert technical and critical assistance with the MS analyses.

---

[1]S.L. Fowler*, A.C. McLean*, and S.A.L. Bennett (2009). **Tissue-specific cross-reactivity of connexin32 antibodies: Problems and solutions unique to the central nervous system.** *Submitted to Cell Communication and Adhesion, in press.*
*Both authors contributed equally

Leigh Anne Swayne is gratefully acknowledged for her scientific ingenuity related to the methodologies explored in this study.

2.3: Introduction

Connexin proteins are a highly conserved family of single and double membrane channels characterized, in part, by four TM-spanning domains. The connexin family consists of 21 members; 11 of which are expressed in the mammalian central nervous system (CNS) (Rouach et al., 2002b; Nakase and Naus, 2004; Sohl et al., 2005). Hexamerization of compatible connexins form structures called connexons that incorporate as hemichannels in non-junctional membranes (single membrane channels) or dock with compatible connexons donated from adjacent cells to form intercellular gap junction channels (double membrane channels) (Goodenough and Paul, 2003). Gap junctions are present in membranes as plaques composed of hundreds of channels of various connexin combinations that allow for the transfer of ions and metabolites less than one kDa in size between neighboring cells (Bruzzone et al., 1996).

Connexin32 (Cx32) is the predominant liver connexin, and was first isolated in 1986 from purified calf liver gap junctional preparations (Paul, 1986a). Hydropathy analysis of the Cx32 cDNA clone predicted a protein with four transmembrane segments flanked by alpha helical loops. Shortly thereafter, the cytoplasmic localization of both N- and C-termini, and a hydrophilic domain corresponding to the loop between the second and third TM regions, were confirmed (Fig 1). It is generally accepted that

these cytoplasmic regions are the least conserved amongst connexin family members, and thus provided the most attractive sites for connexin-specific antibody development (Hertzberg, 1985; Goodenough et al., 1988).

The first Cx32 antibodies were prepared from purified calf liver gap junction preparations (Traub et al., 1982; Paul, 1986a) or from peptides localized to the CT, and the IL (Hertzberg, 1985; Goodenough et al., 1988). Each of these antibodies recognized a monomeric protein with a molecular weight of approximately 27 kDa, as well as the predicted Cx32 dimer migrating at approximately 54 kDa. Specificity was confirmed by peptide competition and by qualitative observations of target protein oligomerization upon heating in sodium dodecyl sulfate (SDS), a defining characteristic of connexin proteins (Hertzberg, 1985; Goodenough et al., 1988). However, the ultimate negative control for any immunogenic protein analysis lies in the examination of samples from a null-mutant animal. The Cx32 null-mutant mouse, generated by the Willecke laboratory, has greatly facilitated the investigation of Cx32 localization and function (Nelles et al., 1996b). This control has confirmed that Cx32 is predominantly expressed in myelinating glia (oligodendrocytes and Schwann cells) of the CNS and peripheral nervous system (Scherer et al., 1995; Dermietzel et al., 1997; Li et al., 1997; Altevogt et al., 2002; Melanson-Drapeau et al., 2003a; Nagy et al., 2003a).

While great care has been taken to ensure antibody specificity in tissues with high levels of target connexin expression (i.e., specific

detection of Cx32 in liver, Cx45 in heart), few studies have assessed the potential for cross-reactivity in the CNS wherein an extensive repertoire of connexins is expressed in different cell types (Traub and Willecke, 1982; Nagy et al., 2003b). Unpublished data from our laboratory and anecdotal reports from other groups have detected a 27-32 kDa anti-Cx32 reactive band in murine brain and spinal cord homogenates of Cx32-null animals by Western blot analysis using antibodies that have been repeatedly verified for appropriate immunofluorescent analyses (Melanson-Drapeau et al., 2003a; Nagy et al., 2003a; Nagy et al., 2004). Because laboratories are understandably reticent to publish the appearance of spurious artifacts, these observations have not been systematically evaluated; however the presence of a cross-reactive band, with the same approximate mobility in null-mutant animals, represents an important complication in the analysis of Cx32 by Western analysis following CNS injury.

To address this issue, we compared reactivity of ten commonly used Cx32 antibodies in brain and liver using IB, immunofluorescence (IF), and IP applications. Surprisingly, we found that eight antibodies cross-reacted with a protein present in $Cx32^{Y/-}$ brain but not liver. We show that this cross-reactivity is only observed when proteins were subjected to reducing/denaturing conditions prior to immunodetection. To further distinguish Cx32 from CNS-specific cross-reactive protein(s), we used using sucrose gradient fractionation demonstrating that Cx32 and the cross-reactive protein(s) localize to distinct subcellular compartments and

exhibit a 4 kDa size difference. Finally, combined bioinformatics and molecular approaches provide converging evidence that the cross-reactive protein is likely not another connexin but rather an immature (Golgi-localized) or partially degraded (lysosome-localized) subunit of a larger unidentified protein complex. Together, these data highlight a key concern for the interpretation of changes in Cx32 protein expression in the CNS that can be easily controlled by the choice of methodology and the optimized reagents described in this study.

2.4: Methods

Cx32 Antibodies

Table 2.1 describes the Cx32 antibodies employed, the peptides used to generate each antibody, the antigenic sites within these peptide sequences, the source of each antibody, and the concentrations employed.

$Cx32^{Y/+}$ and $Cx32^{Y/-}$ animals

Cx32 null-mutant breeding pairs (Nelles et al., 1996b), kindly provided by Dr. Klaus Willecke (Universitat Bonn, Germany), were backcrossed for 13 generations into a C57Bl/6 background in our laboratory. Congenic wild-type mice were derived from heterozygote matings. Male mice used in this study were 3-4 months of age at the time

of sacrifice. A total of 15 $Cx32^{Y/+}$ and 15 $Cx32^{Y/-}$ mice were analyzed. Genotyping was confirmed at time of weaning and again at time of sacrifice (Supplemental Fig 2.1). DNA isolated from tail snips was amplified using Primers A, B, and C (A: 5' – TCA TTC TGC TTG TAT TCA GGT GAG AGG CGG – 3', B: 5' – ATA CAC CTT GCT CAG TGG CGT GAA TCG GCA – 3', C: 5' – TCT TAC TCC ACA CAG GCA TAG AGT GTC TGC – 3'). A and B amplified a 750 bp fragment of the $Cx32^{Y/+}$ WT allele, while A and C produced a 1.3 kb fragment indicating the $Cx32^{Y/-}$ KO allele (Supplemental Fig 2.1). Polymerase chain reaction (PCR) amplification was performed on a Whatman Biometra TGradient96 system. Cycling parameters were: 95°C for 10 minutes, followed by 30 cycles of 95°C for 60 seconds, 67°C for 60 seconds, and 72°C for 60 seconds.

Immunoblotting

Brain tissue (encompassing either cerebrum and cerebellum or dissected hippocampus as indicated) was isolated from $Cx32^{Y/+}$, $Cx32^{Y/-}$, $Cx32^{Y/-}Cx29^{-/-}$, and $Cx30^{-/-}$ mice. $Cx29^{-/-}$ mice (Altevogt et al., 2002) were kindly provided by Dr David Paul (Harvard Medical School) and crossed onto a Cx32 null-mutant background in our laboratory. $Cx30^{-/-}$ breeding pairs (Teubner et al., 2003) were obtained through the European Mouse Mutant Archive with the kind assistance of Dr Klaus Willecke. Liver was obtained from the same animals. Human brain from a 67 yr old female

who suffered sudden death due to non-neurological complications was obtained from the Douglas Hospital Research Centre Brain Bank (Montreal, Canada). At autopsy, parahippocampal gyri were removed and flash-frozen in liquid nitrogen without fixation for protein extraction. Post-mortem delay was 17 hours. The hippocampus was dissected from this sample for Western analysis. All tissues were homogenized in fresh RIPA buffer (1% Nonidet P-40, 0.5% sodium deoxycholate, 0.1% SDS, 1 mM NaF, 50 g/ml aprotinin, 1 mM sodium orthovanadate, 1 mg/mL phenylmethylsulfonyl fluoride, 10 mM phosphate buffered saline (PBS) [10 mM phosphate, 154 mM NaCl]) and assayed for protein concentration using a Bio-Rad DC protein assay kit (Bio-Rad, Hercules, CA). Brain and liver samples were diluted in 2X SDS sample buffer (Tris-HCl/SDS pH 6.8, 5% glycerol, 1.67% SDS, 100mM dithiothreitol (DTT), 0.002% bromophenol blue) with 10% β-mercaptoethanol (BME) and solubilized at room temperature (RT) for 30 minutes. All experiments were performed and repeated using 30 µg of hippocampal or whole brain protein and 10 µg of liver protein to allow for comparable signal and exposure times given the differences in abundance of Cx32 protein between liver and brain tissue. Proteins were resolved under reducing/denaturing conditions on 12.5% or 15% (sucrose fractions only) Tris-HCl polyacrylamide gels and transferred onto Immobilon P^{SQ} polyvinylidene fluoride (PVDF) membrane (Millipore, MA) at 100 V for 60 minutes. Membranes were blocked in 5% (w/v) skim milk powder-PBS with 0.1% Tween-20 (blocking buffer) for 1-3 hours and incubated in primary antibody diluted in the same buffer

overnight at 4°C (see Table 1 for working concentrations of all connexin antibodies). Membranes were rinsed twice in 0.1% PBST and twice in blocking buffer for 10 minutes prior to a 1-3 hour incubation in horseradish peroxidase (HRP)-conjugated anti-mouse or anti-rabbit (Jackson ImmunoResearch Laboratories, Inc., PA; 1:2000 and 1:5000) secondary antibody diluted in blocking buffer. Signal was detected on X-ray film using SuperSignal West Pico Chemiluminescent Substrate (Pierce, IL).

Immunofluorescence

Male mice ($Cx32^{Y/+}$ and $Cx32^{Y/-}$) were anesthetized with Euthansol (65 mg/mL) and intracardially perfused with 10 mM PBS (pH 7.2) followed by 3.7% molecular grade paraformaldehyde (Sigma) in 10 mM PBS diluted immediately prior to use. Brain and liver were removed and post-fixed for 24 hours at 4°C in the same fixative followed by 48 hours of cryoprotection in 20% sucrose solution containing 0.001% sodium azide at 4°C. Serial cryostat sections (10 mm) were obtained (Leica Microsystems Inc.). Sections were immunoreacted with anti-Cx32 primary antibodies (Table 2.1) diluted in antibody buffer (Ab buffer) (10mM PBS, 0.3% Triton-X100, 3% bovine serum albumin (BSA)). Optimal concentrations were determined by serial dilution on both liver and brain sections with the antibody concentration giving the most robust signal employed for the rest of the study. Where antibodies were not reactive or showed cross-reactivity on brain tissue, the optimal concentration determined using liver

cryosections was employed. Secondary antibodies used were Cy3- or FITC- conjugated anti-mouse IgG (diluted 1:800 and 1:400 respectively) and Cy3- or FITC- conjugated anti-rabbit IgG (1:600, 1:100, Jackson ImmunoResearch Laboratories, Inc., PA). Details are as described in Melanson-Drapeau et al. (2003). Sections were coverslipped in 0.05% p-phenylenediamine in PBS/glycerol, pH 8.0 and imaged by epifluorescent microscopy using OpenLab 5.0.2 (Improvision) on a DMXRA2 epifluorescent microscope (Leica Microsystems Inc.).

Immunoprecipitation

Cx32-coupled protein G agarose beads were prepared as follows: One mL of protein G agarose bead slurry (1:1 PBS; Roche, Germany) was incubated with 25 µg of AB1 (Table 2.1) overnight at 4°C. The beads were washed with 10 mL of 0.1 M borate buffer (pH 9.0) and resuspended in 10 mL of the same buffer. AB1 was chemically coupled to the protein G beads by the addition of solid dimethylpimelimidate (DMP) (Pierce, IL) to a final concentration of 20 mM. Beads were incubated for 30 minutes at RT. The reaction was stopped by washing the beads twice with 0.2 M ethanolamine. Beads were resuspended in 10 mL of 0.2 M ethanolamine and incubated at RT for 2 hours, followed by two washes with 10 mL of PBS. Beads were resuspended in 1 mL PBS and stored at 4°C.

Human and mouse hippocampal and brain lysates as well as mouse liver lysates were prepared for Western analyses in RIPA buffer with fresh protease inhibitors and assayed for protein concentration.

Protein lysates were diluted to 100 µg in 200 µL volumes for preclearing with 50 µL of uncoupled protein G agarose beads for 1 hour at 4°C. Precleared lysates were added to 50 µL of prepared AB1-coupled beads and incubated overnight at 4°C. Beads were washed twice in RIPA buffer and three times in PBS. Proteins were eluted from the IgG molecules at RT for 30 minutes with inversion in 200 µL of ammonium hydroxide elution buffer (0.5 M NH_4OH, 0.5 mM EDTA). Samples were lyophilized in a SpeedVac and solubilized in 45 µL 2X SDS sample buffer and 5 µl BME at room temperature for 30 minutes. The SDS-solubilized proteins were resolved on 12.5% Tris-HCl polyacrylamide gels, transferred to PDVF membranes, and blotted with polyclonal AB6.

Sucrose Gradient Fractionation

Whole brain and whole liver were extracted from $Cx32^{Y/+}$ and $Cx32^{Y/-}$ mice and immediately frozen in liquid nitrogen. For each experiment, one brain hemisphere or one lobe of liver was homogenized in 1.5 mL PTN buffer (50 mM sodium phosphate, 1% Triton X-100, 50 mM NaCl, 30 µL protease inhibitor cocktail, pH 7.4) using a Teflon Potter-Elvehjem homogenizer fitted to a 30 mL glass tube. Homogenates were incubated on ice for 30 minutes and centrifuged at 16,000 xg for 10 minutes at 4°C. The Triton X-100 soluble supernatant was reserved on ice. One mL of supernatant was mixed with 1 mL 80% sucrose. Samples were carefully overlaid with 1.5 mL 30% sucrose followed by 1.5 mL of 5% sucrose. Prepared tubes were centrifuged at 130,000 xg in an SW-40 Ti

swinging-bucket rotor overnight (18 hours) at 4°C (Beckman 50 Ultra-Clear Tubes [14x95 mm] for rotor; #344060). Gradients were carefully aliquoted (10 fractions at 500 µL each) with fraction 1 being the uppermost, lightest fraction. Protein quantification was performed using the BioRad DC protein assay kit, and samples were analyzed by immunoblotting using AB1 and the fractionation markers coxIV (Molecular Probes [A-21348] 0.4 µg/mL), caveolin-1 (Santa Cruz [SC-894] 1:500), flotillin-1 (BD Transduction Laboratories [610820] 1:1000), syntaxin-1 (Sigma [S0664] 1:2000), LAMP1 (Cell Signalling [C54H11] 1:1000), and golgin-97 (Molecular Probes [A-21270] 1:1000).

Mass spectrometric identification of proteins after western analysis.

Blotting and removal of nitrocellulose (BARN) methodology followed by tryptic digest and mass spectrometry analysis were performed as described in Luque-Garcia et al. (2008) to identify the Cx32 cross-reactive protein under reducing/denaturing conditions. Briefly, 20 µg of liver fractions 4, 5, and 6 from a $Cx32^{Y/+}$ fractionation were resolved in each of eight lanes of a 12.5% SDS-PAGE gel and transferred to a nitrocellulose membrane (Triton-free, pore size 0.2 µm) at 400 mA for 1 hour on ice in transfer buffer (25 mM Tris, 192 mM glycine, 0.1% SDS, 20% methanol). The membrane was blocked with poly(vinylpyrrolidone)-40 (PVP-40) buffer (0.5% w/v PVP in 100 mM acetic acid) for 1 hour at room temperature and rinsed with four changes of PBS (1 minute each) before overnight incubation with AB1 diluted in PBS. Primary antibody was rinsed from the

membrane with four changes of PBS (10 minutes each), and incubated with anti-mouse IgG-HRP secondary antibody diluted in PBS for 1 hour, followed by four rinses in PVP-40 blocking buffer. The membrane was rinsed with four changes of PBS (1 minute each) to remove excess PVP-40 buffer. Chemiluminescent detection was performed as usual except that all surfaces coming into contact with the membrane were washed with 70% ethanol and rinsed with ddH_20 to prevent keratin contamination. The developed film was aligned with the chemiluminescent stain on the membrane to facilitate accurate detection of the Cx32-containing region of the membrane. Each of the eight Cx32-containing bands were excised with #11 scalpel blades and washed three times with 1.5 mL 20 mM sodium bicarbonate buffer (pH 7.4) for 5 minutes each at room temperature. The membrane sections were then washed three times with 1.5 mL 100 mM glycine (pH 2.4) for 10 minutes to remove all traces of antibody before a final 5 minute wash in 1.5 mL 20 mM sodium bicarbonate buffer. The non-specific sites on the membrane sections were blocked with 0.5 mL PVP-40 buffer for 30 minutes at 37°C and rinsed six times with ddH_2O. Trypsin (Promega) prepared in 50 mM NH_4HCO_3 buffer (pH 8) was added at 12.5 ng/µL to the membrane sections and incubated at 37°C overnight. The samples were dried under vacuum and dissolved by vortexing in acetone (90 µL acetone/4 mm^2 nitrocellulose) followed by a 30 minute incubation at room temperature. The acetone containing the nitrocellulose was removed, and the peptides were air-dried

and re-suspended in 20 µL 2% acetonitrile in 0.1% formic acid. LC-MS/MS was used to analyze peptide mixtures derived from these on-membrane digestions as described by (Luque-Garcia et al., 2008) and data were analyzed as in (Lambert et al., 2009).

Epitope Mapping

Three algorithms were used to identify the peptides most likely to raise an immunogenic response within the IL and in the CT domain of Cx32: (1) Antigenic Peptide Tool [Immunomedicine group at Universidad Complutense de Madrid; Kolaskar & Tongaonkar method] and (2) Abie Pro 3.0 [Chang Biosciences; Hopp-Woods and Kyte Doolittle hydrophillicities]. For each prediction tool, the peptide size was set to 8.

2.4: Results

A cross-reactive protein with the same mobility as Cx32 is detected in null-mutant brain but not liver

Protein lysates prepared from murine tissue (liver, brain, and isolated hippocampus) as well as human hippocampus were resolved by SDS-PAGE under reducing conditions. Western analysis was performed using ten different Cx32 antibodies (Table 2.1, Fig 2.1). Five antibodies were directed against epitopes localizing to the IL (Fig 2.1,2.2); five antibodies were directed against epitopes found within the CT tail of Cx32 (Fig 2.1,2.3). Because six of the antibodies tested were raised against

proprietary peptide sequences (Table 2.1), three algorithms (Hopp and Woods, 1981; Kyte and Doolittle, 1982; Kolaskar and Tongaonkar, 1990) were used to identify the peptides most likely to raise an immunogenic response within the targeted region. Three potential antigenic sequences were detected within the IL of Cx32 (Fig 2.2A-E, Table 2.2). Two of these sequences were present in the peptide used to generate AB1. All three sequences were present in AB2 and AB3. Because AB1, AB2, and AB3 are monoclonal antibodies and generated identical banding patterns (Fig 2.2A-C), it is likely that they recognize the same epitope, either the EEVKRHKV or EGHGDPLH/GDPLHLEE antigenic sequences, located towards the CT of the IL encompassed by the peptides used to generate AB1 (Table 2.2). Although the exact peptide sequence used to generate AB4 and AB5 was not disclosed by the manufacturer, both antibodies were distinguished from AB1-3 by a species variation in the doublet detected in human samples (Fig 2.2D). Based on this difference, we hypothesized that they likely detect one of the two potential epitope variants (EGHGDPLH/GDPLHLEE) (Table 2.2). Only polyclonal AB5 demonstrated specificity and thus we hypothesized recognizes the only antigenic sequence that does not overlap with AB1 (i.e., QQHIEKKM)located towards the N-terminus of the intracellular loop (Table 2.2). This analysis predicted that the cross-reactive protein would contain contiguous amino acid sequences, exposed under denaturing/reducing conditions that share the EEVKRHKV and EGHGDPLH/GDPLHLEE but

Table 2.1: Connexin Antibodies

Code	Catalogue Number	Source	Epitope Location[1]	Type[2]	[Western]	[Immuno]
AB1	CX32C13-M	Alpha Diagnostics	IL 110-128	Monoclonal	0.5 µg/mL	1:200
AB2	Hybridoma	David Paul	IL 95-125	Monoclonal	No dilution	No dilution
AB3	MAB3069	Chemicon	IL 95-125	Monoclonal	1:1000	1:100
AB4	13-8200	Zymed	IL[3]	Monoclonal	1:250	1.0 µg/mL
AB5	71-0600	Zymed	IL[3]	Polyclonal	1:125	2.0 µg/mL
AB6	C3470	Sigma	C-term 265-279	Polyclonal	1:200	1:600
AB7	C7854-05E	USBiological	C-term 19aa	Polyclonal	0.7 µg/mL	1:400
AB8	C7854-04	USBiological	C-term	Polyclonal	3.0 µg/mL	1:800
AB9	34-5700	Zymed	C-term[4]	Polyclonal	1:125	1.0 µg/mL
AB10	35-8900	Zymed	C-term[4]	Monoclonal	3.0 ug/mL	1:800
AB11	51-2800 (Cx26)	Zymed	C-term	Polyclonal	1:125	NA
AB12	71-2200 (Cx30)	Zymed	C-term	Polyclonal	1:200	NA

[1]Peptides used to generate each antibody are listed by amino acid position where known (see Figure 1). Position and/or length of the peptides used to generate AB4, AB5, AB7-10 were not disclosed by the manufacturer. Abbreviations: IL, intracellular loop; C-term, C-terminus. [2]All monoclonal antibodies were raised in mouse. All polyclonal antibodies were raised in rabbit. [3]AB4 and AB5 were raised against the same proprietary IL antigen. [4]AB9 and AB10 were raised against the same proprietary C-term antigen. NA, not applicable.

Figure 2.1: Schematic of the transmembrane structure of Cx32 highlighting the position of the peptides used to generate each of the antibodies assessed.
Additional details are provided in Table 2.1.

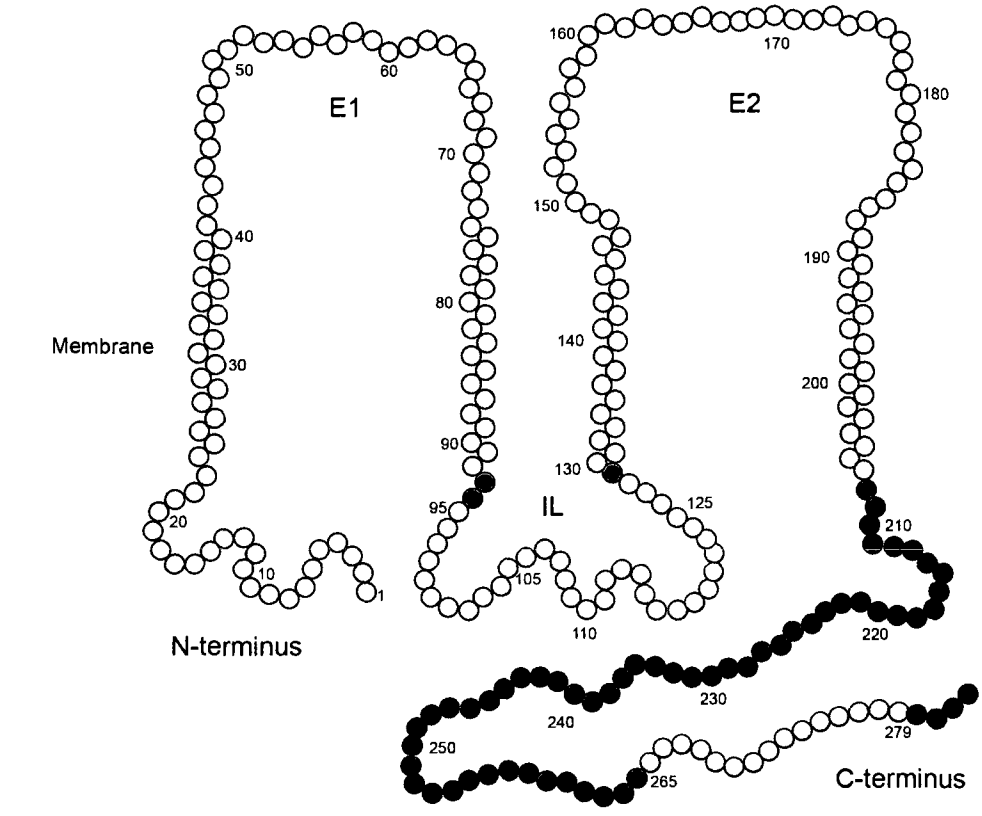

○ Immunogen for AB1
○ ○ Immunogen for AB2, AB3
○ ● ○ ○ Immunogen for AB4, AB5
● ○ Immunogen for AB7, AB8, AB9, AB10
○ Immunogen for AB6

Figure 2.1

Figure 2.2: Four of the five Cx32 antibodies directed against the intracellular loop cross-react with a protein exhibiting the same mobility as Cx32 in $Cx32^{Y/-}$ brain but not $Cx32^{Y/-}$ liver under reducing/denaturing conditions.

(A-E, left panel), Transmembrane schematics of the peptides for each Cx32 antibody with the colored circles representing available information about each immunizing peptide sequence. Black brackets indicate primary sequence with the highest antigenic potential (See Table 2.2). (A-E, right panel), Cx32 immunoblots were performed using 10 µg liver or 30 µg of human (Hu) and murine hippocampus or brain lysates. Lines indicate size markers. Black arrowheads point to Cx32 specifically detected by all antibodies in liver (A-E) and AB5 in brain (E). White arrowheads indicate isoform variations specific to human samples (D,E). Arrows indicate the cross-reactive protein(s) detected by AB1-4 in both $Cx32^{Y/+}$ brain tissue and the $Cx32^{Y/-}$ control (A-D). Note that this particular cross-reactive protein(s) migrates with the same mobility as Cx32 when separated on 12.5% Tris-HCl polyacrylamide gels.

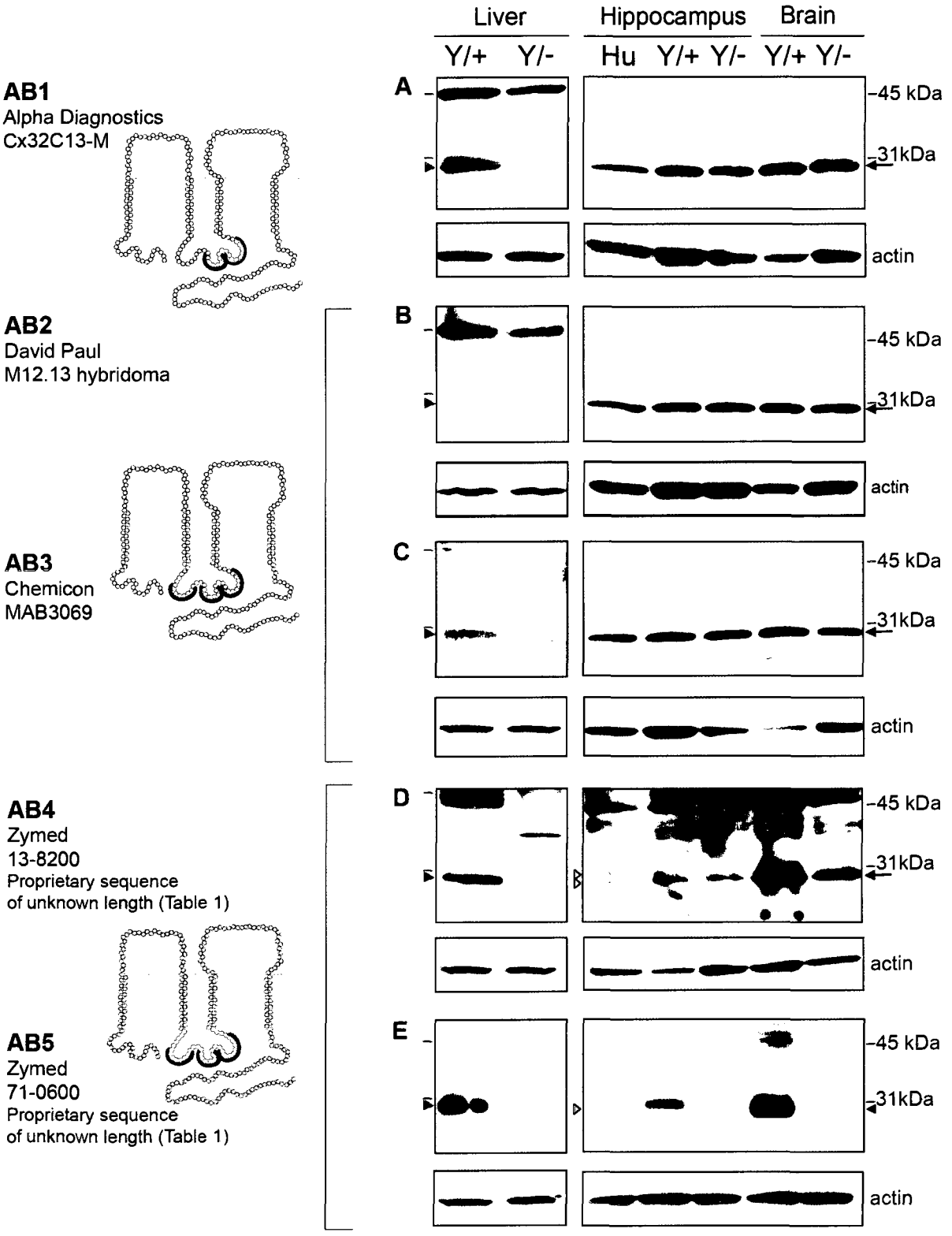
AB1
Alpha Diagnostics
Cx32C13-M
AB2
David Paul
M12.13 hybridoma
AB3
Chemicon
MAB3069
AB4
Zymed
13-8200
Proprietary sequence
of unknown length (Table 1)
AB5
Zymed
71-0600
Proprietary sequence
of unknown length (Table 1)
Liver
Hippocampus
Brain
Y/+ Y/-
Hu Y/+ Y/-
Y/+ Y/-
A
B
C
D
E
-45 kDa
-31kDa
actin

Figure 2.2

Figure 2.3: Four of the five Cx32 antibodies directed against the C-terminal tail cross-react with a protein exhibiting the same mobility as Cx32 in $Cx32^{Y/-}$ brain but not $Cx32^{Y/-}$ liver under reducing/denaturing conditions.

As in Figure 2.2, lines indicate size markers. Closed arrowheads point to Cx32 specifically detected by all antibodies in liver (A-E) and AB10 in brain (E). White arrowheads indicate isoform variations specific to human samples (C-E). Arrows indicate the cross-reactive protein(s) detected by AB6-9 in both $Cx32^{Y/+}$ brain tissue and the $Cx32^{Y/-}$ control (A-D). Note that this particular cross-reactive protein(s) migrates with the same mobility as Cx32 when separated on 12.5% Tris-HCl polyacrylamide gels. All other details are as in Figure 2.2.

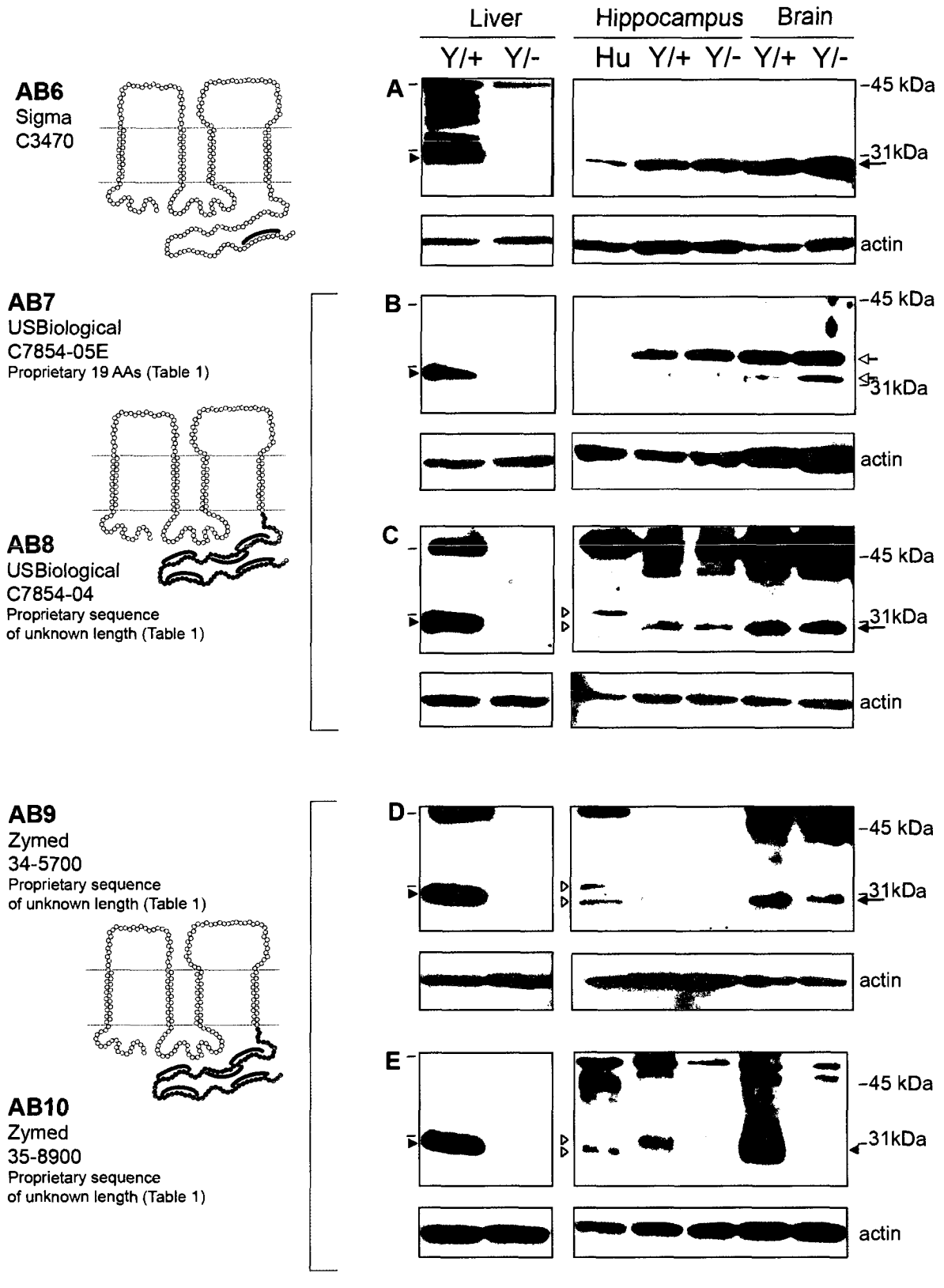
Liver
Hippocampus
Brain
Y/+ Y/-
Hu Y/+ Y/-
Y/+ Y/-
AB6
Sigma
C3470
A
-45 kDa
-31kDa
actin
AB7
USBiological
C7854-05E
Proprietary 19 AAs (Table 1)
B
-45 kDa
-31kDa
actin
AB8
USBiological
C7854-04
Proprietary sequence
of unknown length (Table 1)
C
-45 kDa
-31kDa
actin
AB9
Zymed
34-5700
Proprietary sequence
of unknown length (Table 1)
D
-45 kDa
-31kDa
actin
AB10
Zymed
35-8900
Proprietary sequence
of unknown length (Table 1)
E
-45 kDa
-31kDa
actin

Figure 2.3

Table 2.2: Antigenic sites along the IL and CT of the Cx32 protein

	Site (aa's)[1]	Sequence	Hopp-Woods	Kyte-Doolittle	Kolaskar & Tongaonkar
IL epitopes	118-125	EEVKRHKV	✔	✔	
	98-105	QQHIEKKM	✔	✔	
	109-116 (112-119)	EGHGDPLH	✔	✔	✔ (GDPLHLEE)
CT epitopes	220-227	AQRRSNPP	✔	✔	
	225-232	NPPSRKGS	✔	✔	
	239-246 (235-242)	SPEYKQNE	✔	✔	✔ (FGHRLSPE)
	252-259	SEQDGSLK	✔	✔	
	271-278	GLAEKSDR	✔	✔	

[1]Sites are listed from most to least likely to raise an antibody response determined using three different bioinformatic tools: (1) Antigenic Peptide Tool [Immunomedicine group at Universidad Complutense de Madrid; Kolaskar & Tongaonkar method]; (2) Abie Pro 3.0 [Chang Biosciences; Hopp-Woods and Kyte Doolittle hydrophilicities]. Abbreviations are as in Table 2.1.

not the QQHIEKKM epitopes with Cx32.

In the CT of Cx32, five potentially antigenic sequences were detected (Fig 2.3A-E, Table 2.2). Polyclonal AB6 (Fig 2.3A) was directed against a known sequence that encompassed the most distal CT antigen (GLAEKSDR, Table 2.2). Polyclonal AB7 generated a pattern distinct from all of the other reagents and thus likely recognizes epitope(s) distinct from AB6 (Fig 2.3B). AB8 and AB9 detected a doublet in human brain samples and thus likely recognize the same species-specific antigenic sequences (Fig 2.3C,D). AB10 was Cx32-specific and, as a monoclonal antibody, is raised against a single epitope (Fig 2.3E). Based on this pattern, we predicted that the cross-reactive protein would contain, in addition to the epitopes recognized by the IL antibodies, contiguous sequences in primary sequence homologous to at least three and likely four of the Cx32 CT epitopes but no significant homology with the fifth predicted antigenic sequences (recognized by Cx32-specific AB10).

Only Cx30 met these criteria. The IL EEVKRHKV epitopes exhibited a significant alignment score of 62% whereas alignment of the EGHGDPLH/GDPLHLEE antigenic sequences met the minimum number of adjacent amino acids required to raise an antigenic response (contiguous alignment score of 25). Further, as predicated, the QQHIEKKM epitope was not found in the Cx30 primary sequence (alignment score of 12%). Four of the five Cx32 C-terminal tail epitopes produced significant alignment scores of 25-62. The fifth epitope NPPSRKGS did not exhibit any significant alignment in contiguous

sequence (≤12%). Despite this potential homology, stringent testing with null-mutant controls provided conclusive evidence that Cx32 antibodies do not cross-react with Cx30 (Fig 2.8).

In immunoblots of rat liver lysates, Cx32 migrates with a mobility of approximately 27 kDa under reducing/denaturing conditions (Paul, 1986a). As expected, this same pattern was detected in murine liver (Fig 2.2,2.3, Liver). All of the antibodies tested reacted specifically with a protein migrating just below the 31 kDa protein standard that was absent from the $Cx32^{Y/-}$ controls (Fig 2.2,2.3, Liver, closed arrowhead). However, in lysates prepared from either whole brain or dissected hippocampus, seven of the antibodies (AB1-4, AB6,8,9) detected a cross-reactive protein(s) with the same mobility as Cx32 in both $Cx32^{Y/+}$ and $Cx32^{Y/-}$ samples (Fig 2.2A-D, Fig 2.3A,C,D, arrow). Some species variation in reactivity was also observed. AB4 (Fig 2.2D, open arrowhead), AB8 (Fig 2.3C, open arrowhead) and AB9 (Fig 2.3D, open arrowhead) detected a doublet in human hippocampus, but only one species in murine brain/hippocampus. However, this single species was also evident in $Cx32^{Y/-}$ samples (Fig 2.2D, 2.3C,D, arrow). AB7 detected a doublet that migrated above the 31 kDa marker in all murine CNS samples (Fig 2.3B, open arrow) but failed to react with human protein (Fig 2.3B).

Only AB5 and AB10 detected Cx32 specifically in brain tissue (Fig 2.2E, Fig 2.3E closed arrowhead). Some species variations were again observed in that the human protein appeared to migrate faster than murine Cx32 in hippocampal lysates (Fig 2.2E, open arrowhead), possibly as a

doublet (Fig 2.3E, open arrowheads). The Cx32-specific signal detected using AB5 and AB10 was more abundant in lysates prepared from whole brain (and thus enriched in protein isolated from myelinated fibre tracts containing Cx32-expressing oligodendrocytes) than in hippocampal lysates (Fig 2.2E, 2.3E, compare murine brain to hippocampus). This expression pattern is consistent with the expected localization of Cx32. Conversely, the signal intensity of the cross-reactive protein was comparable across samples (Fig 2.2A-D, 2.3A-D, arrow).

Cx32 immunofluorescent analysis is not confounded by cross-reactivity with other proteins in murine brain.

To test whether this tissue-specific cross-reactivity is also detected *in situ*, immunofluorescent analysis of fixed 10 μm liver and brain cryosections was performed. As expected, all ten of the antibodies detected Cx32 at hepatocyte plasma membrane in $Cx32^{Y/+}$ liver tissue, with minimal to no background reactivity in the $Cx32^{Y/-}$ controls (Fig 2.4A-E, 2.5A-E, Liver, arrows) with the exception of low level labeling of rare hepatocyte membranes with AB5 (Fig 2.5E, Liver, arrowhead). Some of the antibodies detected intracellular pools of Cx32 in addition to robust immunostaining at the membrane (AB2, AB7, and AB9) (Fig 2.4B, 2.5B,D, Liver). None of the antibodies exhibited significant cross-reactivity with $Cx32^{Y/-}$ brain tissue (Fig 2.4A-E, 2.5A-E, $Cx32^{Y/-}$ hippocampus) with the possible exception of AB6 at the highest concentration tested (Fig 2.5A). Each reagent was examined over a minimum of three concentrations.

Figure 2.4: Specific immunofluorescent detection of Cx32 in liver and brain using intracellular loop-directed antibodies.

All five antibodies directed against epitopes localizing to the Cx32 IL detected Cx32 at hepatocyte plasma membrane in $Cx32^{Y/+}$ liver tissue (arrows, inset, Liver), with minimal to no background reactivity in the $Cx32^{Y/-}$ controls. Four antibodies detected fixed protein *in situ* in $Cx32^{Y/+}$ mouse hippocampal sections (A,B,D, and E) with AB5 providing the most robust signal (D). Hippocampal immunostaining was evident at the plasma membrane of cells with the expected oligodendrocyte and/or oligodendrocyte precursor cell morphology (arrows, inset, Hippocampus). None of the antibodies exhibited significant cross-reactivity with $Cx32^{Y/-}$ brain tissue. Abbreviations: GrDG, granule cell layer of the dentate gyrus; PMNL, polymorphonuclear layer of the dentate gyrus; CA3c, CA pyramidal cell field 3c of the hippocampus. Scale bars, 50μm.

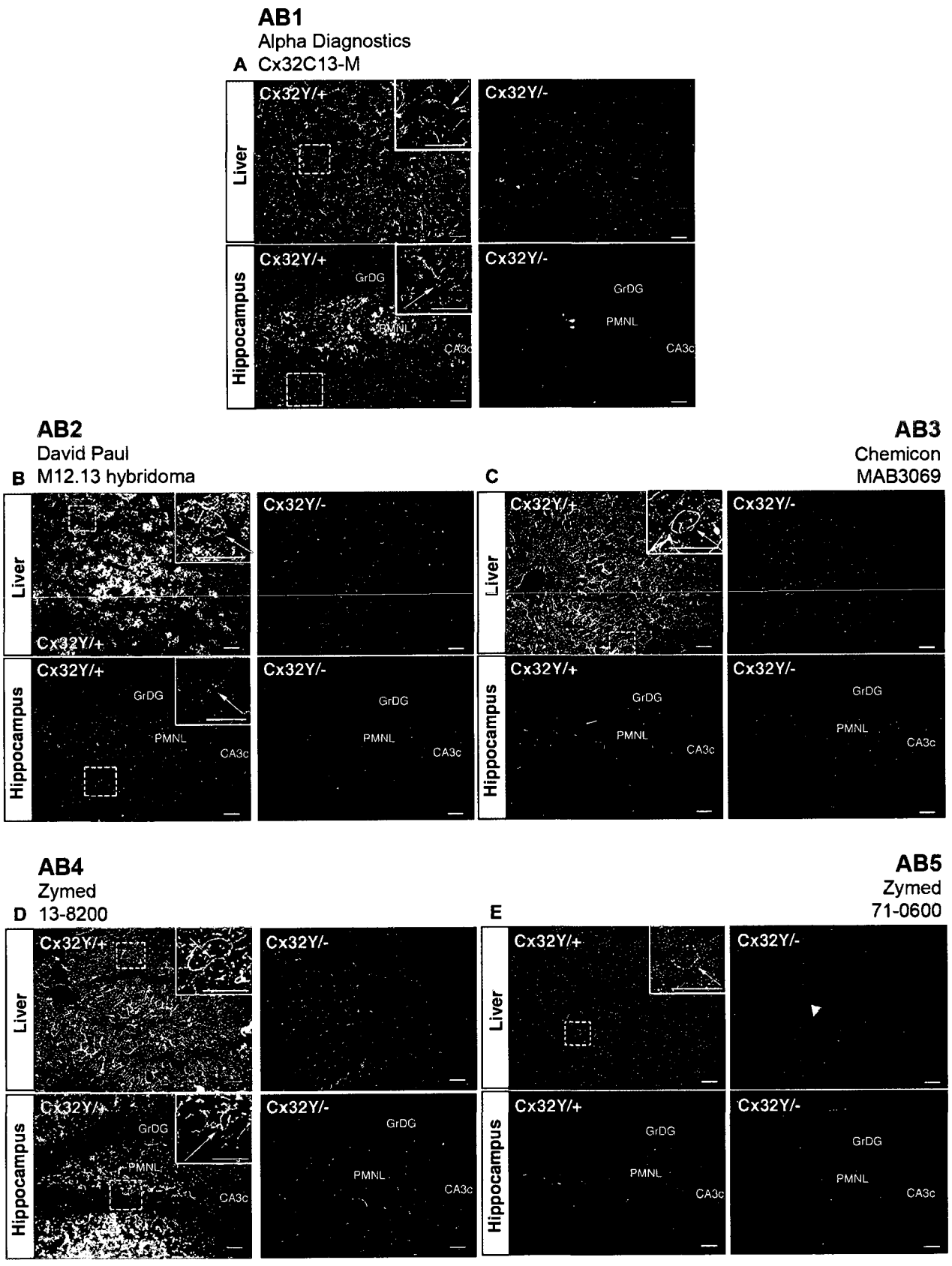
AB1
Alpha Diagnostics
A Cx32C13-M
Liver
Hippocampus
Cx32Y/+
Cx32Y/-
GrDG
PMNL
CA3c
AB2
David Paul
B M12.13 hybridoma
AB3
Chemicon
C
MAB3069
AB4
Zymed
D 13-8200
AB5
Zymed
E
71-0600

Figure 2.4

Figure 2.5: Specific immunofluorescent detection of Cx32 in liver but not brain using CT-directed antibodies.

(A-E) All five C-terminal antibodies detected Cx32 at hepatocyte plasma membrane in $Cx32^{Y/+}$ liver tissue (arrows, inset, Liver), with minimal to no background reactivity in the $Cx32^{Y/-}$ controls. No specific immunosignal was seen in the $Cx32^{Y/+}$ hippocampus under the specific fixation and processing conditions employed in this study. Abbreviations are as in Figure 2.4. Scale bars, 50 μm.

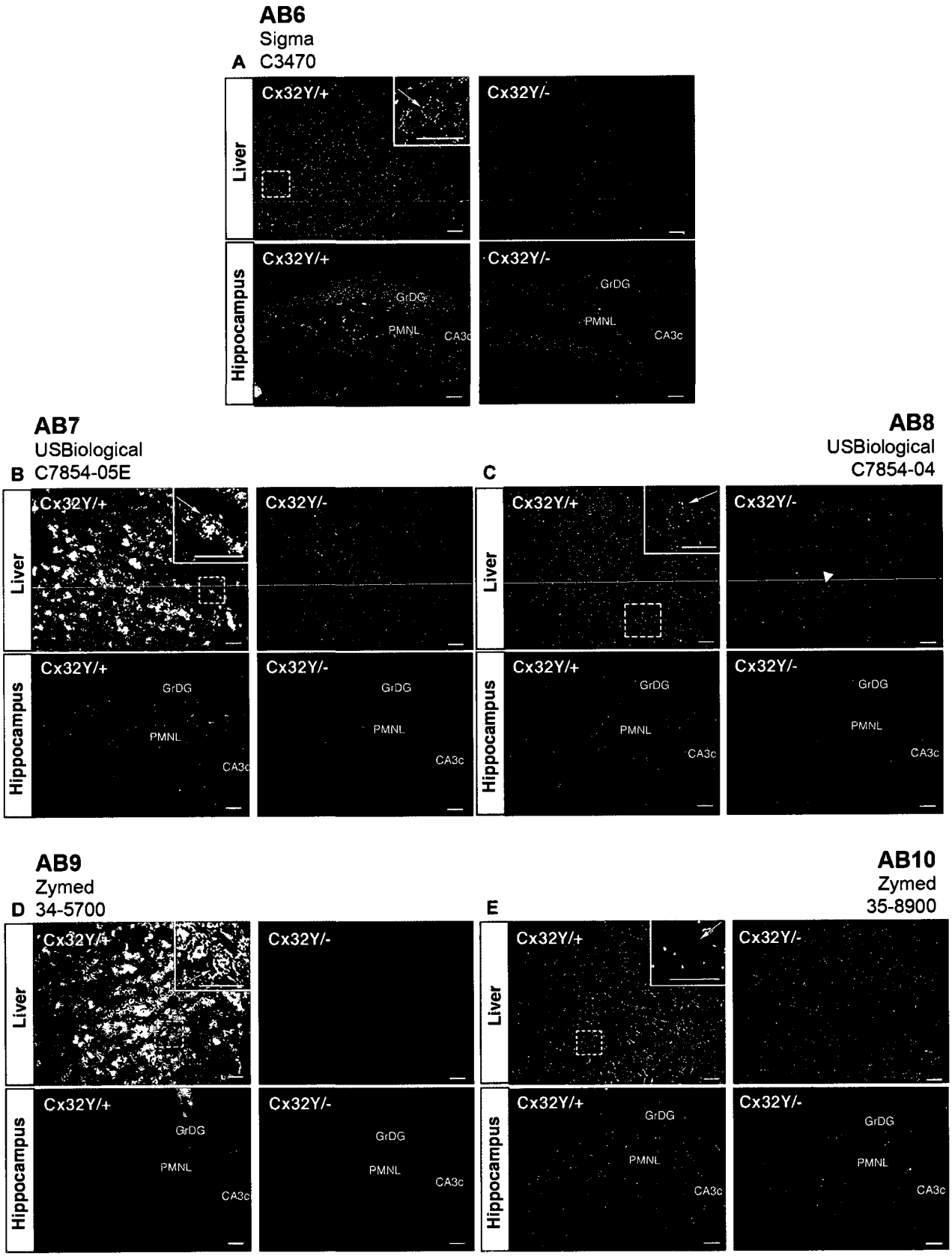
AB6
Sigma
A C3470
Liver
Hippocampus
Cx32Y/+
Cx32Y/-
GrDG
PMNL
CA3c
AB7
USBiological
B C7854-05E
AB8
USBiological
C7854-04
C
AB9
Zymed
D 34-5700
AB10
Zymed
35-8900
E

Figure 2.5

The dilution that gave optimal signal in brain sections is presented in Fig 2.4 and Table 2.1. Where specific signal was not detected in hippocampus (Fig 2.4C, Fig 2.5) or corpus callosum (not shown), the dilution optimal for detection of Cx32 in liver sections is shown (Table 2.1, Fig 2.4,2.5). Four of ten antibodies tested (AB1, AB2, AB4, and AB5) reliably detected fixed protein *in situ* in mouse hippocampal sections (Fig 2.4A,B,D,E $Cx32^{Y/+}$ hippocampus) under the perfusion, post-fixation, and cryoprotection protocol employed here with AB4 providing the most robust signal (Fig 2.4D). All of these antibodies were directed against epitopes localizing to the IL of Cx32. Immunostaining was evident at the plasma membrane of cells with the expected oligodendrocyte and/or oligodendrocyte precursor cell morphology (Fig 2.4A,B,D,E $Cx32^{Y/+}$ hippocampus). None of the CT-directed antibodies produced a specific immunosignal under the fixation protocol defined in the Materials and Methods (Fig 2.5A-E, $Cx32^{Y/+}$ hippocampus). Moreover, AB6 exhibited some artifactual labeling of neurons in both $Cx32^{Y/+}$ and $Cx32^{Y/-}$ sections (Fig 2.5A, compare labeling in the GrDG).

Cross-reactivity is not observed when tertiary structure is maintained during initial detection.

Taken together, these results suggested that cross-reactivity is primarily detected in CNS tissue under denaturing/reducing conditions. These data led us to hypothesize that antibody cross-reactivity was dependent upon protein conformation. To test this hypothesis, the tertiary

conformation of Cx32 was maintained during IP before being subjected to denaturing/reducing conditions in IB detection. This approach restored specific detection of Cx32 in brain tissue (Fig 2.6A, Hippocampus and Brain, arrow). No cross-reactivity was observed in $Cx32^{Y/-}$ samples (Fig 2.6A). Mobility was consistent with that observed in liver lysate controls subjected to IB only (Fig 2.6A, Liver, arrow). To further confirm that this specificity was conformation-dependent, aliquots of the same protein samples used in the IPs (Fig 2.6A) were analyzed by IB (Fig 2.6B). Fig. 2.6B reiterates the presence of a cross-reactive species in $Cx32^{Y/-}$ brain lysates immunoblotted under reducing/denaturing conditions.

The brain-specific cross-reactive protein(s) is expressed at higher levels than endogenous Cx32 and exhibits a distinct subcellular localization.

While demonstrating that Cx32 can be detected specifically in brain tissue by IP, this finding also limited our capacity to identify cross-reactive CNS protein(s) by standard proteomic protocols. As an alternative, we attempted BARN to identify proteins present in the anti-Cx32 immunoreactive bands under reducing/denaturing conditions (Luque-Garcia et al., 2008). We were, however, unable to detect Cx32 from on-membrane digestions of $Cx32^{Y/+}$ liver samples despite successful identification of other co-migrating proteins (data not shown). As such, we lacked the appropriate positive control required to apply this profiling approach to identify the anti-Cx32-reactive proteins in $Cx32^{Y/+}$ and $Cx32^{Y/-}$

Figure 2.6: Brain-specific cross-reactivity is not observed following immunoprecipitation.

(A) Cx32 lysates were purified from native RIPA lysates using monoclonal AB1, resolved under denaturing conditions by SDS-PAGE, and immunoblotted using polyclonal AB6. In the first two lanes WT ($Cx32^{Y/+}$) and null-mutant ($Cx32^{Y/-}$) liver lysates were subjected to Western analysis under reducing/denaturing conditions. The following three lanes represent human hippocampus and murine brain samples from WT ($Cx32^{Y/+}$) and null-mutant ($Cx32^{Y/-}$) controls immunoprecipitated with AB1 under native conditions before denaturing/reducing SDS-PAGE separation and immunoblotting with AB6. Specific immunoaffinity purification of Cx32 is observed under these conditions. (B) Standard Western analysis with aliquots of the same samples used in (A) reiterate the cross-reactivity observed when protein is first detected under reducing/denaturing conditions.

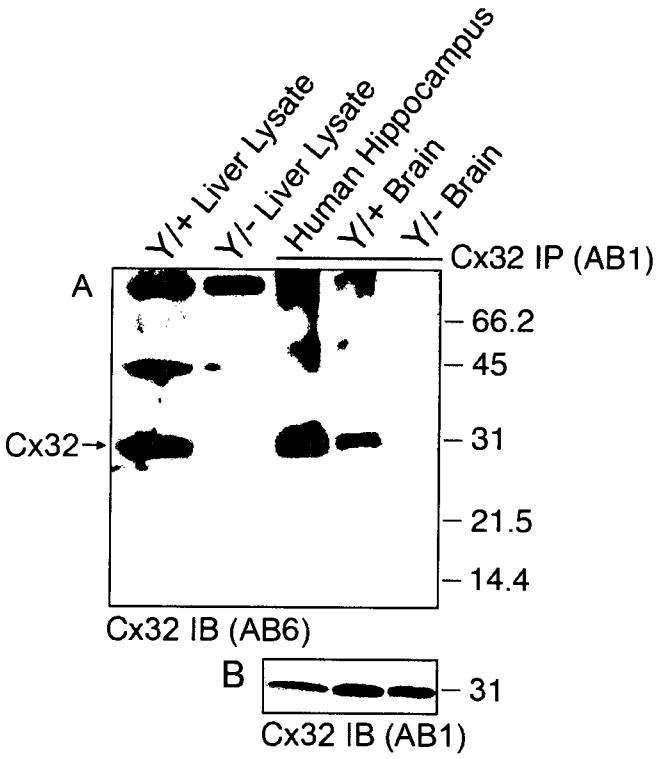
Y/+ Liver Lysate
Y/- Liver Lysate
Human Hippocampus
Y/+ Brain
Y/- Brain
Cx32 IP (AB1)
A
66.2
45
Cx32
31
21.5
14.4
Cx32 IB (AB6)
B
31
Cx32 IB (AB1)

Figure 2.6

brain samples.

We turned to an analysis of AB1-reactive proteins under denaturing/reducing conditions using sucrose flotation gradients (Fig 2.7). In $Cx32^{Y/+}$ liver lysates, a single immunoreactive band was detected in the Triton X-100 insoluble pellet (Fig 2.7A, P) and fractions 4-6 (Fig. 2.7A, fractions 4-6). This distribution reflected predominant localization to detergent-insoluble and detergent-soluble lipid raft and plasma membrane fractions and possibly to mitochondria. No reactivity was detected in any of the fractions derived from control $Cx32^{Y/-}$ lysates (Fig 2.7B). Artifactual labeling was evident in $Cx32^{Y/+}$ and $Cx32^{Y/-}$ brain samples, as demonstrated in Fig 2.2 and 2.3, but with a detectable difference that could be used to distinguish specific Cx32 signal. Using a 15% SDS-PAGE gel (as compared to 12.5% gels presented in Fig 2.2 and 2.3), a reproducible difference in mobility was evident between brain and liver samples (Fig 2.7A, B). A single AB1 immunoreactive band was present in brain lysates (Fig 2.7A, Brain) migrating approximately 4 kDa faster than in liver lysates (Fig 2.7A, Liver). Following sucrose gradient fractionation of brain protein, this predominant species was evident in both $Cx32^{Y/+}$ and $Cx32^{Y/-}$ lysates (Fig 2.7C,D) but could be distinguished from a less abundant higher molecular weight species (Fig 2.7C, arrow) migrating at approximately the same position as liver-derived Cx32 (compare Fig 2.7A and 2.7C). This band was absent from $Cx32^{Y/-}$ fractions (Fig 2.7D). The fractions enriched for the higher molecular weight Cx32-specific band (fractions 4, 5, and 6) were also enriched for the mitochondrial marker

Figure 2.7: Sucrose gradient fractionation reveals that the brain-specific cross-reactive protein is approximately 4 kDa smaller than Cx32 and exhibits a distinct subcellular localization.

(A-D) Total tissue lysates (T) or the Triton X-100 insoluble pellet (P) and (E) fractions 1-10 obtained through sucrose fractionation were immunoblotted under denaturing/reducing conditions using AB1. To achieve maximal separation, proteins were separated on 15% Tris-HCl polyacrylamide gels. Each lane contains 5 µg of protein. (A) Sucrose gradient fractions of $Cx32^{Y/+}$ liver are compared to total tissue lysates of $Cx32^{Y/+}$ liver or brain. Note the ~ 4 kDa size difference between the species predominating in $Cx32^{Y/+}$ liver compared to brain. (B) Sucrose gradient fractions of $Cx32^{Y/-}$ liver are compared to total tissue lysates of $Cx32^{Y/+}$ liver or brain. No signal was detected in $Cx32^{Y/-}$ control lysates. (C) Sucrose gradient fractions of $Cx32^{Y/+}$ brain are compared to total brain lysates prepared from $Cx32^{Y/+}$ and $Cx32^{Y/-}$ mice (top panel). Exposure times were extended from that shown in A and B to enable detection of endogenous Cx32 in fractions 4 and 5 (arrow), migrating 4 kDa higher than the cross-reactive protein that was present at higher abundance and enriched in fractions 6-10. Lower panels characterize each fraction using organelle-specific markers: mitochondria (coxIV), lipid rafts (Caveolin-1 and Flotillin-1), plasma membrane (Syntaxin-1), lysosomes (LAMP-1) and the trans-golgi network (Golgin-97). The fractionation of liver tissue exhibited the same pattern of organelle-specific immunoreactivity (Chapter 3; Fig. 3.3). (D) Only the lower molecular weight cross-reactive band was present in sucrose gradient fractions prepared from $Cx32^{Y/-}$ mouse brain. (E) Schematic of the sucrose fractionation showing the gradients enriched for Cx32 in both brain and liver.

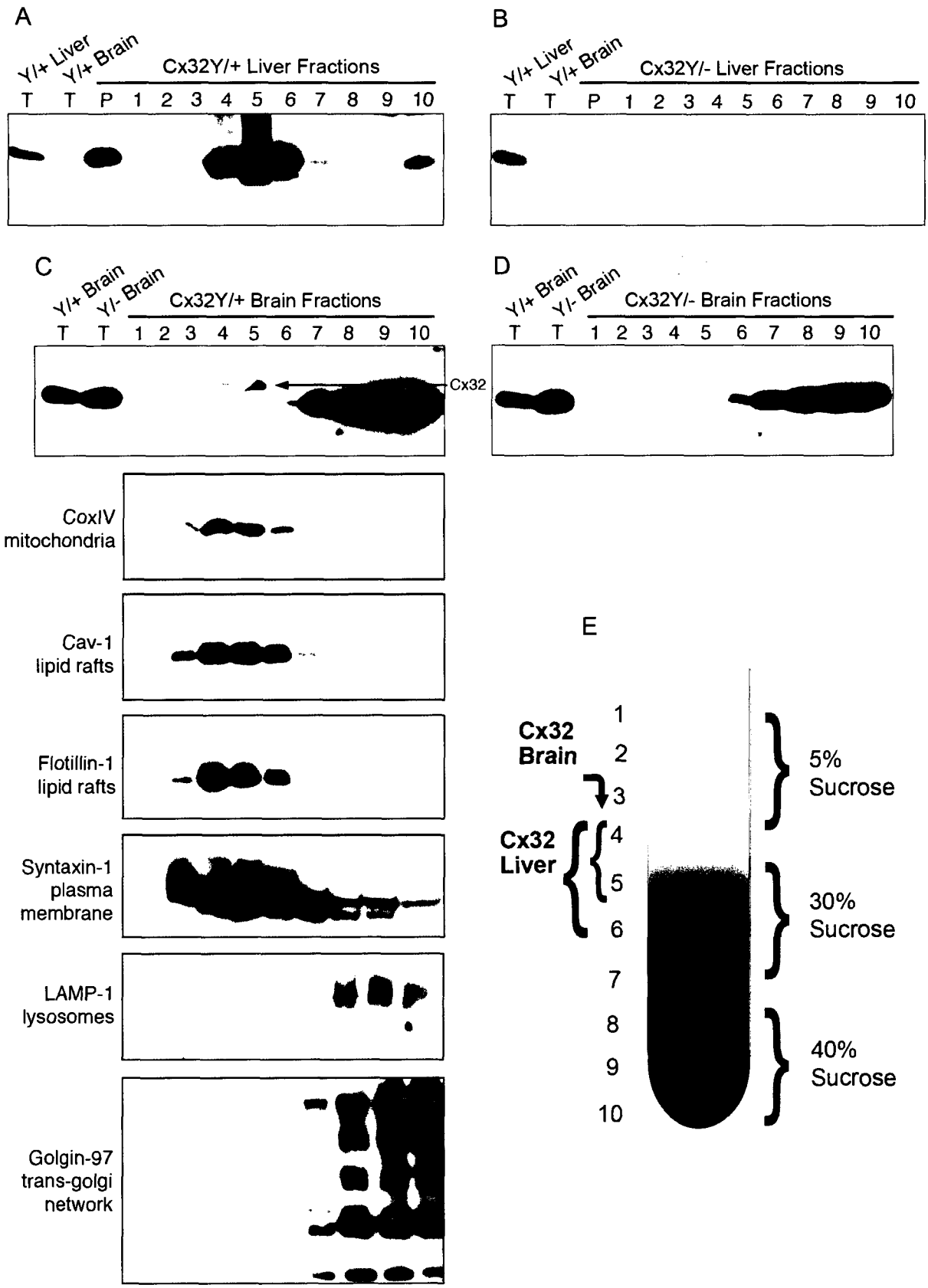
A
Y/+ Liver
Y/+ Brain
Cx32Y/+ Liver Fractions
T T P 1 2 3 4 5 6 7 8 9 10
B
Y/+ Liver
Y/+ Brain
Cx32Y/- Liver Fractions
T T P 1 2 3 4 5 6 7 8 9 10
C
Y/+ Brain
Y/- Brain
Cx32Y/+ Brain Fractions
T T 1 2 3 4 5 6 7 8 9 10
Cx32
D
Y/+ Brain
Y/- Brain
Cx32Y/- Brain Fractions
T T 1 2 3 4 5 6 7 8 9 10
CoxIV
mitochondria
Cav-1
lipid rafts
Flotillin-1
lipid rafts
Syntaxin-1
plasma
membrane
LAMP-1
lysosomes
Golgin-97
trans-golgi
network
E
Cx32
Brain
Cx32
Liver
1
2
3
4
5
6
7
8
9
10
5%
Sucrose
30%
Sucrose
40%
Sucrose

Figure 2.7

coxIV, both lipid-raft associated protein markers caveolin-1 and flotillin-1, and the plasma membrane marker syntaxin-1 (Fig 2.7C). This subcellular fractionation matched that observed in liver (Fig 2.7A). Conversely, the fractions enriched for the smaller cross-reactive protein (fractions 7-10) in both $Cx32^{Y/+}$ and $Cx32^{Y/-}$ lysates (Fig 2.7C,D) were enriched for LAMP-1 (lysosomes) and golgin-97 (trans-golgi network) (Fig. 2.7C). Together, these data suggested that brain, but not liver, tissue expresses Cx32 at both plasma and perhaps mitochondrial membranes, as well as a cross-reactive protein enriched in the golgi apparatus and lysosomes that is ~4 kDa smaller than Cx32.

Bioinformatic and western analyses suggest that the cross-reactive protein is not another connexin

We were surprised that antibodies directed at both the IL and the CT of Cx32 exhibited the same cross-reactivity. To address this, we used a bioinformatics approach to identify candidate proteins based on the pattern of cross-reactivity detected in Figs 2.2 and 2.3, the antigenic sites predicted in Table 2.2, and the tissue-specific expression pattern. This analysis predicted that the cross-reactive protein(s) would contain contiguous amino acid sequences, exposed under denaturing/reducing conditions, that share the EEVKRHKV and EGHGDPLH/GDPLHLEE epitopes (recognized by AB1-4) but not the QQHIEKKM (recognized by Cx32-specific AB5) epitope found within the IL with Cx32 as well as at least three and likely four of the Cx32 CT epitopes (recognized by AB6-9)

but no significant homology with the fifth predicted antigenic sequences (recognized by Cx32-specific AB10).

We used these assumptions to establish search criteria for other connexins with sufficient contiguous antigenic peptide sequences, tissue specificity, and electrophoretic mobility for potential cross-reactivity (Appendix I: Supplemental Methodology). One connexin (Cx30) met all criteria; two other connexins (Cx26 and Cx29) met some but not all parameters. However, direct assessment of lysates prepared from $Cx29^{-/-}$, $Cx29^{-/-}/Cx32^{Y/-}$ or $Cx30^{-/-}$ brain tissue provided conclusive evidence that the cross-reactive protein was still present in double and single null-mutant brain tissue and thus was not Cx29 or Cx30 (Fig 2.8A,B). Further, although Cx26 could be detected abundantly in wild-type mouse liver and, weakly in brain, Cx26 protein levels were substantively reduced in $Cx32^{Y/-}$ brain or liver tissue (Fig 2.8C) and thus Cx26 is unlikely to represent the cross reactive protein. This reduction in Cx26 protein levels in Cx32 null-mutant animals is consistent with previous studies (Nelles et al., 1996).

When placed in context with the subcellular localization evident in sucrose gradient fractionation (Fig 2.7), these data provide converging evidence to indicate that the cross-reactive protein is likely not another connexin but rather an immature (Golgi-localized) or partially degraded (lysosome-localized) subunit of a larger unidentified protein complex with homologous epitopes unmasked only after protein denaturation and the reduction of disulfide bonds.

2.5 Discussion

Here, we characterize a tissue-specific cross-reactivity with multiple commonly used Cx32 antibodies that impacts upon the interpretation of Western blots performed using CNS tissue. While all ten of the reagents tested reliably detect Cx32 in liver as expected, we found that eight of these reagents cross-react with a CNS protein(s) that exhibits the same approximate electrophoretic mobility as Cx32. Comparing IB, IF, and IP detection methods using $Cx32^{Y/+}$ and $Cx32^{Y/-}$ brain and liver tissue, we concluded that this artifactual cross-reactivity is only observed under denaturing/reducing conditions and does not complicate analyses that retain tertiary protein structure during initial immunodetection or immunopurification (i.e., *in situ* IF or IP studies). These data indicate that cross-reactivity is likely the result of the unmasking of epitopes found in primary sequence not accessible *in situ* upon proper protein folding.

Finally, two antibodies, polyclonal AB5 and monoclonal AB10 (Table 2.1), reliably detected Cx32 in Western analysis of brain tissue. These data are consistent with previous reports wherein AB5 and AB10 were shown to specifically recognize Cx32 in brain and liver(Nagy et al., 2003b) emphasizing the need for careful choice of antibody and methodology in the study of Cx32 in brain tissue.

To provide further insight into this tissue-specificity, we identified three highly antigenic sites in the IL and five highly antigenic sites in the CT of the Cx32 protein sequence. Based on these sites and the banding

Figure 2.8. Cx32 antibodies do not cross-react with Cx26, Cx29, or Cx30 under denaturing/reducing conditions.

(A) Liver and brain samples were prepared from wild-type ($Cx32^{Y/+}$), $Cx32^{Y/-}$, $Cx29^{-/-}$. $Cx32^{Y/-}/Cx29^{-/-}$, or $Cx30^{-/-}$ null-mutant mice, separated on 15% Tris-HCl polyacrylamide gels, and immunoblotted for Cx32 using monoclonal AB1. To distinguish between the cross-reactive protein(s) and endogenous Cx32 in brain samples, fraction 5 lysate from sucrose gradient separations (see Fig 2.7) of WT ($Cx32^{Y/+}$) was included as a positive control. All brain samples, except WT brain fraction 5 exhibited the lower molecular weight cross-reactive band. Arrowheads indicate Cx32; arrows indicate the cross-reactive (CR) protein. (B) Immunoblotting of Cx30 in lysates prepared from human brain, wild-type mouse brain and liver, and $Cx30^{-/-}$ brain confirmed the presence of Cx30 in CNS tissue (arrowhead), absent from liver. Specificity was established using null-mutant controls. (C) Cx26 protein, present in $Cx32^{Y/+}$ brain and liver (arrowhead) was below detection levels in $Cx32^{Y/-}$ tissue.

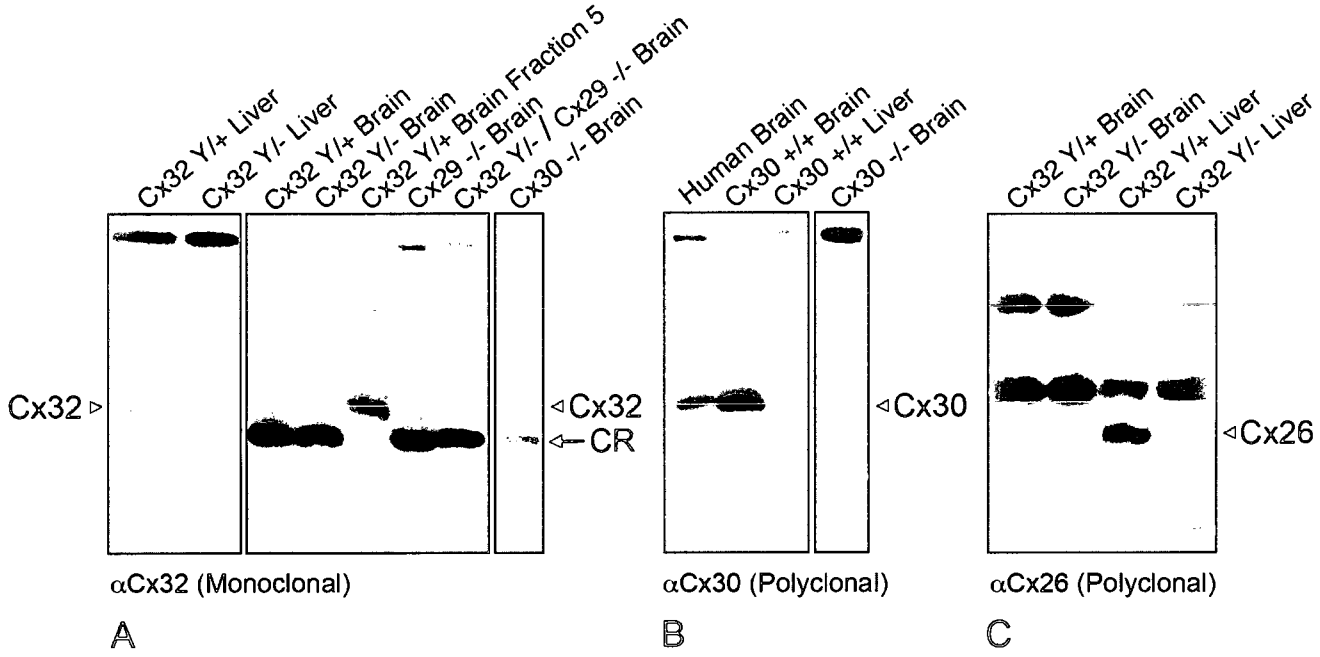
Cx32 Y/+ Liver
Cx32 Y/- Liver
Cx32 Y/+ Brain
Cx32 Y/- Brain
Cx32 Y/+ Brain Fraction 5
Cx29 -/- Brain
Cx32 Y/- / Cx29 -/- Brain
Cx30 -/- Brain
Cx32
Cx32
CR
αCx32 (Monoclonal)
A
Human Brain
Cx30 +/+ Brain
Cx30 +/+ Liver
Cx30 -/- Brain
Cx30
αCx30 (Polyclonal)
B
Cx32 Y/+ Brain
Cx32 Y/- Brain
Cx32 Y/+ Liver
Cx32 Y/- Liver
Cx26
αCx26 (Polyclonal)
C

Figure 2.8

patterns produced by each of antibodies tested in Cx32 null-mutant tissue, we predicted that the primary sequence of the cross-reactive protein(s) would exhibit strict homology to six of these eight antigenic sites but would not contain the two unique epitopes that rendered AB5 and AB10 Cx32-specific. Moreover, the protein would be expressed in brain but not liver. Bioinformatic analyses encompassing all of these criteria identified only one protein, Cx30, with potential to cross-react under denaturing/reducing conditions. However, direct assessment revealed that the brain-specific cross-reactive protein was still present in brain lysates prepared from not only $Cx30^{-/-}$ but also $Cx29^{-/-}/Cx32^{Y/-}$ mice and in the absence of Cx26. Further, sucrose gradient fractionation analyses revealed that the antigenically related cross-reactive protein(s) exhibited an ~4 kDa size difference, localized to different subcellular compartments, and was expressed at higher levels than Cx32 in brain tissue. Cx32 was found in fractions enriched for plasma membrane, lipid rafts, and mitochondrial markers; the brain-specific cross-reactive protein was found in fractions enriched for golgi and lysosome markers. This subcellular localization indicates that the cross-reactive protein is likely not a member of the connexin family.

In summary, this study addresses a CNS-specific problem in Cx32 antibody cross-reactivity that has been reported anecdotally but not analyzed directly. We show that, while all of the reagents tested are specific for Cx32 in liver, protein denaturation/reduction unmasks epitopes present in primary sequence of a CNS-specific protein, likely not another

connexin, that exhibits the same approximate electrophoretic mobility as Cx32 and is present in mouse brain prepared from multiple connexin null-mutants. We show that this technical obstacle can be easily overcome by choice of antibody, careful size analysis, or exclusive use of IP to quantify changes in Cx32 protein expression. These data are presented with the intent of reducing the amount of time laboratories currently expend in validating changes in Cx32 expression in CNS.

2.6 Acknowledgements

We wish to thank Dr Jim Nagy (University of Manitoba) for critical reading of the manuscript and helpful suggestions as to how to further improve immunofluorescent detection of Cx32 *in situ*.

2.7 References

Altevogt BM, Kleopa KA, Postma FR, Scherer SS, and Paul DL (2002). Connexin29 is uniquely distributed within myelinating glial cells of the central and peripheral nervous systems. *J Neurosci.* 22: 6458-6470.

Bruzzone R, White TW, and Paul DL (1996). Connections with connexins: the molecular basis of direct intercellular signalling. *Eur J Biochem.* 238: 1-27.

Dahl E, Manthey D, Chen Y, Schwarz HJ, Chang YS, Lalley PA, Nicholson BJ, and Willecke K (1996). Molecular cloning and functional expression of mouse connexin-30,a gap junction gene highly expressed in adult brain and skin. *J Biol Chem.* 271: 17903-17910.

Dermietzel R, Farooq M, Kessler JA, Althaus H, Hertzberg EL, and Spray DC (1997). Oligodendrocytes express gap junction protein connexin32 and connexin45. *Glia.* 20: 101-114.

Goodenough DA, and Paul DL (2003). Beyond the gap: functions of unpaired connexon channels. *Nat Rev Mol Cell Biol.* 4: 285-294.

Goodenough DA, Paul DL, and Jesaitis L (1988). Topological distrubution of two Connexin32 antigenic sites in intact and split rodent hepatocyte gap junctions. *J Cell Biol.* 107: 1817-1824.

Hertzberg EL (1985). Antibody probes in the study of gap junctional communication. *Annu Rev Physiol.* 47: 305-318.

Hopp TP, and Woods KR (1981). Prediction of protein antigenic determinants from amino acid sequences. *Proc Natl Acad Sci U S A.* 78: 3824-3828.

Kolaskar AS, and Tongaonkar PC (1990). A semi-empirical method for prediction of antigenic determinants on protein antigens. *FEBS Lett.* 276: 172-174.

Kyte J, and Doolittle RF (1982). A simple method for displaying the hydropathic character of a protein. *J Mol Biol.* 157: 105-132.

Lambert JP, Mitchell L, Rudner A, Baetz K, and Figeys D (2009). A novel proteomics approach for the discovery of chromatin-associated protein networks. *Mol Cell Proteomics.* 8: 870-882.

Li J, Hertzberg EL, and Nagy JI (1997). Connexin32 in oliogdendrocytes and association with myelinated fibers in mouse and rat brain. *J Comp Neurol.* 379: 571-591.

Luque-Garcia JL, Zhou G, Spellman DS, Sun TT, and Neubert TA (2008). Analysis of electroblotted proteins by mass spectrometry: protein identification after Western blotting. *Mol Cell Proteomics.* 7: 308-314.

Melanson-Drapeau L, Beyko S, Davé S, Hebb ALO, Franks DJ, Sellito C, Paul DL, and Bennett SAL (2003). Oligodendrocyte progenitor enrichment in the connexin32 null-mutant mouse. *J Neurosci.* 23: 1759-1768.

Nagy JI, Dudek FE, and Rash JE (2004). Update on connexins and gap junctions in neurons and glia in the mammalian nervous system. *Brain Res Brain Res Rev.* 47: 191-215.

Nagy JI, Ionescu AV, Lynn BD, and Rash JE (2003). Connexin29 and connexin32 at oligodendrocyte and astrocyte gap junctions and in myelin of the mouse central nervous system. *J Comp Neurol.* 464: 356-370.

Nakase T, and Naus CC (2004). Gap junctions and neurological disorders of the central nervous system. *Biochim Biophys Acta.* 1662: 149-158.

Nelles E, Buetzler C, Jung D, Temme A, Gabriel HD, Dahl U, Traub O, Stuempel F, Jungermann K, Zielasek J, Toyka KV, Dermietzel R, and Willecke K (1996). Defective propagation of signals generated by sympathetic nerve stimulation in the liver of connexin32-deficient mice. *Proc Natl Acad Sci USA.* 93: 9565-9570.

Paul DL (1986). Molecular cloning of cDNA for rat liver gap junction protein. *J Cell Biol.* 103: 123-134.

Rouach N, Avignone E, Meme W, Koulakoff A, Venance L, Blomstrand F, and Giaume C (2002). Gap junctions and connexin expression in the normal and pathological central nervous system. *Biol Cell.* 94: 457-475.

Scherer SS, Deschenes SM, Xu Y, Grinspan JB, Fischbeck KH, and Paul DL (1995). Connexin32 is a myelin-related protein in the PNS and CNS. *J Neurosci.* 15: 8281-8294.

Senda M, and Natsumeda Y (1994). Tissue-differential expression of two distinct genes for human IMP dehydrogenase (E.C.1.1.1.205). *Life Sci.* 54: 1917-1926.

Sohl G, Maxeiner S, and Willecke K (2005). Expression and functions of neuronal gap junctions. *Nat Rev Neurosci.* 6: 191-200.

Supplemental Figure 2.1: Genotyping for Cx32 WT or null mutant KO allele.

All mice were genotyped at both the time of weaning and time of sacrifice for a 750 bp amplicon generated from the WT allele (Panel B) and a 1300 bp amplicon generated from KO allele (Panel A). Representative genotyping from four of the fifteen null mutant mice (Cx32Y/-) and five of the fifteen WT mice (Cx32Y/+) is shown. NT is the no template control to confirm lack of reagent contamination.

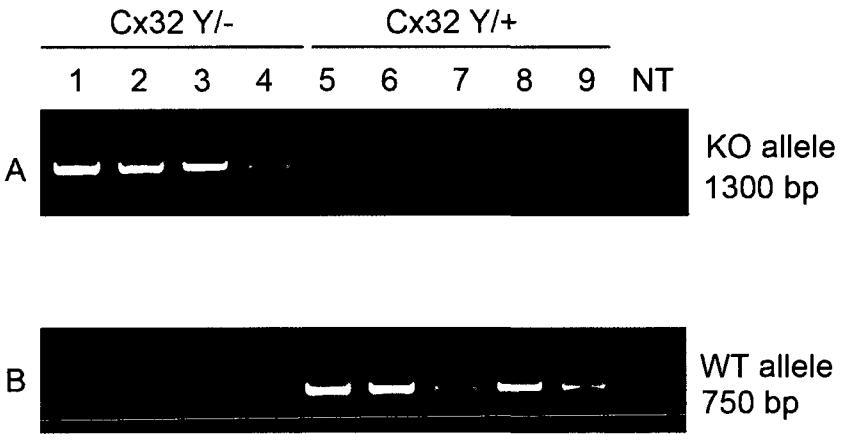

Supplemental Figure 2.1

Chapter 3: Identification of Cx32 interacting proteins: preliminary identification of a novel connexin mitochondrial interactome

3.1: Objectives of this study

Having established that Cx32 can be accurately identified in brain and liver by IP and that protein localizes both to plasma membrane, and possibly mitochondria, the objectives of this study were to (1) validate the potential for protein-protein interactions between Cx32 and other mitochondrial proteins by immunoaffiniity purification and LC-MS/MS, (2) confirm these interactions by co-IF and co-IP, and, in doing so, predict potential channel-independent signalling roles at this subcellular location.

3.2: Statement of author contributions

I am extremely grateful to members of the Ottawa Institute for Systems Biology (OISB) under the guidance of Dr. Figeys and Dr. Kristin Baetz for both methodological guidance and technical assistance. Jean-Phillipe Lambert, Julian Vascilescu, and Leslie Mitchell provided expert advice in the planning stages of these experiments. I was mentored by Jean-Phillipe on band excision from silver stained gels, and training for trypsin digestions and MS sample preparation was provided by Danielle

Dewar-Darch. Danielle also ran and analyzed the samples I prepared, and her technical support has been invaluable.

3.3: Introduction

The use of liver as a starting point for these studies was based on both historical and practical considerations. The idea that intercellular communication exists between many cell types in the body was first introduced and described by Loewenstein and Kanno in the early 1960s (Loewenstein and Kanno, 1967). The study of intercellular junctions began with the salivary glands of *Drosophila* but soon after, hepatocytes of the liver became the cell model of choice due to their large size, stability, and degree of intercellular communication. Thus, the structural components of intercellular junctions were first isolated and cloned from this tissue in the 1970s and 80s (Goodenough, 1974; Kumar and Gilula, 1986; Paul, 1986; Nicholson et al., 1987; Zhang and Nicholson, 1989), and were given the name, "connexin". Cx32 and Cx26 family members make up 90% and 5%, respectively of all the connexin proteins in the liver, with the other 5% being represented by Cx43 in the stellate and Kupffer cells (Cascio et al., 1995; Neveu et al., 1995). Cx32/26 heteromeric gap junctions are abundant in hepatocytes, and are involved in many aspects of liver biology including cell growth, proliferation, differentiation, normal functioning, and apoptotic death (Vinken et al., 2008).

There are three main ways that connexin proteins can participate in cellular communication. The first is through the formation of the classical

gap junction channel, which in hepatocytes, can be either homotypic, heterotypic, or heteromeric consisting two homotypic connexons made up of identical connexins, two homotypic connexons made of six Cx32 connexins and six Cx26 connexins, or two heterotypic Cx32/Cx26 connexons respectively (Fig 1.2, Chapter 1). Homotypic Cx26 gap junctions tend to favour cation transfer, whereas homotypic Cx32 channels preferentially pass anions (Bukauskas et al., 1995). Although both homotypic Cx26-containing and Cx32-containing channels pass inositol phosphates with equal efficiency, heteromeric channels exhibit selective permeability to discrete family members (Ayad et al., 2006). The second form of communication can occur via hemichannels, which are connexons elaborated at the plasma membrane that do not dock with a neighboring connexon, but instead mediate paracrine signalling within the microenvironment. Electrophysiological data shows that both Cx32 and Cx26 form hemichannels in hepatocyte membranes, and that Cx32 hemichannels are more abundant than Cx26 hemichannels (Valiunas et al., 1999). The third method of communication is channel-independent, and can be accomplished in two ways: 1.) connexins at the plasma membrane can act as adhesion molecules to aid in the proper migration of differentiating cells (Elias et al., 2007), and 2.) connexins can interact with specific proteins or complexes to modulate intracellular signalling pathways.

While we know that gap junctions and hemichannels contribute significantly to the effects of connexin-mediated communication in the

liver, there is mounting evidence that protein-protein interactions with connexin proteins have important regulatory and signalling roles (Moorby and Patel, 2001; Giepmans, 2004; Herve et al., 2004; Stout et al., 2004; Herve et al., 2007). Most of this evidence comes from the study of the ubiquitously expressed Cx43, for which there are approximately twenty known binding partners that include various kinases, transcription factors, and members of tight and adherens junctions (Giepmans, 2006). Given the rich associations of Cx43 with proteins known to possess transcriptional and intracellular signalling activities, it has been suggested that connexins may sequester transcription factors until needed or act as scaffolds to bring key intracellular effecters together (Dbouk et al., 2009). In this role, varying the level of connexin expression would alter the equilibrium of bound and non-bound factors, the latter of which would be free to activate their specific targets in the cell or translocate to the nucleus and alter gene expression (Ai et al., 2000). Furthermore, we know that the C-terminal domain of Cx43 itself is able to translocate to the nucleus and act as a transcription factor (Dang et al., 2003). Much less is known about the proteins associated with other connexins, thus, this chapter will focus on identifying Cx32 binding partners from liver, a tissue wherein Cx32 protein expression is maximal and where positive controls have been identified, in hopes of discovering how these proteins contribute to connexin-mediated, channel-independent communication in hepatocytes. This information will then be applied to the brain, in future studies, wherein Cx32 levels are lower but linked to NPC proliferation,

migration, and fate determination (Melanson-Drapeau et al., 2003; Elias et al., 2007; Elias and Kriegstein, 2008; Imbeault et al., 2009).

While we know that Cx32 associates with members of other junctional complexes and modulatory proteins that promote formation of gap junctions, it is likely, given the plethora of Cx43 interactions, that we have an incomplete list of the possible Cx32-binding proteins (see Chapter 1.6.1 and Table 1.1). The overarching goal of this study was to identify Cx32 interacting partners in liver tissue, and given the surprising finding that mitochondrial membranes co-fractionated with Cx32-rich membranes, we also sought to test the hypothesis that perhaps some Cx32 protein was contained within mitochondria.

This chapter describes the purification of endogenous Cx32 from mouse liver, and the identification of 19 novel Cx32 binding partners by LC-MS/MS of which 11 were identified as mitochondrial proteins co-purifying with Cx32. Further, we verified by both co-IF and co-IP that one of these mitochondrial proteins, SFXN-1, does indeed interact and partition with Cx32 in both liver and Cx32-transfected Human Embryonic Kidney (HEK) 293A cells. The mitochondrial localization of Cx32 is a novel finding, and its interaction with mitochondrial proteins unveils a possibly novel mechanism by which intracellular connexins can exert effects likely separate from their role in gap junctional intercellular communication.

3.4 Materials and Methods

Animals

$Cx32^{Y/+}$ and $Cx32^{Y/-}$ were bred, genotyped, and sacrificed as described in Chapter 2 (Materials and Methods).

Sucrose gradient fractionation

Fractionation and IB analyses were performed as described in Chapter 2 (Materials and Methods). Anti-SFXN-1 was used at 1.5 µg/µL as described below for the co-IP assays, and anti-**Bi**nding **P**rotein (BiP; marker of endoplasmic reticulum) was used at 1:125 (BD Transduction Laboratories [610978]).

Immunoaffinity purification

Anti-Cx32-coupled protein G agarose beads were prepared as follows: One mL of protein G agarose bead slurry (1:1 PBS; Roche, Germany) was incubated with 30 µg monoclonal anti-Cx32 (AB1) overnight at 4°C. The beads were washed with 10 mL of 0.1M borate buffer (pH 9.0) and resuspended in 10 mL of the same buffer. Anti-Cx32 antibody was chemically coupled to the protein G beads by the addition of solid DMP (Pierce, IL) to a final concentration of 20 mM. Beads were incubated for 30 minutes at RT. The cross-linking reaction was stopped by washing the beads twice with 0.2M ethanolamine (pH 8.2). Beads were resuspended in 10 mL of 0.2 M ethanolamine and incubated at RT for 2 h,

followed by two washes with 10 mL of PBS. Beads were resuspended in PBS to a final volume of 1 mL and stored at 4°C.

To specifically address the issue of biological significance of Cx32 detected at the mitochondria in brain (Fig 2.7) and liver (Fig 2.7, fraction identifications not shown), the liver lysates used here for IP were prepared from pooling sucrose fractions 4, 5, and 6 as these were enriched for Cx32 as well as the mitochondrial marker CoxIV and the plasma membrane marker Syntaxin-1 (brain) or lipid raft markers Caveolin-1 and Flotillin-1 (liver) (see Fig 2.7 and Fig 3.3). The pooled fractions were diluted 1:2 in fresh RIPA buffer with protease inhibitors prior to preclearing with 100 µL of uncoupled protein G agarose beads per 1 mL of protein lysate for 1 hour at 4°C. From the pooled fractions, 1 mg total protein was used as starting material for the 1X reaction, and 5 mg total protein was used for the 5X reaction. Precleared lysates (or an equal volume of RIPA buffer for the no lysate control) were added to either 400 µL (1X reaction) or 2 mL (5X reaction) prepared anti-Cx32-coupled beads and incubated overnight at 4°C. Beads were washed twice in RIPA buffer and three times in PBS for two minutes each with gentle inversion. Proteins were eluted at RT for 30 min with inversion in one bead-volume of ammonium hydroxide elution buffer (0.5 M NH_4OH, 0.5 mM EDTA). Samples were lyophilized in a speedvac and solubilized in 45 µL 2X SDS buffer and 5 µl BME at room temperature for 30 min. The SDS-solubilized proteins were run on NuPAGE Novex 4-12% Bis-Tris Gels (Invitrogen, CA) at 100 V for 20 minutes, followed by 150 V until desired resolution was obtained. Gels

were fixed for 30 mins in a 5% acetic acid:methanol solution, and rinsed twice with ddH_20 for two minutes each. To minimize background, the gel was washed in ddH_20 overnight with shaking at 4°C. The wash was discarded and the gel was sensitized for 1-2 mins in a 0.02% sodium thiosulfate solution, before being rinsed twice for 30 sec each with ddH_20. Fresh silver nitrate (0.1%) solution was incubated with the gel for 30 mins, followed by another two 30 sec washes in ddH_20. The gel was developed with two changes of freshly prepared 0.01% formaldehyde in 2% sodium carbonate solution, rinsed with 1% acetic acid, and stored in the same solution at 4°C.

LC-MS/MS analysis

All surfaces in contact with the gel were wiped with 70% ethanol and precautions were taken to minimize contamination of gel and gel pieces with keratin and dust from the air. Protein bands present in the $Cx32^{Y/+}$ sample and absent from the $Cx32^{Y/-}$ sample were excised from the gel on a clean glass plate with a #11 scalpel blade (blade was wiped with 70% ethanol before use, and changed between each band). Gel bands were cut into smaller pieces approximately 3 mm^2 and transferred to clean 0.6 mL Eppendorf tubes and washed by vortexing in 50 µL Solution A (50 mM ammonium bicarbonate), centrifuged briefly, and the liquid was discarded. The gel pieces were shrunk in 50 µL Solution B (50% acetonitrile, 25 mM ammonium bicarbonate) for 15 mins at RT, centrifuged briefly, and the liquid was discarded. Samples were dried in a

speedvac for 5 mins with no heat, followed by an incubation in 30 µL Solution C (50 mM ammonium bicarbonate, 10 mM DTT) for 15 mins at 56°C to re-hydrate the gel pieces and reduce disulfide bonds. Tubes were removed from the hot plate and allowed to cool at RT for 15 mins, after which time they were centrifuged briefly and the liquid was discarded. To inhibit re-formation of disulfide bonds, thiols were quenched by adding 30 µL Solution D (100 mM iodoacetamide in 50 mM ammonium bicarbonate) for a15 min incubation in the dark. Samples were centrifuged briefly and the liquid was discarded. Gel pieces were washed in Solution A for 15 mins, and shrunk in Solution B for 15 mins. Samples were centrifuged briefly and the liquid was discarded. Gel pieces were dried in a speedvac for 5 mins with no heat. Trypsin enzyme solution was prepared by adding 100 µL re-suspension buffer to 20 µg porcine trypsin (Promega, USA) and mixing the re-suspended enzyme with 310 µL of Solution A (sufficient for 10 samples). The enzyme solution was added to each sample at 28 µL/tube, let stand on ice for 10 mins, and the excess solution was removed. 10 µL of Solution E (25 mM ammonium bicarbonate) was added to each tube and samples were incubated at 37°C overnight. Tubes were centrifuged briefly and the solution was transferred to a clean tube. 50 µL of Solution E was added to the gel pieces and incubated at RT for 20 mins with occasional vortexing. This liquid was pooled with the other 10 µL of Solution E from the previous step. Peptides were extracted from the gel pieces by incubating each sample in 50 µL Solution F (5% formic acid and 50 % acetonitrile) for 20 mins. The tubes were centrifuged and the

peptide solution was pooled into the Solution E washes. Samples were dried in a speedvac with no heat and stored at -20°C.

LC-MS/MS was performed by dissolving the peptide samples in 5% formic acid and loading them into a 200 µm x 5 cm precolumn packed in-house with 5 µm YMC ODS-A C18 beads (Waters, USA) using a micro Agilent 1100 HPLC system (Agilent Technologies, USA). The peptides were desalted on-line with 95% water, 5% acetonitrile and 0.1% formic acid (V/V) for 10 mins at 10 µL/min. The flow rate was split before the precolumn to produce a flow of rate of approximately 200 µl/min at the column. Following their elution from the precolumn, the peptides were directed to a 75 µm x 5 cm analytical column packed with 5 µm YMC ODS-A C18 beads. The peptides were eluted using a 1 h gradient (15 to 80% acetonitrile with 0.1% formic acid) into a LTQ linear ion-trap mass spectrometer (Thermo-Electron, USA). MS/MS spectra were acquired in a data-dependant acquisition mode that automatically selected and fragmented the five most intense peaks from each MS spectrum generated.

Peak lists were generated from the MS/MS .raw file using Mascot Distiller 2.0.0.0 (Matrix Science, UK) to produce .mgf file with default parameters with the exception that for each MS/MS individual peak lists were generated assuming a 2+ and a 3+ charge. All .mgf files were analyzed and matched to the 52735 mouse protein sequences in the IPI database (released November 2007) using the Mascot 2.1.04 database search engine (Matrix Science) with trypsin as digestion enzyme,

carbamidomethyl of cysteine as a fixed modification and methionine oxidation as a variable modification. Peptide and MS/MS mass tolerances were set at ± 2 Da and ± 0.8 Da, respectively, with 1 miss-cleavage allowed and the significance threshold set to 0.01 ($p < 0.01$). Finally, an ion score cut-off of 30 was chosen to produce a false-positive rate of less than 1% in the MS data (Elias et al., 2005). The most logical assignment of the peptide in the database was reported, and when peptides matched to more than one database entry, only the highest scoring protein was considered.

Co-IP of Cx32, Cx26, and SFXN-1

Validation of protein-protein interaction was performed essentially as described above with the following modifications. Protein G beads were coupled with polyclonal Cx26 and SFXN-1 antibodies as previously described for the Cx32 IPs (Chapter 2 and above). Input protein amounts and bead volumes were scaled down to 250 ug, and 100 uL, respectively. Again, no lysate controls were performed in which protein lysate was substituted with an equal volume of RIPA buffer. Eluted, dried, and re-suspended IP product was run on 15% Tris-HCl polyacrylamide gels and transferred onto Immobilon P^{SQ} PVDF membrane (Millipore, MA) at 100 V for 60 min or overnight at 22 V. Blots were processed as described in the IB section above. Primary antibody concentrations were as follows: polyclonal anti-Cx32 (AB6; 1:200), polyclonal anti-Cx26 (Zymed, 51-2800,

1:200), and polyclonal anti-SFXN-1 (Proteintech Group 12296-1-AP, 1.5 µg/mL).

HEK293A cell transient transfection

The full cDNA coding sequence of the human Cx32 gene (Accession #: NC_000023) was cloned into a pcDNA3.1/*Myc*-His(-)A backbone (Invitrogen, CA). The resultant vector contained the Cx32 sequence followed by a single myc epitope and six histidine residues attached via a short linker sequence to the 3′ end of the Cx32 gene. The original empty vector was used as a negative control, and the pcDNA3.1/*Myc*-His(-)/*lacZ* plasmid was used to monitor transient transfection efficiency via β-galactosidase staining (β-gal Staining Kit, Invitrogen, CA).

HEK293A cells were maintained and passaged at ~70% confluence in Dulbecco's modified Eagle medium (DMEM; Gibco) with 10% fetal bovine serum (HyClone) and 1% penicillin/streptomycin antibiotic cocktail. Cells were plated at 4.25×10^5 in 6-well tissue culture plates on coverslips coated with 0.1% gelatin 24 h pre-transfection in 2 mL of regular culture medium. Just before transfection, 4 µg of respective plasmid DNA and 10 µL of Lipofectamine reagent (Invitrogen, CA) were each diluted in 250 µL warmed Opti-Mem low serum media (Invitrogen, CA) and incubated for 5 minutes. The diluted plasmid and Lipofectamine solutions were gently mixed together and incubated for 20 mins. During this time, the medium on each plate was replaced with 1.5 mL warmed DMEM+serum with no

antibiotics. After the incubation period, 500 µL of DNA:Lipofectamine complexes were added to each well of cells (~60% confluent) followed by gentle rotation to mix. Cells were incubated with transfection reagents overnight.

Mitotracker Red labeling of mitochondria

Twenty-four h post-transfection mitochondria were labeled with Mitotracker red or washed twice with PBS prior to fixation. Lyophilized Mitotracker Red (M7512; excitation λ = 579 nm, emission λ = 599 nm, Invitrogen, CA) powder was dissolved in dimethylsulfoxide (DMSO) to a final concentration of 1 mM and stored protected from the light at -20°C. Following the 24 h transfection period, the 1 mM Mitotracker Red stock solution was diluted in DMEM without serum to a concentration of 100 nM and pre-warmed to 37°C. The medium containing transfection complexes was removed from the cells and replaced with the warmed Mitotracker Red solution. Following 30 min incubation with the cells, the Mitotracker Red solution was removed in preparation for cell fixation.

Immunocytochemistry for Cx32 and SFXN-1

Following incubation with transfection complexes and/or the Mitotracker Red solution, cells were washed with 10 mM cold tissue culture PBS, fixed with 3.7% formaldehyde/PBS for 10 mins, and washed again in PBS. Fixed coverslips were removed from the wells and anchored onto a microscope slide with nailpolish. Coverslips were

incubated with monoclonal anti-Cx32 (AB4; 1 µg/mL) and/or polyclonal anti-SFXN-1 (1:50) diluted in antibody buffer (10 mM PBS [10 mM phosphate, 154 mM NaCl], 3% BSA, 0.3% Triton-X, pH 7.2) overnight at 4°C. Cells were washed 3X in 10 mM PBS for 5 mins at room temperature (RT), and incubated with Cy3 anti-mouse IgG secondary antibody (1:800, Jackson ImmunoResearch Labs, Inc.) or Alexa488 anti-rabbit IgG secondary antibody (1:200, Invitrogen, CA) in antibody buffer for 1 h at RT. Coverslips were washed 3X in 10 mM PBS for 5 mins at RT. Vectashield (Vector Labs) was applied to each coverslip and another coverslip was attached with clear nailpolish. Slides were stored at -20°C until imaging. Fluorescence was visualized using a Leica DMRXA2 microscope (Leica Microsystems, Germany) and analyzed using Openlab 5.0.2 software (Improvision, England).

Purification of liver mitochondria

Two whole livers were extracted from each of $Cx32^{Y/-}$ and $Cx32^{Y/-}$ mice immediately upon sacrifice and put in ice-cold PBS. The PBS was decanted and the livers were weighed on a pre-tared scale, and minced with scissors until homogenous. The liver pieces were washed with 3 changes of ice-cold PBS, or until no blood remained. Buffer A (20 mM Hepes, pH 7.4, 220 mM mannitol, 68 mM sucrose, 80 mM KCl, 0.5 mM ethylene glycol tetraacetic acid (EGTA), 2 mM $Mg(Ac)_2$, 10 mM DTT, fresh protease inhibitors) was added to the liver pieces at twice the volume per wet weight (g) of liver tissue (eg. 5 mL buffer A per 2.5 g liver tissue) and

homogenized using a dounce homogenizer and Teflon pestle until very smooth. The lysates were transferred to 30 mL centrifuge tubes and buffer A was added to fill the tube prior to centrifugation at 3000 rpm in a JA-25.5 rotor at 4°C for 20 mins. The supernatant was collected with a pasteur pipette, transferred to a new tube, and centrifuged at 8000 rpm at 4°C for 15 mins. The supernatant (containing the cytosol and light membranes) was discarded, and the mitochondrial pellet was washed with 30 mL of buffer A and carefully resuspended in this same buffer. The resuspended pellet was centrifuged at 8000 rpm as before. The supernatant wash was discarded and the mitochondrial pellet was resuspended in 500 uL buffer A without DTT.

Sucrose solutions (80%, 50%, 40% and 30%) were prepared in buffer A without DTT or protease inhibitors. 500 µL of the resuspended mitochondrial pellet was mixed with 1.5 mL 80% sucrose (~60% sucrose final). A discontinuous sucrose gradient was prepared on ice by slowly overlaying 2 mL of the mitochondrial:sucrose solution with 2 mL of each 50%, 40% and 30% sucrose solutions into a 13.2 mL (14 x 89 mm) polyallomer centrifuge tube (Beckman Coulter #331372). Buffer A (without DTT or protease inhibitors) was added to a point 1 mm below the surface of the tube (~5 mL). Tubes were carefully balanced and adjusted with buffer A if necessary before assembly into an SW41 Ti rotor (Beckman Coulter). Gradients were centrifuged at 35,000 rpm at 4°C for 16 h. Twenty-four fractions were carefully collected from the top of the tube (500 µL/fraction) into 1.5 mL eppendorf tubes and assayed for protein

concentration using the Bio-Rad DC protein assay kit (Bio-Rad, Hercules, CA). Samples (5 µg) were analyzed by IB as described in Chapter 2 for Cx32 (AB1), SFXN-1 (1.5 µg/mL), CoxIV (0.4 µg/mL), and Na+K+ATPase (0.5 µg/mL; Millipore [05-369]).

3.5 Results

Endogenous purification of Cx32-interacting proteins

To address the question of which proteins physically interact with Cx32 in liver lysates, we performed an endogenous pull-down of pooled sucrose gradient fractions enriched for Cx32 using a monoclonal Cx32 antibody (AB1) chemically coupled to protein G agarose beads. Control reactions were similarly coupled beads incubated in RIPA buffer in place of protein lysate (Fig 3.1A,B No lysate). The $Cx32^{Y/+}$ purification produced several bands that were visually absent in the $Cx32^{Y/-}$ purification. These areas of the gel delineated by black boxes were excised for LC-MS/MS analysis, and include distinct bands at 15 kDa, 22 kDa, 31 kDa, 42 kDa, and 45 kDa. The region between 31 and 40 kDa contained a smear of proteins that was darker than the corresponding region in the $Cx32^{Y/-}$ lane, and was split into two regions to simplify the analyses. Specific purification of Cx32 was confirmed by IB with a polyclonal anti-Cx32 antibody (AB6; 1:200; Fig 3.1B).

Figure 3.1: Endogenous liver Cx32 co-purifies with proteins primarily distributed between 20 and 50 kDa.

(A) Silver stain of immunoaffinity purified Cx32 and interacting proteins resolved by 4-12% gradient SDS-PAGE. Protein was immunoprecipitated with AB1 from sucrose gradient fractions 4-6 from $Cx32^{Y/+}$ liver. Lyophilized IP products were re-constituted in 2X SDS-containing sample buffer. Negative controls included IP reactions using of fractionated $Cx32^{Y/-}$ liver or IPs reactions carried out without tissue lysate (no lysate) representing light chain and heavy chain IgG/protein G background. Black boxes indicate gel regions excised for tryptic digest from both Y/+ and Y/- lanes (B). Western blot of pooled fractions (5 µg) and 1 µl of the IP products analyzed in (A) blotted with AB6.

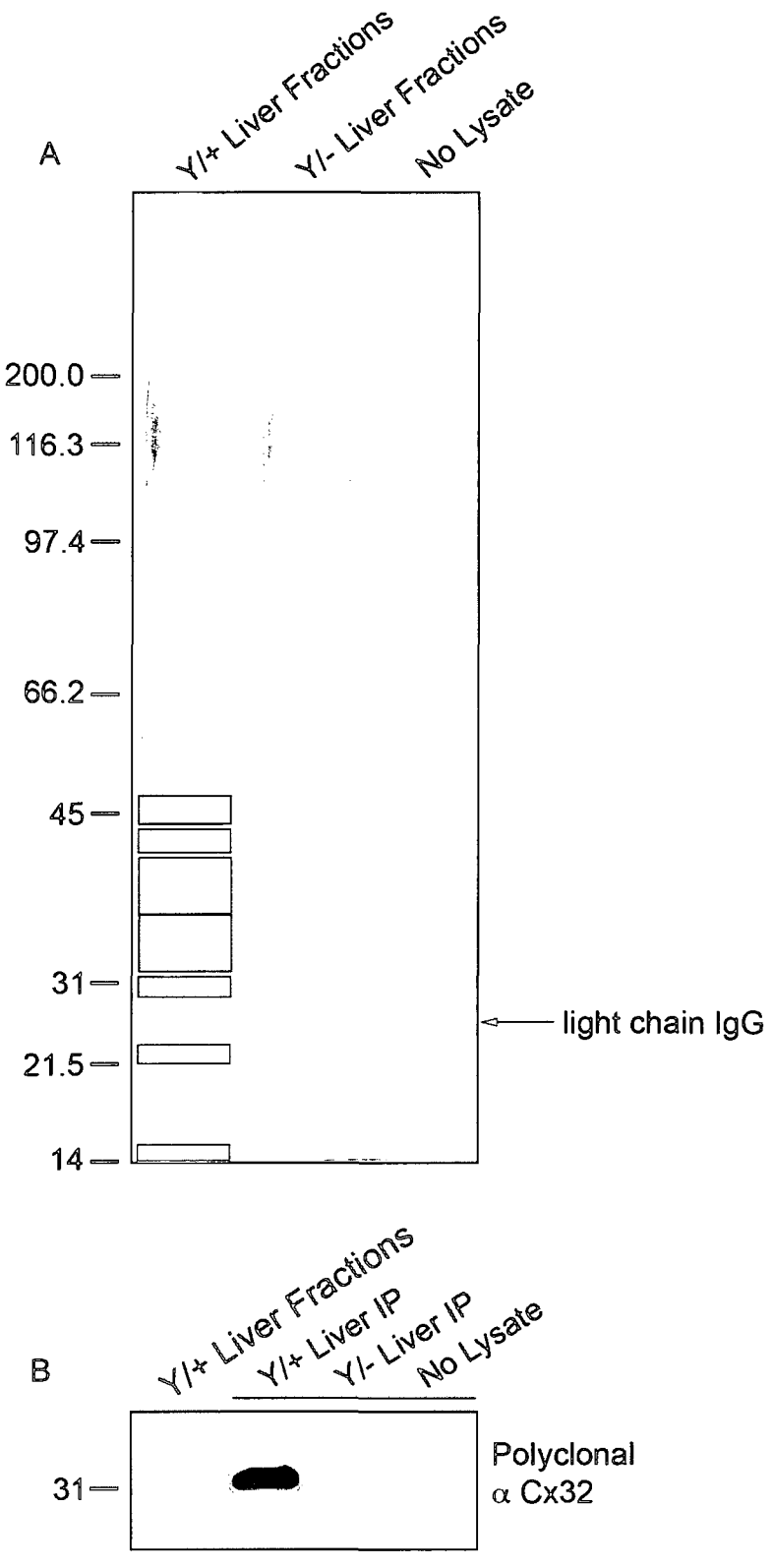
A
Y/+ Liver Fractions
Y/- Liver Fractions
No Lysate
200.0
116.3
97.4
66.2
45
31
21.5
14
light chain IgG
B
Y/+ Liver Fractions
Y/+ Liver IP
Y/- Liver IP
No Lysate
31
Polyclonal
α Cx32

Figure 3.1

Cx32 interacts with proteins found in the mitochondria, the cytoplasm, and at the plasma membrane

Following excision of the silver-stained bands from both $Cx32^{Y/+}$ and $Cx32^{Y/-}$ lanes, proteins were eluted from the gel pieces, treated with trypsin, and analyzed by LC-MS/MS to determine protein identities. With 1 mg of input protein, we identified Cx32 and Cx26 at ~ 31 kDa and 24 kDa, respectively (Fig3.2A). Also identified were SFXN-1, ADP/ATP translocase 2, and a protein similar to the ubiquitin A-52 ribosomal fusion protein product 1 (UbA52). These same proteins were confirmed after a 5X scale-up of the IP reaction as well as 15 additional proteins exhibiting mascot scores of 77 or greater. We reported two proteins (ADP/ATP translocase 2, and similar to UbA52) with scores significantly lower than 100 because they were present in both rounds of MS. The membrane-associated progesterone receptor with a mascot score of 77 was reported because it is of particular interest to our laboratory. Most proteins reported were multiple-peptide hits, and absent from the $Cx32^{Y/-}$ negative control lanes.

Despite using fractions enriched for both plasma membrane and mitochondrial markers, the majority (11 of 19) of Cx32-interacting proteins identified were mitochondrial; four were plasma membrane-associated; another four were cytoplasmic. Detection of protein-protein interaction with Cx32 and mitochondrial proteins further validates the novel localization for Cx32 as suggested in Chapter 2. The mitochondrial interacting proteins include membrane-bound members of the electron

Figure 3.2: MS/MS analyses confirmed Cx32 purification and identified Cx26 and 18 novel proteins as interacting partners of Cx32. (A) Mascot software identified 5 proteins from the first round of MS (1 mg input). Upon 5X scale-up of reaction (5 mg input), 15 additional proteins were identified. (B) Interaction map showing predicted localizations of Cx32-binding partners. Predicted cytoplasmic, mitochondrial, and plasma membrane localizations are represented by green, purple and blue circles, respectively. Black lines and smaller circles represent proteins identified from the 1X reaction, while heavier grey lines and larger circles represent proteins identified from both 1X and 5X reactions.

A

IPI #	Protein Name	Mascot Score			
		WT (5X)	WT (1X)	Cx32 KO (5X)	Cx32 KO (1X)
IPI00118459	**Tax_Id=10090 Gap junction beta-1 protein**	370	160	0	0
IPI00125162	Tax_Id=10090 Gap junction beta-2 protein	208	179	0	0
IPI00115454	Tax_Id=10090 Sideroflexin-1	97	102	0	0
IPI00127841	Tax_Id=10090 ADP/ATP translocase 2	241	57	0	0
IPI00377342	Tax_Id=10090 similar to ubiquitin A-52 residue ribosomal protein fusion product 1	58	51	0	0
IPI00226430	Tax_Id=10090 3-ketoacyl-CoA thiolase, mitochondrial	396	0	0	0
IPI00130280	Tax_Id=10090 ATP synthase subunit alpha, mitochondrial precursor	228	0	0	0
IPI00135646	Tax_Id=10090 ATP-binding cassette sub-family D member 3	183	0	0	0
IPI00408961	Tax_Id=10090 3-hydroxyanthranilate 3,4-dioxygenase	176	0	0	0
IPI00124223	Tax_Id=10090 Proteasome activator complex subunit 1	165	0	0	0
IPI00317074	Tax_Id=10090 Mitochondrial dicarboxylate carrier	161	0	0	0
IPI00461407	Tax_Id=10090 similar to ATP synthase, H+ transporting, mitochondrial F1 complex, O subunit	153	0	0	0
IPI00109275	Tax_Id=10090 Mitochondrial glutamate carrier 1	145	0	0	0
IPI00134746	Tax_Id=10090 Argininosuccinate synthase	118	0	0	0
IPI00116770	Tax_Id=10090 Ras-related protein Rab-18	110	0	0	0
IPI00124225	Tax_Id=10090 Proteasome activator complex subunit 2	108	0	0	0
IPI00122549	Tax_Id=10090 Isoform PI-VDAC1 of Voltage-dependent anion-selective channel protein 1	101	0	0	0
IPI00126042	Tax_Id=10090 Ras-related protein Rab-14	99	0	0	0
IPI00330754	Tax_Id=10090 D-beta-hydroxybutyrate dehydrogenase, mitochondrial precursor	95	0	0	0
IPI00319973	Tax_Id=10090 Membrane-associated progesterone receptor component 1	77	0	0	0

B

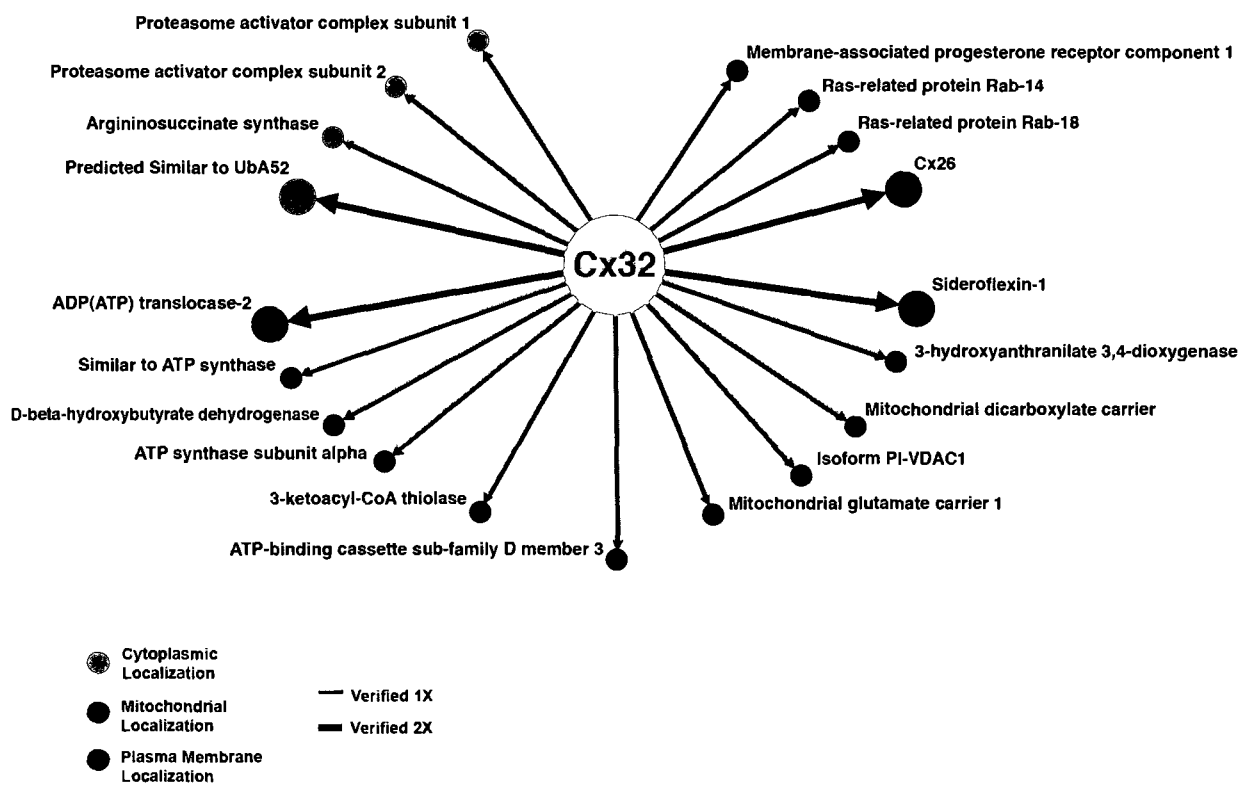

Figure 3.2

transport chain, enzymes involved in metabolism, and other membrane transport channels. The plasma membrane associated proteins consisted of two Rab GTPases, a membrane-associated progesterone receptor component, and Cx26, while the cytoplasmic proteins were mostly related to the proteosome (Fig 3.2B). At least one protein from each subcellular localization was identified in both rounds of MS.

Cx32 co-purifies with Cx26 and SFXN-1

To verify the expected interaction of Cx26 and the novel interaction of SFXN-1 with Cx32 in the liver, we performed reverse-IP studies. Cx32 was immunoprecipitated from mitochondrial and plasma membrane-enriched sucrose gradient fractions (fractions 4-6), and the products were immunoblotted for each binding partner. Conversely, we purified for Cx26 and SFXN-1 from these same pooled fractions and immunoblotted each of the products for Cx32. In Fig. 3.3A, immunoblotting for Cx26 produced a band at approximately 24 kDa that was present in $Cx32^{Y/+}$ liver fractions, but absent in $Cx32^{Y/-}$ control fractions, consistent with the observation that the loss of Cx32 results in a concomitant reduction in levels of Cx26 protein (Nelles et al., 1996). When Cx32 was immunopurified from liver fractions, Cx26 protein was present in the IP products from $Cx32^{Y/+}$, but not $Cx32^{Y/-}$ lysates (Fig 3.3A). This finding was confirmed by reverse IP. Liver lysates immunopurified for Cx26 contained Cx32 protein in the

Figure 3.3: Liver Cx32 is primarily localized to sucrose gradient fractions containing the interacting protein SFXN-1, and the mitochondrial inner membrane protein CoxIV.

Liver homogenates were prepared using 1% Triton X-100 and overlayed with decreasing concentrations of sucrose. (A) Schematic of the sucrose gradient showing the ten 500 µL fractions that were harvested and analyzed in (B) with Cx32 being primarily localized to fractions 4, 5, and 6. (B). Immunoblots for Cx32, SFXN-1, CoxIV, Caveolin-1, Flotillin-1, and BiP, of 5 µg whole liver tissue before fractionation and 5 µg of each fraction 1-10.

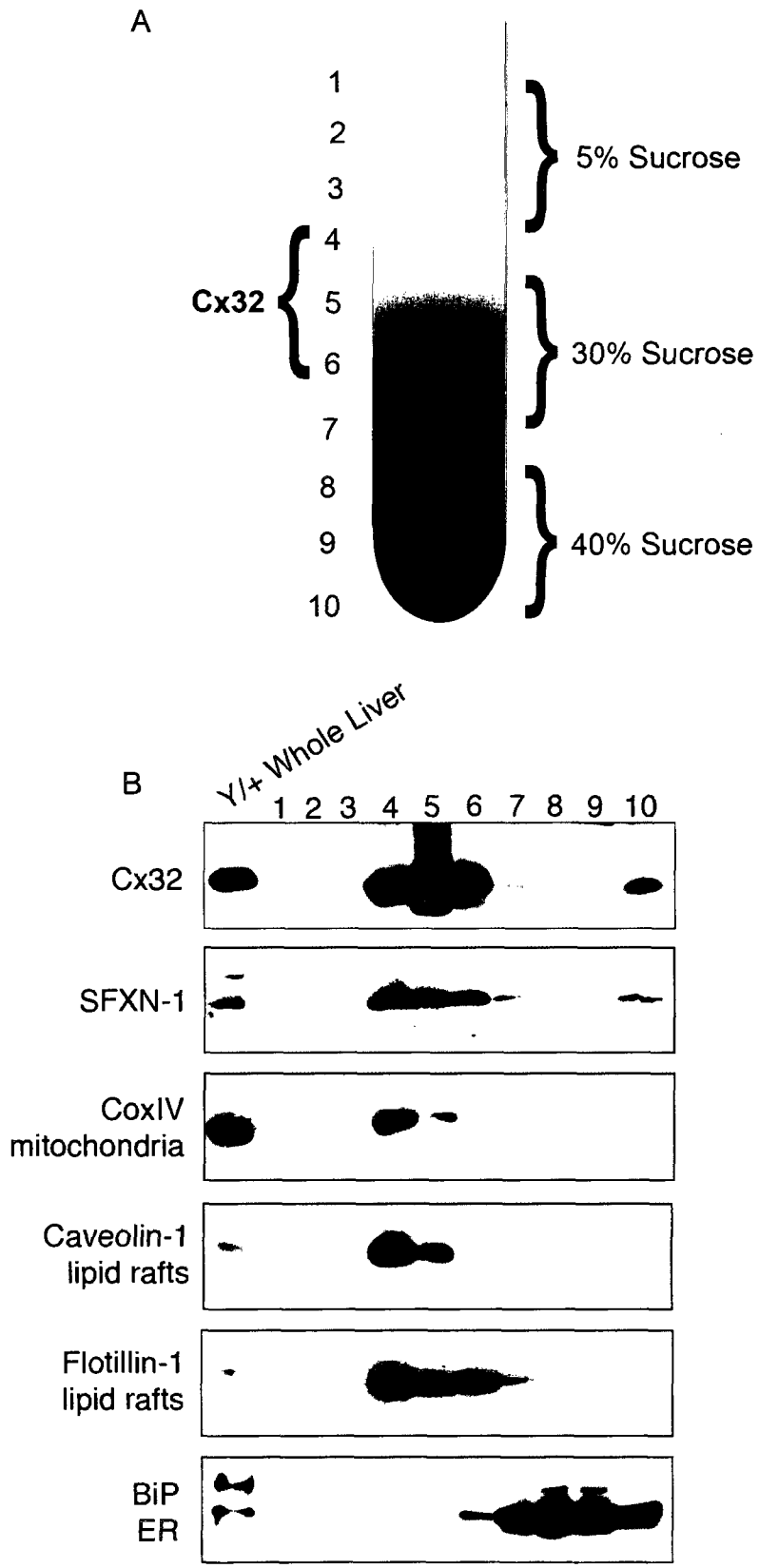
A
1
2
3
4
5
6
7
8
9
10
Cx32
5% Sucrose
30% Sucrose
40% Sucrose
B
Y/+ Whole Liver
1 2 3 4 5 6 7 8 9 10
Cx32
SFXN-1
CoxIV
mitochondria
Caveolin-1
lipid rafts
Flotillin-1
lipid rafts
BiP
ER

Figure 3.3

$Cx32^{Y/+}$ reaction only (Fig 3.3B). Together, panels A and B confirm that Cx26 interacts with Cx32 in the liver as previously reported for Cx26 (Vinken et al., 2008).

With this positive control validated, we assessed the putative SFXN-1/Cx32 interaction. IB for SFXN-1 from $Cx32^{Y/+}$ and $Cx32^{Y/-}$ liver fractions produced bands of equal intensity in each genotype at approximately 35 kDa. When liver fractions were immnopurified for Cx32, SFXN-1 was detected in the $Cx32^{Y/+}$ purification only (Fig 3.3C). When liver fractions were immunopurified for SFXN-1, Cx32 was detected in the $Cx32^{Y/+}$ purification only. As above, panels C and D confirm that SFXN-1 interacts with Cx32 in the liver. Together, these data provide strong evidence that Cx32 and SFXN-1 are part of the same complex but, unlike Cx26 (Fig 3.4A), loss of Cx32 does not impact upon SFXN-1 protein expression (Fig 3.3C).

Cx32 is contained within cell fractions also enriched for the binding partner SFXN-1 and the mitochondrial protein CoxIV.

It is, however, possible that the detection of mitochondrial interacting proteins with Cx32 does not necessarily indicate a potential function at the mitochondria, but rather that association with a Cx32-containing complex at the plasma membrane serves to sequester these proteins from the mitochondria. To validate that these interactions could occur in the mitochondria, we analyzed the ten sucrose gradient fractions (schematic shown in Fig. 3.4A) for their expression of Cx32, SFXN-1,

Figure 3.4: Cx26 and SFXN-1 co-IP with Cx32. All co-IPs were performed using protein G beads cross-linked with either Cx32 (monoclonal AB1), Cx26 (polyclonal), or SFXN-1 (polyclonal) antibodies.

(A) Liver fractions 4, 5, and 6 were immunoprecipitated for Cx32 and immunoblotted for Cx26. Negative controls included Y/- lysates. Cx26 was only present in Y/+ liver fractions. (B) Liver fractions were affinity-purified for Cx26 and immunoblotted for Cx32 using AB1. Cx32 was present only in the Y/+ lanes. (C) Purification for Cx32 also verified the interaction between Cx32 and SFXN-1. The loss of Cx32 had no impact on the expression of SFXN-1 as shown in lane 2 of this panel. (D) Similarly, purification for SFXN-1 allowed for the detection of Cx32 in the WT lane only.

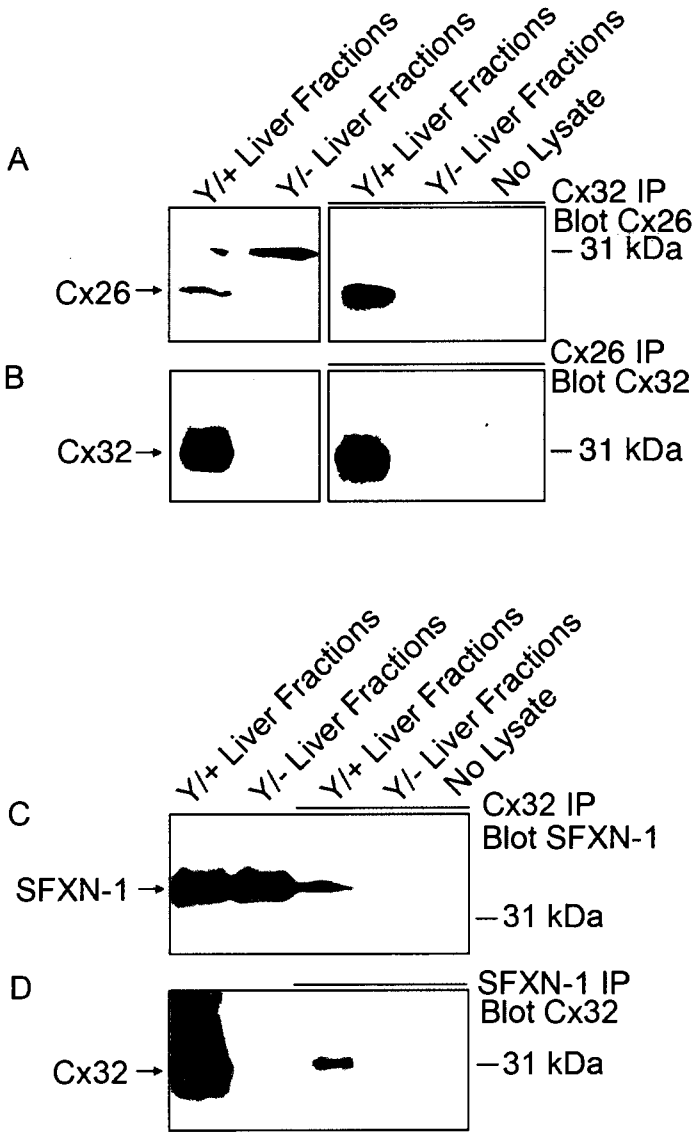
A
Y/+ Liver Fractions
Y/- Liver Fractions
Y/+ Liver Fractions
Y/- Liver Fractions
No Lysate
Cx32 IP
Blot Cx26
– 31 kDa
Cx26 →
B
Cx26 IP
Blot Cx32
Cx32 →
– 31 kDa
C
Y/+ Liver Fractions
Y/- Liver Fractions
Y/+ Liver Fractions
Y/- Liver Fractions
No Lysate
Cx32 IP
Blot SFXN-1
SFXN-1 →
– 31 kDa
D
SFXN-1 IP
Blot Cx32
Cx32 →
– 31 kDa

Figure 3.4

CoxIV, Caveolin-1, Flotillin-1, and BiP by IB. We found that fractions 4, 5, and 6 were enriched for Cx32 protein (Fig 3.3B). These fractions were located between the 5% and 30% sucrose layers. SFXN-1 was also enriched in fractions 4, 5, and 6, and possessed a nearly identical pattern of distribution as Cx32. Because SFXN-1 is a putative mitochondrial protein, we analyzed the liver fractions for expression of the mitochondrial marker Cox IV, which was found in fractions 4 and 5. Further, fractions 4, 5, and 6 (Flotillin-1 only) were enriched for the lipid raft markers Caveolin-1 and Flotillin-1. The marker of the endoplasmic reticulum, BiP, was enriched in fractions 6-10.

While it appears that Cx32 and its binding partner SFXN-1 are contained within fractions enriched for both plasma membrane and mitochondria, these data must be interpreted with caution. The fractionations described above were performed on liver lysates solubilized in 1% Triton X-100, thus, proteins identified in these fractions consist of both detergent-insoluble membranes and their protein constituents, in addition to proteins disrupted from detergent-soluble membranes that have retained interaction with part of their lipid environment (i.e, membrane components). Indeed, these types of fractionations are prone to artifactual identification of more soluble membrane proteins within fractions containing detergent-insoluble membranes from other organelles (Shogomori and Brown, 2003; Zheng et al., 2009). It is possible that the identification of mitochondrial proteins (particularly large mitochondrial membrane complexes) within detergent-insoluble plasma membrane and

lipid raft fractions may simply reflect their partial solubilization in 1% Triton X-100, which imparts the ability to float in the density gradient. Given this caveat, we prepared liver mitochondria from $Cx32^{Y+}$ and $Cx32^{Y/-}$ animals by differential centrifugation using detergent free buffers, and further purified the samples by sucrose gradient fractionation (Fig 3.5).

Mitochondrial fractionations reveal that while enriched in plasma membrane, Cx32 is also present in mitochondria, and that SFXN-1 is detected at both plasma membrane and mitochondria membranes

A detergent-free purification was performed to more definitively assess whether Cx32 could be present in intact mitochondrial membranes. It is well-known that plasma membrane lipids and their associated proteins are common contaminants of mitochondrial purifications by differential centrifugation (Zheng et al., 2009), thus, a sucrose gradient was necessary to conclusively separate these two organelles (Fig 3.5A). Twenty-four fractions (~500 µL each) were collected, and as expected, plasma membrane constituents floated above the mitochondrial constituents as assessed by their respective enrichment in Na^+K^+ATPase ($Cx32^{Y/+}$: fractions 10-15 (Fig 3.5B); $Cx32^{Y/-}$: fractions 9-15 (Fig 3.5C)) and CoxIV ($Cx32^{Y/+}$: fractions 13-22 (Fig 3.5B); $Cx32^{Y/-}$: fractions 13-21 (Fig 3.5C)). Cx32 was predominantly identified within the fractions enriched for the Na^+K^+ATPase (fractions 10-15; Fig 3.5B), however was also detected at much lower levels in the mitochondrial fractions enriched for CoxIV (fractions 13-22; Fig 3.5B). SFXN-1 was detected in all of the

mitochondrial fractions ($Cx32^{Y/+}$: fractions 17-22), but was clearly present in plasma membrane fractions ($Cx32^{Y/+}$: fractions 12-15 and). Note that $Cx32^{Y/+}$ fractions 10 and 12 and $Cx32^{Y/-}$ fractions 9 and 10 contained plasma membrane devoid of mitochondrial contamination (Fig 3.5B,C), while $Cx32^{Y/+}$ fractions 20-22 and $Cx32^{Y/-}$ fractions 19-21 contained mitochondria devoid of plasma membrane contamination (Fig 3.5B,C).

Co-IP of Cx32 and SFXN-1 from pure plasma membrane and pure mitochondrial fractions suggest that the interaction occurs in both locations

Given the apparent dual localization of both Cx32 and SFXN-1 to the plasma membrane and to mitochondria, we performed an IP for SFXN-1 using the distinct plasma membrane and pure mitochondrial fractions indicated above. The fractions were pooled from each genotype, re-assayed, and incubated with protein G agarose beads coupled to anti-SFXN-1 antibody as previously described. IB for Cx32 (AB1) from 2.5 µg $Cx32^{Y/+}$ plasma membrane fractions and 2.5 µg mitochondrial fractions indicates that the plasma membrane fractions contain significantly more Cx32 than the mitochondrial fractions (Fig 3.6). IB of the SFXN-1 IP products for Cx32 shows that the interaction is present at both the plasma membrane and the mitochondrion, however, the interaction is much more prevalent at the plasma membrane than in mitochondria (Fig 3.6).

Figure 3.5: Although mostly present at the plasma membrane, Cx32 is detected in purified mitochondrial fractions, while SFXN-1 displays a dual enrichment to both mitochondrial and plasma membrane fractions.

(A) Following enrichment for mitochondria from $Cx32^{Y/+}$ and $Cx32^{Y/-}$ liver by differential centrifugation, the sample was further purified by discontinuous sucrose gradient. Twenty-four fractions were collected and 5 µg each immunoblotted for Cx32, Na^+K^+ATPase, CoxIV, and SFXN-1 ($Cx32^{Y/+}$ only) (B) $Cx32^{Y/+}$: Cx32 is enriched in fractions containing the Na^+K^+ATPase (fractions 10-15), however, is also detected in fractions containing CoxIV (fractions 17-22). SFXN-1 is equally enriched in fractions 12-15 (plasma membrane), and fractions 17-22 (mitochondria). (C) $Cx32^{Y/-}$: Cx32 is present in $Cx32^{Y/+}$ CM but absent in $Cx32^{Y/-}$ CM and corresponding sucrose fractions. The Na^+K^+ATPase is enriched in fractions 9-15, while CoxIV is enriched in fractions 13-21. Relative enrichment is indicated in reference to 5 µg of the crude mitochondrial (CM) preparation ($Cx32^{Y/+}$ CM or $Cx32^{Y/-}$ CM).

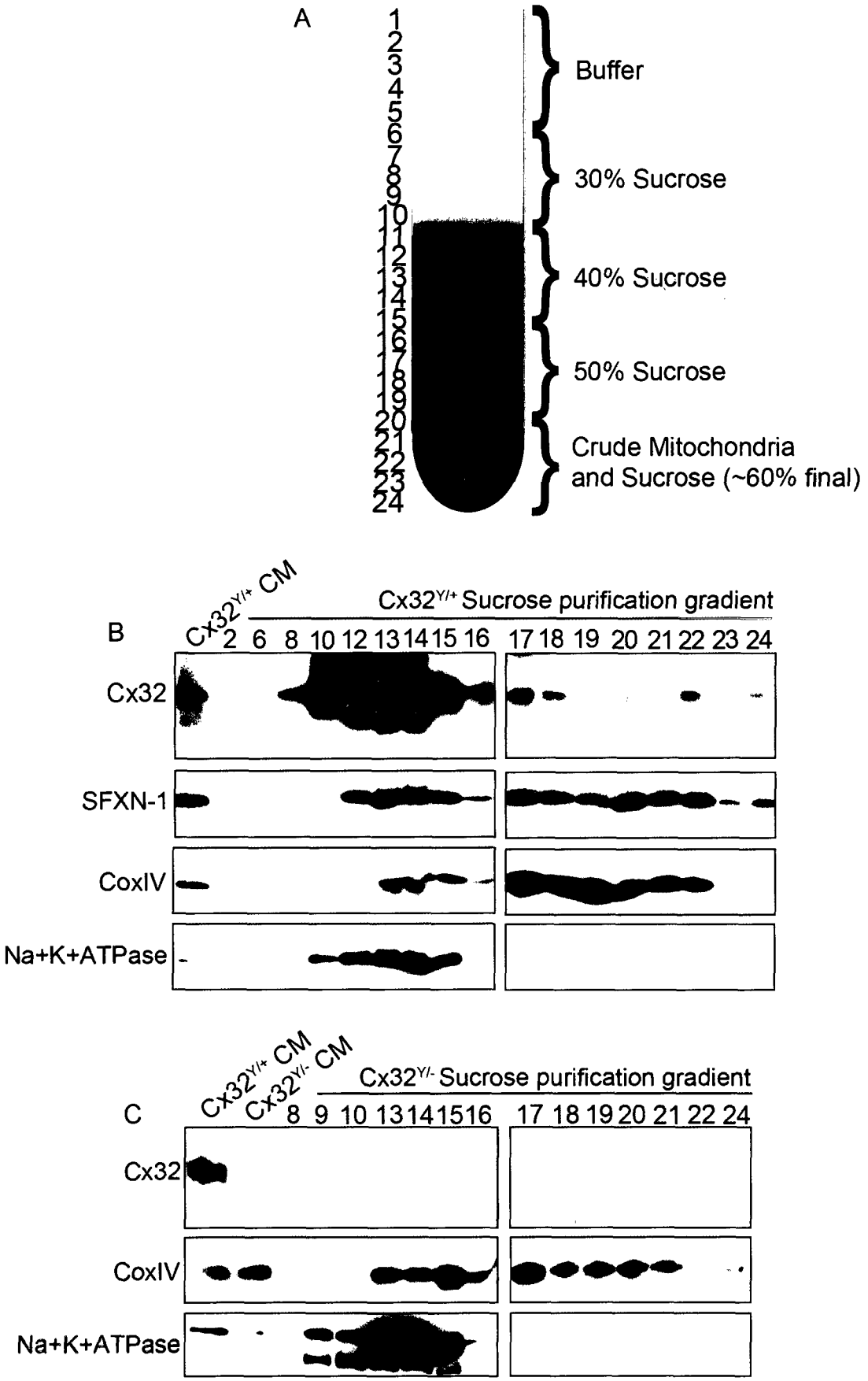
A
1
2
3
4
5
6
7
8
9
10
11
12
13
14
15
16
17
18
19
20
21
22
23
24
Buffer
30% Sucrose
40% Sucrose
50% Sucrose
Crude Mitochondria
and Sucrose (~60% final)
B
Cx32Y/+ CM
Cx32Y/+ Sucrose purification gradient
2 6 8 10 12 13 14 15 16 17 18 19 20 21 22 23 24
Cx32
SFXN-1
CoxIV
Na+K+ATPase
C
Cx32Y/+ CM
Cx32Y/- CM
Cx32Y/- Sucrose purification gradient
8 9 10 13 14 15 16 17 18 19 20 21 22 24
Cx32
CoxIV
Na+K+ATPase

Figure 3.5

Figure 3.6: Cx32 interacts with SFXN-1 predominately at the plasma membrane, however, the interaction also occurs in mitochondria.
$Cx32^{Y/+}$ fractions 10 and 12 and $Cx32^{Y/-}$ fractions 9 and 10 were each pooled to generate plasma membrane only fractions for each genotype. Similarly, $Cx32^{Y/+}$ fractions 20-22 and $Cx32^{Y/-}$ fractions 19-21 were pooled to generate mitochondria only fractions. The first four lanes contain 2.5 µg plasma membrane and mitochondrial fractions from each genotype immunoblotted for Cx32 using AB1, and re-iterate the dual localization of Cx32 in pure samples of each subcellular fraction. The last four lanes contain plasma membrane and mitochondrial fractions (50 µg) purified for SFXN -1 and immunoblotted for Cx32 using AB1. The interaction between Cx32 and SFXN-1 is strongest at the plasma membrane, yet is present in mitochondria.


WT Plasma Membrane
KO Plasma Membrane
WT Pure Mitochondria
KO Pure Mitochondria
WT Plasma Membrane
KO Pure Mitochondria
WT Pure Mitochondria
KO Pure Mitochondria
IP SFXN-1
50ug input
Cx32
2.5ug protein

Figure 3.6

Intracellular Cx32 co-localizes with SFXN-1 *in situ*

The finding that Cx32 interacts with SFXN-1 both at the mitochondrion and at the plasma membrane by detergent-free subcellular fractionation prompted further validation of the apparent dual localization of both Cx32 and SFXN-1 by co-immunocytochemistry. HEK293A cells do not express Cx32 as established by reverse transcription polymerase chain reaction (RT-PCR) (Supplemental Fig 3.1). In HEK293A cells transiently transfected with myc/his-tagged human Cx32 cDNA, Cx32 protein localizes to both the plasma membrane and to intracellular/perinuclear regions of the cell as demonstrated by Cx32 immunocytochemistry (Fig 3.7A-F). Fig 3.7 panels A-C demonstrate the punctate staining characteristic of gap junction plaques located at the plasma membrane (arrows), while panels D-F show an example of strong perinuclear staining for Cx32 (arrows). Together, these data reveal that Cx32 protein localizes both to the plasma membrane where it displays plaque-like staining, but is also present in intracellular regions of the cell, particularly surrounding the nucleus.

Immunocytochemistry for Cx32 and SFXN-1 revealed that the intracellular portion of Cx32 in transiently transfected HEK293A cells co-localizes with SFXN-1, the Cx32 binding partner twice validated by LC-MS/MS (Fig 3.2) and co-IP from both Triton-solubilized (Fig 3.4) and detergent-free (Fig 3.5) liver lysates. When mitochondria were imaged with Mitotracker Red and co-stained with SFXN-1, it appeared that SFXN-1 was primarily restricted to the mitochondria (Fig 3.7, III (g-i)). However,

when we examined the co-localization of Cx32 and SFXN-1 by confocal microscopy (Fig 3.8), SFXN-1, Cx32, and Mitotracker Red all displayed significant co-localization at both cell surface (arrowhead), and intracellular regions of the cell (arrow).

Based on the identification of Cx32 and SFXN-1 at both the plasma membrane and in mitochondria by subcellular fractionation and these preliminary immunocytochemical analyses, it appeared that Cx32 and SFXN-1 may indeed interact at both locations. However, it will be important to pursue this finding with confocal microscopy for Cx32 and SFXN-1 of isolated liver mitochondria from both $Cx32^{Y/+}$ and $Cx32^{Y/-}$ animals. To address the question of whether Cx32 and SFXN-1 localize to the inner or outer mitochondrial membrane will require selective permeabilization of the outer mitochondrial membrane by digitonin, followed by simultaneous detection of both proteins with known markers of each membrane compartment as described by Rodriguez-Sinovas and colleagues (Rodriguez-Sinovas et al., 2006). Further, from the data presented in this chapter regarding the dual localization of the supposed mitochondrial protein, SFXN-1, it is unclear whether or not the interaction with Cx32 impacts upon its localization. Examination of SFXN-1 localization in HEK293A cells with and without ectopically expressed Cx32, in hepatocytes cultured from both $Cx32^{Y/+}$ and $Cx32^{Y/-}$ animals, and in $Cx32^{Y/-}$ mitochondrial fractions (from Fig 3.5) will be performed to assess whether Cx32 is responsible for SFXN-1 localization at the plasma membrane, or if SFXN-1 is able to traffic there independently.

Figure 3.7: Cx32 localizes both to the plasma membrane and to intracellular membrane structures, and SFXN-1 co-localizes with Mitotracker Red in transiently transfected HEK293A cells.

HEK293A cells were transfected with human Cx32 cDNA using the Lipofectamine (Invitrogen) reagent. Cells were fixed 24 h post-transfection prior to immunocytochemical analyses. (A) Example of Cx32 localizing primarily to the plasma membrane in plaque-like puncta. (B) Example of Cx32 present at intracellular/perinuclear regions. (C) SFXN-1 co-localizes almost exactly with mitochondria imaged using Mitotracker Red. Scale bars, 50 μm.

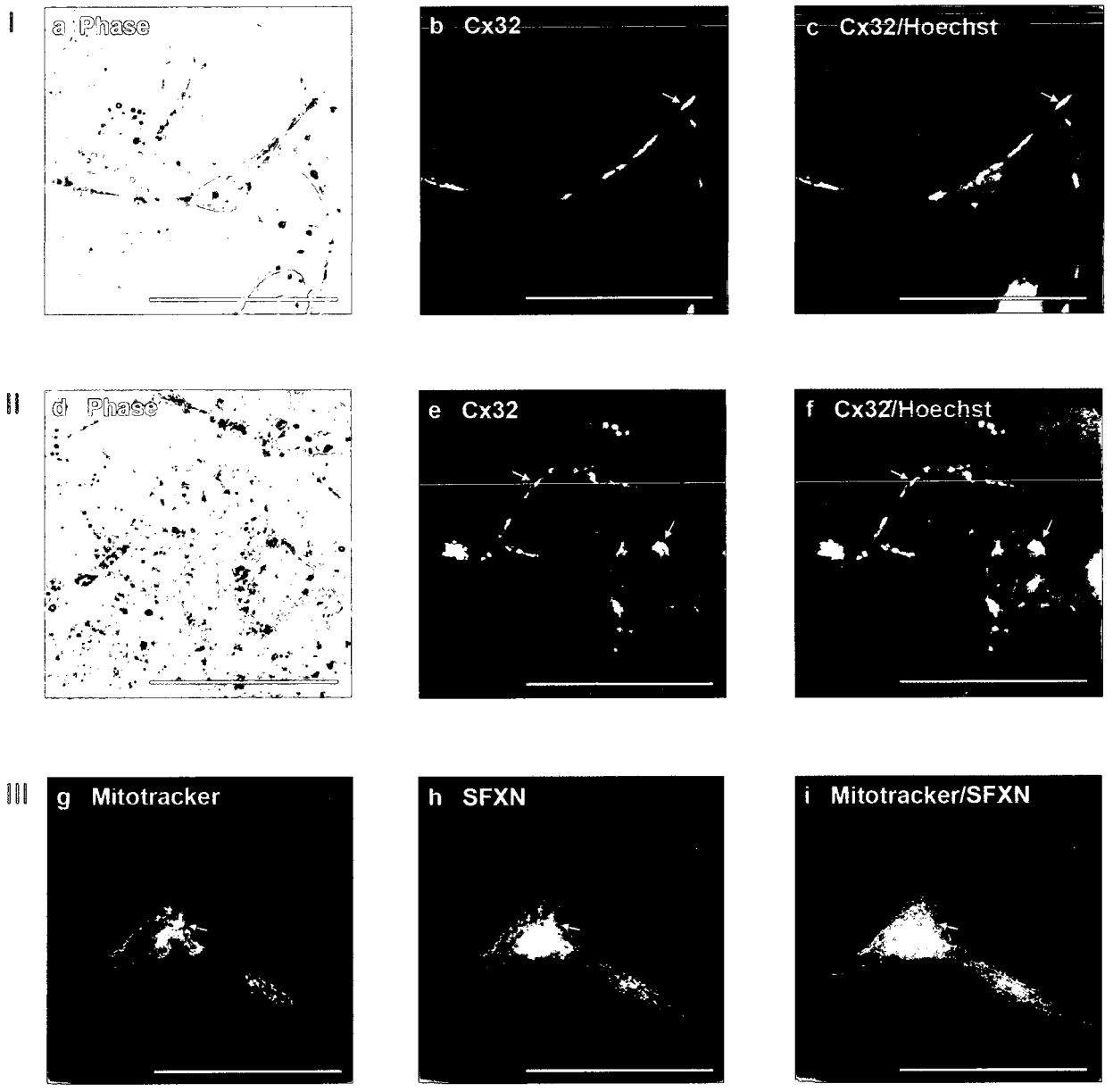
I
a Phase
b Cx32
c Cx32/Hoechst
II
d Phase
e Cx32
f Cx32/Hoechst
III
g Mitotracker
h SFXN
i Mitotracker/SFXN

Figure 3.7

Figure 3.8: Cx32, SFXN-1 and Mitotracker Red display significant co-localization in transiently transfected HEK293A cells as assessed by three-colour confocal microscopy.

HEK293A cells were transiently transfected with human Cx32 cDNA, incubated with 100 nM Mitotracker Red prior to fixation, and subjected to immunocytochemistry for SFXN-1 and Cx32. Co-localization of SFXN-1, Cx32, and Mitotracker Red by confocal microscopy occurred both in proximity to the cell surface (arrowhead), and intracellularly (arrow). Scale bar, 50 μm.

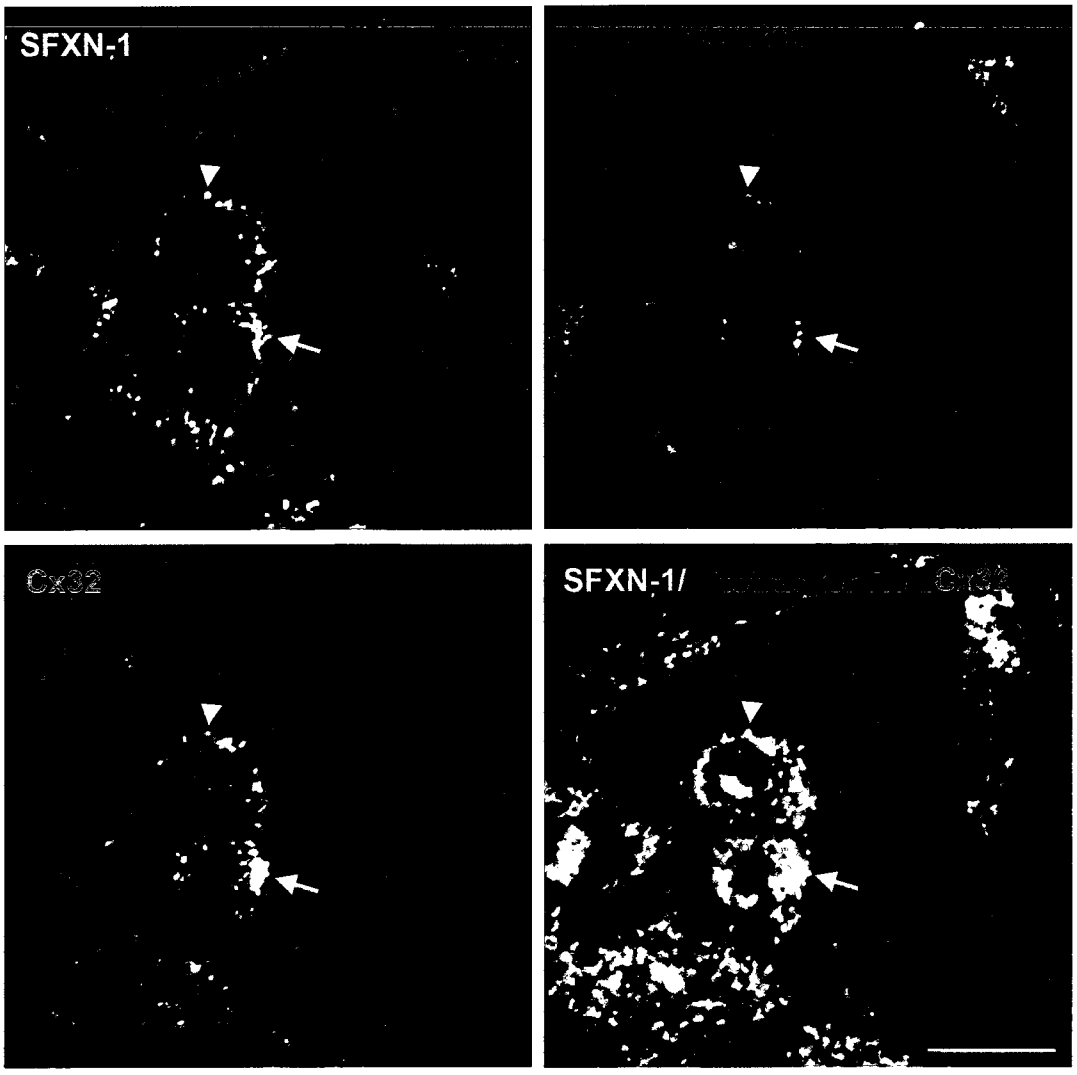

Figure 3.8

3.6 Discussion

In the present chapter we describe the purification of Cx32 and associated binding partners from murine liver, and their identification by LC-MS/MS. We show that Cx32 co-purifies with Cx26, a known Cx32 binding partner (Vinken et al., 2008), thereby verifying our method of protein identification, and providing the first proteomic demonstration of the physical association between these connexin family members. Furthermore, we have identified a list of eighteen novel proteins associated with Cx32, three of which have been verified by repeated rounds of mass spectrometry.

In this study, we used an absolute negative control, null-mutant tissue, immunoaffinity purified with same antibodies used in WT tissue. Visual inspection of the silver stained Cx32 IP products (see Fig.3.1) revealed that most of the differences between the $Cx32^{Y/+}$ and $Cx32^{Y/-}$ samples were evident between molecular weights of approximately 20-50 kDa. Above that mass, it was harder to discern bands that were not present in the $Cx32^{Y/-}$ lane, thus, only lower molecular weight products were excised for MS/MS. The validity of our methodology was demonstrated in the identification of the expected interaction between Cx32 and Cx26. In both purifications, the probability of the interaction between Cx32 and Cx26 was very high (Mascot scores: 1X-179; 5X-208). We know from electrophysiological and immunofluorescent studies that Cx32 forms gap junctions and hemichannels with Cx26 (Bukauskas et al.,

1995; Valiunas et al., 1999; Kojima et al., 2001) thus, this interaction provided an excellent positive control for the identification of *bona fide* Cx32 interacting partners. However, our identification of Cx26 represents, to our knowledge, the first time this interaction was verified directly by mass spectrometry from an endogenous Cx32 purification.

Surprisingly, the majority of Cx32-interacting partners were mitochondrial proteins. These data support the subcellular localization of Cx32 to both plasma membrane and mitochondrial membrane in both brain and liver as suggested by sucrose gradient fractionation of both Triton X-100 solubilized and detergent free liver lysates. These data provide further evidence that channel-independent actions (with respect to pore formation at the level of the plasma membrane) represents a largely unexplored means of connexin communication. We have yet to determine whether these interactions indicate channel function in complex with other proteins at the level of the inner (or outer) mitochondrial membrane or some other signalling aspect. However, one of the validated Cx32 interacting proteins identified here, SFXN-1, is predicted to localize to mitochondrial membranes, given its homology to the mitochondrial tricarboxylate carrier, a known inner mitochondrial membrane resident protein (De Palma et al., 2003), and has putative roles in the transport of co-factors related to iron utilization. Interestingly, in addition to SFXN-1 co-fractionation with both Cx32 and the mitochondrial protein CoxIV, and co-localization with Mitotracker Red in Cx32-transfected HEK293A cells,

SFXN-1 is also specifically enriched at the plasma membrane, indicating a dual subcellular localization not previously discussed in the literature.

The remainder of Cx32-interacting molecules include members of the ubiquitin-proteosome complex, various mitochondrial enzymes and transmembrane ion channels, as well as plasma membrane receptors and small GTPases. Together, these data show that Cx32 interacts with the novel protein SFXN-1 in murine liver, and that this interaction occurs predominantly at the plasma membrane, yet is also present in mitochondria. Further studies must directly dissect whether this association is (a) direct or indirect and (b) whether or not the expression of Cx32 impacts upon SFXN-1 subcellular localization. The detailed study of this interaction and of the other proteins identified by MS/MS is likely to provide exciting mechanistic information about the functional significance of protein-protein interactions with Cx32, particularly in relation to the role of connexins in the mitochondria, and potentially, their role in sequestering mitochondrial proteins at the plasma membrane.

The novel family of SFXN proteins

SFXN-1 was first identified as the gene responsible for the flexed-tail phenotype in mice with skeletal abnormalities, and transient embryonic and neonatal anemia characterized by mitochondrial iron deposits in erythrocytes (Fleming et al., 2001). The *SFXN-1* gene mutation at codon 15 produces 15 amino acids of the WT protein, which is followed by a frameshift that results in 17 novel amino acids and an inframe stop codon.

Thus, as verified by IB, flexed-tail mice do not produce any WT SFXN-1 protein (Fleming et al., 2001).

The discovery that a mutation in this yet uncharacterized gene was responsible for the flexed-tail phenotype soon led to the identification of a family of SFXN proteins. This was an exciting breakthrough in the field, because the flexed-tail phenotype had been under investigation since 1933 due to its similarities with sideroblastic anemias in humans. From the analyses of mammalian EST and sequence databases, (Fleming et al., 2001) discovered the existence of 4 other mammalian homologs of SFXN-1, and named them SFXN-2-5. Further, Fleming and colleagues have shown that SFXN-1 is enriched in mitochondrial preparations, and displays significant colocalization with Mitotracker Red (Fleming et al., 2001).

All SFXN family members possess 5 highly conserved TM domains, and long, fairly unconserved N-termini (Miyake et al., 2002). Northern blot analyses of the SFXN family members reveals that SFXN-1 and 2 are most highly expressed in mouse kidney and liver, SFXN-3 is fairly ubiquitously expressed, SFXN-4 is mostly found in kidney, brain, and heart, while SFXN-5 is restricted to the liver and brain (Fleming et al., 2001). Further sequence analyses of the SFXN proteins also revealed the existence of a conserved mitochondrial tricarboxylate carrier (MTC) domain. SFXN-1 shares 48.6% sequence homology with the MTC domain containing-*Rattus* tricarboxylate carrier protein, which enables the transport of tricarboxylates (eg. citrate), dicarboxylates (eg. malate and succinate) and phosphoenolpyruvate across the inner mitochondrial

membrane (Miyake et al., 2002; Ye et al., 2003). It has been hypothesized that SFXN-1 might also share this function (Azzi et al., 1993), although more recently this function has been questioned in favour of a role in iron regulation (Fleming et al., 2001). Thus, another plausible role for SFXN-1 is as a transporter for pyridoxine (vitamin B6), a cofactor for delta-aminolevulinate synthase 2 (ALAS2), the enzyme that catalyzes the first step in heme synthesis (Fleming et al., 2001; Zheng et al., 2003). Evidence for this hypothesis comes from the detection of similar siderocytic granules in pyridoxine deficiency, presumably as a consequence of ALAS2 deficiency (Hurford et al., 2002).

Evidence for the dual localization of mitochondrial proteins at the plasma membrane

Surprisingly, following purification of mitochondrial preparations by sucrose gradient fractionation, we discovered that SFXN-1 was enriched in mitochondrial fractions, but also that it was specifically enriched in fractions containing the plasma membrane associated Na^+K^+ATPase. This result was unexpected given previous reports (Fleming et al., 2001). Although we expected to find SFXN-1 only in mitochondrial fractions, the presence of mitochondrial proteins at the plasma membrane is not unprecedented. For example, there are numerous accounts of both F_1 and F_0 subunits of the mitochondrial ATP synthase present at the plasma membrane (Arakaki et al., 2003; Martinez et al., 2003; Kim et al., 2004; Kim et al., 2006; Lindqvist et al., 2008; Lyly et al., 2008; Mangiullo et al.,

2008). This example is particularly interesting given that in mammals, the *a* subunit (part of the integral membrane proton channel) and the A6L subunit (provides a physical link between the proton channel and the stator stalk) of the F_0-complex are encoded by the mitochondrial genome, and thus must exit the mitochondrion and travel via an unknown trafficking pathway to the plasma membrane (Kucharczyk et al., 2009). Interestingly, purification for Cx32 in Ch. 3 resulted in the identification of the ATP synthase *a* subunit, and a protein similar to the ATP synthase O-subunit of the F_1-complex, however, we cannot at this point determine whether the interaction with Cx32 occurs at the plasma membrane, in the mitochondria, or at both locations.

Another example of a mitochondrial protein with dual localization is Slit3, a member of the Slit family of proteins involved in developmental patterning. Unlike Slit1 and 2, Slit3 does not appear to be a secreted protein, rather it localizes to the mitochondrion in kidney epithelial cells (Little et al., 2001) and macrophages (Tanno et al., 2007). In confluent cell layers, or following macrophage activation by lipopolysaccharide, a discrete portion of Slit3 is re-directed to the plasma membrane (Little et al., 2001; Tanno et al., 2007). Little and colleagues report that Slit3 contains an N-terminal mitochondrial localization sequence, and hypothesize that another specific N-terminal sequence also targets Slit3 to the secretory pathway.

According to Karniely and Pines, dual localization of single translation products can result from a.) competition between two

localization signals on the same protein, b.) an ambiguous signal that is recognized by two organelles, c.) inaccessibility of localization signals by folding, protein interactions, and/or protein modification, d.) export of proteins from organelles (vesicular) or retrograde translocation (membrane transport), or e.) release from membrane-compromised organelles (Karniely and Pines, 2005). Given that SFXN-1 localizes fairly equally to the mitochondrion and to the plasma membrane in intact liver tissue independent of cell confluency or activation, I would hypothesize that this dual localization results either due to competition between two cryptic localization signals, or occurs as a result of transient protein interactions that block the mitochondrial targeting sequence in a portion of translated proteins. It is tempting to speculate that interaction with Cx32 is responsible for SFXN-1 trafficking to the membrane, however, examination of SFXN-1 subcellular localization in liver tissue and in hepatocytes isolated from both $Cx32^{Y/+}$ and $Cx32^{Y/-}$ animals will determine if the expression of Cx32 is indeed sufficient to direct SFXN-1 to the plasma membrane.

Evidence for the mitochondrial localization of connexins

While the identification of a mitochondrial pool of Cx32 with its own "interactome" is a novel finding in terms of Cx32 localization/function, this finding is consistent with recent demonstration that approximately 4.3% of the total Cx43 protein in heart tissue and isolated cardiomyocytes is mitochondrial (Rodriguez-Sinovas et al., 2006; Ruiz-Meana et al., 2008).

In addition to the numerous immunological co-localization techniques performed to validate this localization, Jorge and colleagues have recently identified Cx43 in mitochondrial membrane preparations using a modified method of LC tandem linear ion trap MS (Jorge et al., 2007).

Thus, a new and growing body of evidence shows that this small Cx43 pool in the mitochondria is important for mediating the ischemic and diazoxide-induced preconditioning of cardiomyocytes (Rodriguez-Sinovas et al., 2006; Ruiz-Meana et al., 2006; Ruiz-Meana et al., 2007). Genetic ablation of Cx43 completely abrogates both the ischemic and diazoxide modes of cardiomyocyte preconditioning, whereas a modest depletion (approximately 33%) by treatment with the benzoquinone antibiotic geldanamycin destroys only the diazoxide-induced mode of preconditioning. Diazoxide is a potassium channel activator, which increases membrane permeability to potassium ions. This type of preconditioning is thought to be mediated by the generation of reactive oxygen species, which, in small amounts, builds resistance against larger ischemic insults. The treatment of cardiomyocytes with geldanamycin inhibits the ATPase function of the chaperone HSP90, which in concert with HSP70 and the Translocase of the outer membrane (Tom) protein complex is responsible for the import of Cx43 into the mitochondria (Rodriguez-Sinovas et al., 2006). These data implicate the depletion of Cx43 in the diazoxide-induced production of reactive oxygen species (ROS) (K^+-dependent), and the complete ablation of Cx43 in the inhibition

of both K^+-dependent and K^+-independent modes of cardiac preconditioning.

In addition to the role of Cx43 in cardiac preconditioning to ischemic stress, mitochondria from Cx43-deficient mice ($Cx43^{Cre\text{-}ER(T)/fl}$) have attenuated ADP-stimulated respiration, and a reduced respiratory control ratio as compared to their WT littermates (Boengler et al., 2006). Mitochondrial Cx43 has also been implicated in the regulation of mitochondrial matrix volume, however, whether this is accomplished through its interaction with other mitochondrial molecules, or through the formation of Cx43 hemichannels is unknown (Miro-Casas, 2007). Furthermore, Goubaeva and colleagues report that treatment of isolated mitochondria with the gap junction blocker 18-β-glycyrrhetinic acid (β-GA) causes concomitant release of calcium and cytochrome C (Goubaeva et al., 2007). This effect appears to be specific to mitochondrial Cx43 because β-GA treatment induces apoptosis in low density (no cell-cell contacts) myocyte cultures as assessed by terminal dUTP nick end labeling (TUNEL). Li and colleagues have shown that the induction of ROS in endothelial cells following treatment with homocysteine results in a dramatic re-distribution of plasma membrane-associated Cx43 to the mitochondria, which is hypothesized to be protective (Li et al., 2002). Indeed, reduction in Cx43 movement to the mitochondria via pharmacological intervention, or as a result of the normal aging process, is detrimental (Boengler et al., 2007; Ruiz-Meana et al., 2008).

Due to the presence of Cx43 in mitochondria, and mounting evidence for its important role in cardiac and endothelial cells, the data presented in this study suggest mitochondrial roles for other connexin family members. Bioinformatic analyses of Cx32 suggest that, unlike Cx43, may be able to translocate to the mitochondria on its own accord rather than in complex with translocases or chaperone proteins as discussed below. The MitoProt software (http://ihg2.helmholtz-muenchen.de/ihg/mitoprot.html) predicts mitochondrial localization based on the analysis of the N-terminal amino acid sequence by comparing it to a database of known mitochondrial proteins and their mitochondrial targeting motifs (Claros and Vincens, 1996). Significant probability of mitochondrial localization occurs with a P value greater than 0.5. Analysis of the Cx32 sequence returned a P value of 0.81, indicating a significant probability that Cx32 can target to the mitochondria. Conversely, Cx43 returns a P value of 0.03, indicating no probability for mitochondrial targeting, a result also observed by Goubaeva et al., 2007.

These studies indicate that Cx43 is likely transported through the outer membrane by specific translocases, independent of the N-terminal signal sequence, and probably in association with Hsp90 (Rodriguez-Sinovas et al., 2006). In fact, approximately 30% of mitochondrial proteins do not contain canonical mitochondrial localization sequences, including all outer mitochondrial membrane proteins, many of the multiple transmembrane metabolite transporters of the inner membrane, and a number of proteins destined for the intermembrane space. Instead, these

proteins possess one or multiple internal cryptic mitochondrial localization sequences, often positioned adjacent to the transmembrane domains (Diekert et al., 1999; Stojanovski et al., 2003; Miotto et al., 2007). Interestingly, analysis of the N-terminal sequence of the Cx32 interacting protein SFXN-1 does not predict its mitochondrial localization, indicating its entry through the TOM transport machinery is likely through a cryptic internal localization sequence.

The generation of a "knock-in" mouse in which Cx43 was replaced with Cx32 introduces some controversy in terms of the ability of Cx32 to be localized to mitochondria. Using this mouse model, Miro-Casas and colleagues demonstrated by Western blotting of myocardium that Cx32 incorporates into the intercalated disk fraction, yet is virtually absent from the mitochondrial fraction (Miro-Casas, 2007). While it is entirely possible that connexins are targeted differently depending on the tissue, these data indicate the need for a separate detailed study concerning the subcellular localization of Cx32 specifically in hepatocytes (liver) and oligodendrocytes and their precursors (brain).

Possible roles of Cx32 in the mitochondria

This thesis will not address function empirically, as these studies will be performed as part of my Ph.D. research, however, as hypothesized for Cx43, Cx32 may interact with the mitochondrial respiration machinery at the inner mitochondrial membrane permitting speculation of function. This interaction could have a number of regulatory roles, and as indicated

for plasma membrane localized connexins, Cx32 may act as a scaffold to sequester necessary co-factors and metabolites of mitochondrial reactions close to where they will be used in the organelle. For example, the Cx32 binding partner, 3-ketoacyl-CoA thiolase, catalyzes the final step of beta-oxidation of lipids, which occurs in the mitochondrial matrix (Haddock et al., 1970). Either outer membrane or inner membrane localized Cx32 hemichannels or stacked assemblages of hemichannels could transiently bind this enzyme in close proximity to where is it needed in the matrix. Similarly, D-β-hydroxybutyric dehydrogenase, a lipid-requiring enzyme involved in butanoate metabolism, is found tightly tethered to the inner mitochondrial membrane (Latruffe et al., 1986). Perhaps, part the regulation of its enzymatic activity or attachment to the membrane is mediated through Cx32 localized to mitochondrial membranes. Finally, arginosuccinate synthase is an enzyme that catalyses the penultimate step in the urea cycle, which occurs on the cytoplasmic side of the mitochondria. While this enzyme is predicted to be cytoplasmic, immunolocalization shows that it is closely associated with the cytoplasmic side of the outer mitochondrial membrane, which may be mediated by its interaction with Cx32 (Cohen and Kuda, 1996).

The other mitochondrial proteins found to associate with Cx32 are transmembrane carrier proteins involved in respiration. Cx32 molecules could be involved in the maintenance of the structure of these complexes, or act as an assembly signal for their proper congregation in the inner membrane. Finally, if Cx32 forms hemichannels or stacked hemichannels

in the inner (or outer) mitochondrial membranes as is hypothesized for Cx43, it could be involved in ion and water regulation, and/or provide a conduit for the transport of molecules between these compartments.

Possible function of cytoplasmic and plasma membrane associated binding partners of Cx32

While the high percentage of mitochondrial interacting proteins represents the more novel findings of this study, new cytoplasmic and plasma membrane-associated binding partners were also identified. The cytoplasmic proteins found to interact with Cx32 include subunits 1 and 2 of the proteasome activator complex, and a protein similar to UbA52. While most Cx32 molecules in the liver are probably degraded by the lysosome pathway (Rahman et al., 1993), as is the case for most plasma membrane proteins, there is also evidence for their proteasomal degradation (Berthoud et al., 2004). The cytoplasmic interaction of Cx32 with these members of the proteasome complex provide more evidence that at least a fraction of Cx32 molecules are likely degraded via the ubiquitin-proteosome pathway.

The plasma membrane localized binding partners of Cx32 included two members of the Rab family of proteins, rab14, and rab18. There are over 60 members of this ras-related family of small GTPases that work in concert to control specific events in membrane fusion, trafficking, vesicle budding, and motility (Zerial and McBride, 2001). Specifically, rab14 is thought to regulate delivery of proteins/vesicles from the trans-golgi

network to the apical domain of the plasma membrane (Kitt et al., 2008), while rab18 is involved in vesicle trafficking between the golgi and endoplasmic reticulum (Dejgaard et al., 2008), and has been implicated in the regulation of secretory vesicle activity (Vazquez-Martinez et al., 2007). The interaction of these two rab proteins could have important roles in the trafficking of Cx32 to different intracellular compartments, and at the plasma membrane, could be implicated in the regulation of hepatocyte bile secretions to the caniculi (Suchy et al., 1997). Indeed, over-expression of Rab20 in Cx43-transfected HeLa cells causes Cx43 to be retained in the endoplasmic reticulum, suggesting an important role for rab proteins in the trafficking and localization of this connexin family member (Das Sarma et al., 2008). Perhaps most interesting however, is the putative role of rab proteins in signal transduction pathways that influence cell proliferation, cell nutrition, and the innate immune response. Moreover, there is evidence for a direct involvement of rab proteins in nuclear signalling (Bucci and Chiariello, 2006). Thus, a second line of future investigation will investigate whether these interactions (either direct or indirect) influence Cx32 sorting and thus function at different organelles.

A final Cx32-interacting protein of interest to our laboratory, in addition to Cx26, is the plasma membrane associated progesterone receptor component 1. There is a large body of literature describing fluctuations in the expression level of connexins, and in the size of gap junction plaques in response to changing levels of steroid hormones (Risek et al., 1995; Meda, 1996). Indeed, unpublished work from our

laboratory reveals the existence of progesterone-responsive elements in the promoter region of the Cx32 gene (McLean, Ph.D. thesis research). The current study suggests that in addition to the probable regulation of Cx32 transcription by steroid hormones, there may exist a second level of control wherein connexins physically bind progesterone and/or their receptor components.

Conclusions

The results from this study describe novel Cx32 interactions with proteins in multiple subcellular localizations whose careful characterization are likely to reveal important functions for the regulation of gap junction formation, function, and most probably most importantly, shed insight into ways connexins can be involved in intracellular signalling pathways. We have verified our method of MS/MS discovery of Cx32 binding partners through the identification of Cx26, the partner connexin of Cx32 in hepatocytes. Furthermore, we have verified by multiple assays that Cx32 interacts with the carrier protein SFXN-1 at both the mitochondrion, and more surprisingly, at the plasma membrane. We are unsure if this interaction is direct, or if it is mediated by one or more other proteins in complex. Future studies will determine if Cx32 plays a role in the plasma membrane localization of SFXN-1, and will elucidate the precise binding domains involved in this interaction. In addition, as part of my Ph.D. research, I will perform functional assays aimed at elucidating the biological significance of such an interaction in both liver, and more

importantly for the overarching rationale for this study, brain. The current study also suggests for the first time that Cx32 may have an important role in mitochondria, as has recently been proposed for Cx43. Indeed, the high percentage of mitochondrial proteins found to interact with Cx32, the co-fractionation and co-localization of Cx32 with mitochondria, and the strong probability that Cx32 could be targeted to mitochondria, are highly suggestive of an important role for Cx32 in this organelle.

References:

Ai Z, Fischer A, Spray DC, Brown AM, Fishman GI (2000) Wnt-1 regulation of connexin43 in cardiac myocytes. J Clin Invest 105:161-171.

Arakaki N, Nagao T, Niki R, Toyofuku A, Tanaka H, Kuramoto Y, Emoto Y, Shibata H, Magota K, Higuti T (2003) Possible role of cell surface H+ -ATP synthase in the extracellular ATP synthesis and proliferation of human umbilical vein endothelial cells. Mol Cancer Res 1:931-939.

Ayad WA, Locke D, Koreen IV, Harris AL (2006) Heteromeric, but not homomeric, connexin channels are selectively permeable to inositol phosphates. J Biol Chem 281:16727-16739.

Berthoud VM, Minogue PJ, Laing JG, Beyer EC (2004) Pathways for degradation of connexins and gap junctions. Cardiovasc Res 62:256-267.

Boengler K, Gres P, Cabestrero A, Ruiz-Meana M, Garcia-Dorado D, Heusch G, Schulz R (2006) Prevention of the ischemia-induced decrease in mitochondrial Tom20 content by ischemic preconditioning. J Mol Cell Cardiol 41:426-430.

Boengler K, Gres P, Dodoni G, Konietzka I, Di Lisa F, Heusch G, Schulz R (2007) Mitochondrial respiration and membrane potential after low-flow ischemia are not affected by ischemic preconditioning. J Mol Cell Cardiol 43:610-615.

Bucci C, Chiariello M (2006) Signal transduction gRABs attention. Cell Signal 18:1-8.

Bukauskas FF, Elfgang C, Willecke K, Weingart R (1995) Heterotypic gap junction channels (connexin26-connexin32) violate the paradigm of unitary conductance. Pflugers Arch 429:870-872.

Cascio M, Kumar NM, Safarik R, Gilula NB (1995) Physical characterization of gap junction membrane connexons (hemi-channels) isolated from rat liver. J Biol Chem 270:18643-18648.

Claros MG, Vincens P (1996) Computational method to predict mitochondrially imported proteins and their targeting sequences. Eur J Biochem 241:779-786.

Cohen NS, Kuda A (1996) Argininosuccinate synthetase and argininosuccinate lyase are localized around mitochondria: an immunocytochemical study. J Cell Biochem 60:334-340.

Dang X, Doble BW, Kardami E (2003) The carboxy-tail of connexin-43 localizes to the nucleus and inhibits cell growth. Mol Cell Biochem 242:35-38.

Das Sarma J, Kaplan BE, Willemsen D, Koval M (2008) Identification of rab20 as a potential regulator of connexin 43 trafficking. Cell Commun Adhes 15:65-74.

Dbouk HA, Mroue RM, El-Sabban ME, Talhouk RS (2009) Connexins: a myriad of functions extending beyond assembly of gap junction channels. Cell Commun Signal 7:4.

Dejgaard SY, Murshid A, Erman A, Kizilay O, Verbich D, Lodge R, Dejgaard K, Ly-Hartig TB, Pepperkok R, Simpson JC, Presley JF (2008) Rab18 and Rab43 have key roles in ER-Golgi trafficking. J Cell Sci 121:2768-2781.

De Palma A, Scalera V, Bisaccia F, Prezioso G (2003) Citrate uniport by the mitochondrial tricarboxylate carrier: a basis for a new hypothesis for the transport mechanism. J Bioenerg Biomembr 35:133-140.

Diekert K, Kispal G, Guiard B, Lill R (1999) An internal targeting signal directing proteins into the mitochondrial intermembrane space. Proc Natl Acad Sci U S A 96:11752-11757.

Elias JE, Haas W, Faherty BK, Gygi SP (2005) Comparative evaluation of mass spectrometry platforms used in large-scale proteomics investigations. Nat Methods 2:667-675.

Elias LA, Kriegstein AR (2008) Gap junctions: multifaceted regulators of embryonic cortical development. Trends Neurosci 31:243-250.

Elias LA, Wang DD, Kriegstein AR (2007) Gap junction adhesion is necessary for radial migration in the neocortex. Nature 448:901-907.

Fleming MD, Campagna DR, Haslett JN, Trenor CC, 3rd, Andrews NC (2001) A mutation in a mitochondrial transmembrane protein is responsible for the pleiotropic hematological and skeletal phenotype of flexed-tail (f/f) mice. Genes Dev 15:652-657.

Giepmans BN (2004) Gap junctions and connexin-interacting proteins. Cardiovasc Res 62:233-245.

Giepmans BN (2006) Role of connexin43-interacting proteins at gap junctions. Adv Cardiol 42:41-56.

Goodenough DA (1974) Bulk isolation of mouse hepatocyte gap junctions. Characterization of the principal protein, connexin. J Cell Biol 61:557-563.

Goubaeva F, Mikami M, Giardina S, Ding B, Abe J, Yang J (2007) Cardiac mitochondrial connexin 43 regulates apoptosis. Biochem Biophys Res Commun 352:97-103.

Haddock BA, Yates DW, Garland PB (1970) The localization of some coenzyme A-dependent enzymes in rat liver mitochondria. Biochem J 119:565-573.

Herve JC, Bourmeyster N, Sarrouilhe D (2004) Diversity in protein-protein interactions of connexins: emerging roles. Biochim Biophys Acta 1662:22-41.

Herve JC, Bourmeyster N, Sarrouilhe D, Duffy HS (2007) Gap junctional complexes: from partners to functions. Prog Biophys Mol Biol 94:29-65.

Hurford MT, Marshall-Taylor C, Vicki SL, Zhou JZ, Silverman LM, Rezuke WN, Altman A, Tsongalis GJ (2002) A novel mutation in exon 5 of the ALAS2 gene results in X-linked sideroblastic anemia. Clin Chim Acta 321:49-53.

Imbeault S, Gauvin LG, Toeg HD, Pettit A, Sorbara CD, Migahed L, DesRoches R, Menzies AS, Nishii K, Paul DL, Simon AM, Bennett SA (2009) The extracellular matrix controls gap junction protein expression and function in postnatal hippocampal neural progenitor cells. BMC Neurosci 10:13.

Jorge I, Casas EM, Villar M, Ortega-Perez I, Lopez-Ferrer D, Martinez-Ruiz A, Carrera M, Marina A, Martinez P, Serrano H, Canas B, Were F, Gallardo JM, Lamas S, Redondo JM, Garcia-Dorado D, Vazquez J (2007) High-sensitivity analysis of specific peptides in complex samples by selected MS/MS ion monitoring and linear ion trap mass spectrometry: application to biological studies. J Mass Spectrom 42:1391-1403.

Karniely S, Pines O (2005) Single translation--dual destination: mechanisms of dual protein targeting in eukaryotes. EMBO Rep 6:420-425.

Kim BW, Choo HJ, Lee JW, Kim JH, Ko YG (2004) Extracellular ATP is generated by ATP synthase complex in adipocyte lipid rafts. Exp Mol Med 36:476-485.

Kim KB, Lee JW, Lee CS, Kim BW, Choo HJ, Jung SY, Chi SG, Yoon YS, Yoon G, Ko YG (2006) Oxidation-reduction respiratory chains and ATP synthase complex are localized in detergent-resistant lipid rafts. Proteomics 6:2444-2453.

Kitt KN, Hernandez-Deviez D, Ballantyne SD, Spiliotis ET, Casanova JE, Wilson JM (2008) Rab14 regulates apical targeting in polarized epithelial cells. Traffic 9:1218-1231.

Kojima T, Kokai Y, Chiba H, Yamamoto M, Mochizuki Y, Sawada N (2001) Cx32 but not Cx26 is associated with tight junctions in primary cultures of rat hepatocytes. Exp Cell Res 263:193-201.

Kucharczyk R, Zick M, Bietenhader M, Rak M, Couplan E, Blondel M, Caubet SD, di Rago JP (2009) Mitochondrial ATP synthase disorders: molecular mechanisms and the quest for curative therapeutic approaches. Biochim Biophys Acta 1793:186-199.

Kumar NM, Gilula NB (1986) Cloning and characterization of human and rat liver cDNAs coding for a gap junction protein. J Cell Biol 103:767-776.

Latruffe N, Berrez JM, el Kebbaj MS (1986) Lipid-protein interactions in biomembranes studied through the phospholipid specificity of D-beta-hydroxybutyrate dehydrogenase. Biochimie 68:481-491.

Li H, Brodsky S, Kumari S, Valiunas V, Brink P, Kaide J, Nasjletti A, Goligorsky MS (2002) Paradoxical overexpression and translocation of connexin43 in homocysteine-treated endothelial cells. Am J Physiol Heart Circ Physiol 282:H2124-2133.

Lindqvist A, Berger K, Erlanson-Albertsson C (2008) Enterostatin up-regulates the expression of the beta-subunit of F(1)F(o)-ATPase in the plasma membrane of INS-1 cells. Nutr Neurosci 11:55-60.

Little MH, Wilkinson L, Brown DL, Piper M, Yamada T, Stow JL (2001) Dual trafficking of Slit3 to mitochondria and cell surface demonstrates novel localization for Slit protein. Am J Physiol Cell Physiol 281:C486-495.

Loewenstein WR, Kanno Y (1967) Intercellular communication and tissue growth. I. Cancerous growth. J Cell Biol 33:225-234.

Lyly A, Marjavaara SK, Kyttala A, Uusi-Rauva K, Luiro K, Kopra O, Martinez LO, Tanhuanpaa K, Kalkkinen N, Suomalainen A, Jauhiainen M, Jalanko A (2008) Deficiency of the INCL protein Ppt1 results in changes in ectopic F1-ATP synthase and altered cholesterol metabolism. Hum Mol Genet 17:1406-1417.

Mangiullo R, Gnoni A, Leone A, Gnoni GV, Papa S, Zanotti F (2008) Structural and functional characterization of F(o)F(1)-ATP synthase on the extracellular surface of rat hepatocytes. Biochim Biophys Acta 1777:1326-1335.

Martinez LO, Jacquet S, Esteve JP, Rolland C, Cabezon E, Champagne E, Pineau T, Georgeaud V, Walker JE, Terce F, Collet X, Perret B, Barbaras R (2003) Ectopic beta-chain of ATP synthase is an apolipoprotein A-I receptor in hepatic HDL endocytosis. Nature 421:75-79.

Meda P (1996) The role of gap junction membrane channels in secretion and hormonal action. J Bioenerg Biomembr 28:369-377.

Melanson-Drapeau L, Beyko S, Dave S, Hebb AL, Franks DJ, Sellitto C, Paul DL, Bennett SA (2003) Oligodendrocyte progenitor enrichment in the connexin32 null-mutant mouse. J Neurosci 23:1759-1768.

Miotto G, Tessaro S, Rotta GA, Bonatto D (2007) In silico analyses of Fsf1 sequences, a new group of fungal proteins orthologous to the metazoan sideroblastic anemia-related sideroflexin family. Fungal Genet Biol 44:740-753.

Miro-Casas E, Ruiz-Meana, M., Agulló, E., Torre, I., Cabestrero, A., Rodríguez-Sinovas, A., Morente, M., Boengler, K., Schulz, R., Heusch G., Garcia-Dorado, D. (2007) Mitochondrial connexin 43 hemichannels. J Mol Cell Cardiol 42:S120.

Miyake S, Yamashita T, Taniguchi M, Tamatani M, Sato K, Tohyama M (2002) Identification and characterization of a novel mitochondrial tricarboxylate carrier. Biochem Biophys Res Commun 295:463-468.

Moorby C, Patel M (2001) Dual functions for connexins: Cx43 regulates growth independently of gap junction formation. Exp Cell Res 271:238-248.

Nelles E, Butzler C, Jung D, Temme A, Gabriel HD, Dahl U, Traub O, Stumpel F, Jungermann K, Zielasek J, Toyka KV, Dermietzel R, Willecke K (1996) Defective propagation of signals generated by sympathetic nerve stimulation in the liver of connexin32-deficient mice. Proc Natl Acad Sci U S A 93:9565-9570.

Neveu MJ, Hully JR, Babcock KL, Vaughan J, Hertzberg EL, Nicholson BJ, Paul DL, Pitot HC (1995) Proliferation-associated differences in

the spatial and temporal expression of gap junction genes in rat liver. Hepatology 22:202-212.

Nicholson B, Dermietzel R, Teplow D, Traub O, Willecke K, Revel JP (1987) Two homologous protein components of hepatic gap junctions. Nature 329:732-734.

Paul DL (1986) Molecular cloning of cDNA for rat liver gap junction protein. J Cell Biol 103:123-134.

Rahman S, Carlile G, Evans WH (1993) Assembly of hepatic gap junctions. Topography and distribution of connexin 32 in intracellular and plasma membranes determined using sequence-specific antibodies. J Biol Chem 268:1260-1265.

Risek B, Klier FG, Phillips A, Hahn DW, Gilula NB (1995) Gap junction regulation in the uterus and ovaries of immature rats by estrogen and progesterone. J Cell Sci 108 (Pt 3):1017-1032.

Rodriguez-Sinovas A, Boengler K, Cabestrero A, Gres P, Morente M, Ruiz-Meana M, Konietzka I, Miro E, Totzeck A, Heusch G, Schulz R, Garcia-Dorado D (2006) Translocation of connexin 43 to the inner mitochondrial membrane of cardiomyocytes through the heat shock protein 90-dependent TOM pathway and its importance for cardioprotection. Circ Res 99:93-101.

Ruiz-Meana M, Abellan A, Miro-Casas E, Garcia-Dorado D (2007) Opening of mitochondrial permeability transition pore induces hypercontracture in Ca2+ overloaded cardiac myocytes. Basic Res Cardiol 102:542-552.

Ruiz-Meana M, Garcia-Dorado D, Miro-Casas E, Abellan A, Soler-Soler J (2006) Mitochondrial Ca2+ uptake during simulated ischemia does not affect permeability transition pore opening upon simulated reperfusion. Cardiovasc Res 71:715-724.

Ruiz-Meana M, Rodriguez-Sinovas A, Cabestrero A, Boengler K, Heusch G, Garcia-Dorado D (2008) Mitochondrial connexin43 as a new player in the pathophysiology of myocardial ischaemia-reperfusion injury. Cardiovasc Res 77:325-333.

Shogomori H, Brown DA (2003) Use of detergents to study membrane rafts: the good, the bad, and the ugly. Biol Chem 384:1259-1263.

Stojanovski D, Johnston AJ, Streimann I, Hoogenraad NJ, Ryan MT (2003) Import of nuclear-encoded proteins into mitochondria. Exp Physiol 88:57-64.

Stout C, Goodenough DA, Paul DL (2004) Connexins: functions without junctions. Curr Opin Cell Biol 16:507-512.

Suchy FJ, Sippel CJ, Ananthanarayanan M (1997) Bile acid transport across the hepatocyte canalicular membrane. FASEB J 11:199-205.

Tanno T, Fujiwara A, Sakaguchi K, Tanaka K, Takenaka S, Tsuyama S (2007) Slit3 regulates cell motility through Rac/Cdc42 activation in lipopolysaccharide-stimulated macrophages. FEBS Lett 581:1022-1026.

Valiunas V, Niessen H, Willecke K, Weingart R (1999) Electrophysiological properties of gap junction channels in hepatocytes isolated from

connexin32-deficient and wild-type mice. Pflugers Arch 437:846-856.

Vazquez-Martinez R, Cruz-Garcia D, Duran-Prado M, Peinado JR, Castano JP, Malagon MM (2007) Rab18 inhibits secretory activity in neuroendocrine cells by interacting with secretory granules. Traffic 8:867-882.

Vinken M, Henkens T, De Rop E, Fraczek J, Vanhaecke T, Rogiers V (2008) Biology and pathobiology of gap junctional channels in hepatocytes. Hepatology 47:1077-1088.

Ye X, Xu J, Cheng C, Yin G, Zeng L, Ji C, Gu S, Xie Y, Mao Y (2003) Isolation and characterization of a novel human putative anemia-related gene homologous to mouse sideroflexin. Biochem Genet 41:119-125.

Zerial M, McBride H (2001) Rab proteins as membrane organizers. Nat Rev Mol Cell Biol 2:107-117.

Zhang JT, Nicholson BJ (1989) Sequence and tissue distribution of a second protein of hepatic gap junctions, Cx26, as deduced from its cDNA. J Cell Biol 109:3391-3401.

Zheng H, Ji C, Zou X, Wu M, Jin Z, Yin G, Li J, Feng C, Cheng H, Gu S, Xie Y, Mao Y (2003) Molecular cloning and characterization of a novel human putative transmembrane protein homologous to mouse sideroflexin associated with sideroblastic anemia. DNA Seq 14:369-373.

Zheng YZ, Berg KB, Foster LJ (2009) Mitochondria do not contain lipid rafts, and lipid rafts do not contain mitochondrial proteins. J Lipid Res 50:988-998.

Supplemental Figure 3.1: HEK293A cells do not express messenger RNA for Cx30, Cx32, or C36.

(A) RT-PCR detection of human connexins from the human brain specimen used in Chapter 2. (B) Shows amplification of human connexins from HEK293A cells which express Cx26 mRNA only.

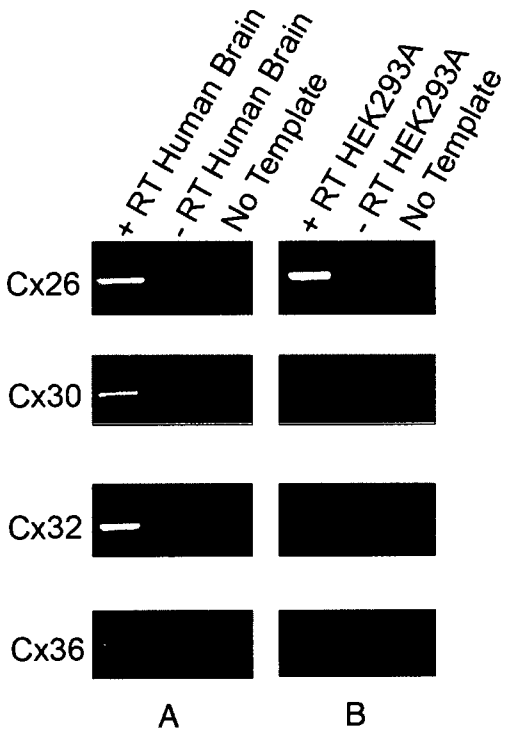

Supplemental Figure 3.1

Chapter 4: General Discussion

4.1 Plasma membrane channel-independent roles of connexins: ascribing new functions to gap junctions

In this thesis, I detected two distinct pools of Cx32 at the plasma membrane and mitochondrial membranes. Localization was validated through both subcellular fractionation and a proteomic approach that has begun to identify and characterize a novel Cx32 interactome with mitochondria-associated proteins. These data expand upon the emerging hypothesis that connexin proteins are more than just pore-forming proteins at the plasma membrane.

It is well established that connexins are the structural units of gap junctions; intercellular channels that mediate electrical and metabolic coupling between virtually all cell types. The variety of signalling molecules permeable to gap junctions, and their complexity at a structural level, permit the transduction of a plethora of cell and tissue-specific responses, enabling coupled cells to efficiently respond to minute changes in the microenvironment (Bruzzone et al., 1996; Rash et al., 2001; Alexander and Goldberg, 2003; Nagy et al., 2003a). The emerging hotspot in connexin biology is the idea that an alternate, yet demonstrably important function of connexin proteins, involves their interactions with other cellular proteins, channel complexes, and/or organelles (Giepmans, 2004; Herve et al., 2004; Giepmans, 2006). In this capacity, connexins do

not participate in communication via gap junctions at junctional plasma membranes or hemichannels at non-junctional plasma membranes, rather, protein-protein interactions are known to alter the proliferate rate of cells through participation in intracellular signalling cascades, or through direct transcriptional effects at the nucleus (Torok et al., 1997; Ai et al., 2000; Toyofuku et al., 2001; Giepmans, 2004; Herve et al., 2004; Giepmans, 2006; Duffy et al., 2007; Herve et al., 2007). Further, connexins can regulate NPC activation, migration, and specification (Dermietzel et al., 1989; Belliveau et al., 1991; Fulton, 1995; Melanson-Drapeau et al., 2003b; Elias and Kriegstein, 2008).

Our laboratory has shown that expression of Cx32 by a subset of NG2+ progenitor cells is a potent inhibitor of neurogenesis and likely restricts their fate to an oligodendrocyte lineage, yet this property was not mediated by direct cell-cell contact (Melanson-Drapeau et al., unpublished). Moreover, we found that brain injury potentiates Cx32 expression in NG2+ progenitors with the majority of activated cells deleted by an apoptotic-like mechanism (Melanson-Drapeau et al, unpublished). We hypothesized that the ability of Cx32 to inhibit neurogenesis, allow NPCs to respond to oligodendrocytic stimuli, and/or promote apoptotic deletion was mediated by protein interactions with Cx32. Therefore, the overarching objective of this thesis was to develop a method to identify protein interactions with Cx32 that could be involved in NPC fate specification. In the process, we identified a brain-specific cross reactivity that was dependent on protein conformation. To address this issue, I

have described a variety of reagents and methodologies to specifically detect Cx32 protein in brain tissues by IB. Furthermore, I developed a method of endogenous immunopurification from positive control liver tissue wherein I was able to identify and verify Cx32 protein interactions by LC-MS/MS. Together, these studies have suggested a novel subcellular localization of Cx32 at the mitochondria, corroborated by co-fractionation of Cx32 with mitochondria, and by the significant enrichment of mitochondrial proteins identified as Cx32-interactors. These methodologies and initial protein interaction screens represent the sum total of my M.Sc. research and provide the framework for my future PhD research.

4.2 Real solutions for solving the Cx32 brain-specific cross-reactivity issue

The connexin proteins are highly conserved amongst family members, a fact that has resulted in considerable difficulties for antibody design, testing, and use, especially prior to the creation of connexin null-mutant animals (Nagy et al., 2003b). Cx32 was the first gap junction protein to be studied in detail, and was isolated from liver, a homogenous tissue of which 80-85% of the total volume is the hepatocyte (Martin et al., 1992). Understandably, given that the liver only expresses small amounts of Cx26 and Cx43, two very divergent connexins compared to Cx32, antigenic determinants were discriminated relatively easily with specificity

proven for existing reagents. Analysis of Cx32 protein in the CNS, however, is more difficult due to the heterogeneity of cell types present, which together express eleven of the connexin family members (Rouach et al., 2002; Nakase and Naus, 2004; Sohl et al., 2005). The Cx32-null mutant mouse has enabled specific detection of Cx32 in myelinating glia and Schwann cells by IF analyses (Nelles et al., 1996; Dermietzel et al., 1997; Li et al., 1997; Nagy et al., 2003b), however, we and others (Freidin and Abrams, personal communication) have found that these same antibodies detect a 27-32 kDa cross reactive species in immunblots of brain and spinal cord that prevents accurate measurement of Cx32 protein levels.

The overarching goal of this thesis was to determine protein interactions with Cx32 that may be involved in channel-independent functions of Cx32 pertaining to the specification of NPC fate. To perform the proteomic analyses necessary to accomplish this task, confirmation of the specificity of the reagents to be used was of utmost importance. In Chapter 2, we tested a panel of ten Cx32 antibodies by IF, IB, and IP to determine the most specific reagents for brain, using the liver as a non-cross-reactive positive control, and confirming all results with tissue derived from null-mutant mice. Most antibodies were specific for Cx32 in both liver and brain by immunofluorescent analyses, and all antibodies were specific for Cx32 in liver immunoblots as expected. However, in brain immunoblots, only two of the antibodies specifically detected Cx32, while the other eight antibodies detected a cross-reactive protein(s) in the

$Cx32^{Y/-}$ lysates. From these results we hypothesized that maintenance of the tertiary structure of the protein during antigen binding was necessary for specific detection of Cx32, and that denaturation of the lysate unmasked linear epitopes recognized by the majority of Cx32 antibodies. As such, we verified that IP of Cx32 with a cross-reactive antibody prior to denaturing IB prevented unmasking of such epitopes, and abrogated antibody cross-reactivity. To further characterize the nature of the cross-reactive epitopes, we performed sucrose gradient fractionation of whole liver and brain tissues, and found that brain Cx32 was specifically localized to intermediate fractions 4, and 5 (only detected in $Cx32^{Y/+}$ fractionations), enriched for mitochondrial and plasma membrane marker proteins, while the cross-reactive species localized to fractions 6-10 in both genotypes with enrichment in lysosomal and golgi compartments. Moreover, liver and brain Cx32 had mobilities of 31-32 kDa, while the cross species was approximately 4 kDa smaller.

We also show that the CNS-specific epitope unmasked following denaturing SDS-PAGE is present in mouse brain prepared from multiple connexin null-mutants, and is likely not another connexin. Ultimately, the results of this study show that Cx32 protein can be specifically detected in the brain by IB, simply by the use of the appropriate reagents (AB5 or AB10, see Chapter 2, Table 2.1), or by initial IP of the protein lysates, a finding that contributes substantially to CNS researchers in the connexin field, and also enables us to proceed confidently with proteomic analyses of Cx32 interaction partners.

4.3 Development of an endogenous purification method from tissue

Due to the technical issues surrounding Cx32 detection in the brain, I used liver, wherein Cx32 is more abundant, to develop a method of immunopurifying endogenous Cx32 from homogenized tissue. The advantages of such purifications are that proteins can be isolated directly from their normal environment, complete with the proper complement of biologically relevant interacting partners. In purifications from tissue culture cells transfected with epitope tagged bait proteins, one must always keep in mind that depending on the size and charge of the tag, it may alter the subcellular location and/or function of the bait protein (Laird et al., 2001; Kumar et al., 2002) and due to the heterologous nature of the expression system, spurious interactions are not uncommon (Kumar et al., 2002; Zhu et al., 2003). Furthermore, from endogenous immunopurifications, we can exclude proteins based on the analyses of null mutant tissues, which represent the most robust negative control.

Our endogenous IPs of liver Cx32 were originally attempted using RIPA-extracted whole protein lysates, however, upon silver staining of the products, there was no visual distinction between the $Cx32^{Y/+}$ $Cx32^{Y/-}$ lanes, indicating the presence of spurious interactions from the complex protein lysate even in liver wherein Cx32 protein levels are highest (Cox and Emili, 2006). To enrich lysates for target protein, we used the sucrose gradient fractionation technique employed in Chapter 2, and purified only

the fractions immunoreactive for Cx32, using their corresponding $Cx32^{Y/-}$ fractions as the negative controls. This technique resulted in clear banding differences between positive and negative control lanes, and the LC-MS/MS analysis of both $Cx32^{Y/+}$ and $Cx32^{Y/-}$ gel sections in parallel provided an excellent way to minimize false positive interactions by the elimination of proteins present in both lanes.

Using this technique, we identified our "bait" protein, Cx32, as well as Cx26, which is known to interact with Cx32 at the plasma membrane of hepatocytes, making it an excellent interaction to highlight the effectiveness of our purification method for membrane proteins. After increasing the amount of input protein from 1 mg to 5 mg, we reproduced many of the original interactions, and were able to identify significantly more proteins in complex with Cx32. While cytoplasmic and plasma membrane-associated interacting proteins were detected, we were particularly excited with the observation that the majority of proteins identified from this screen were mitochondrial, based on our finding in Chapter 2 that Cx32 co-fractionated in sucrose gradients enriched for mitochondrial markers. This result provided another line of evidence supporting our initial observation that perhaps a fraction of cellular Cx32 protein localizes to mitochondria.

4.4 Cx32 interacts with the mitochondrial protein SFXN-1

To further pursue this finding, in addition to verifying the interaction

between Cx32 and Cx26 by co-IP, we chose also to concentrate on the mitochondrial protein SFXN-1. SFXN-1 was identified in both rounds of mass spectrometry, and was also an attractive candidate due to its connection with the (f/f) anemic phenotype. SFXN-1 and its four related family members are widely expressed in the mitochondria of numerous tissues, and may facilitate the transport of a component required for iron utilization into or out of the mitochondria, however, the function of SFXN-1has not been directly assessed (Fleming et al., 2001). We are confident that SFXN-1 is a bona-fide interaction partner of Cx32 due to its presence in both rounds of MS, its successful bi-directional co-IP with Cx32 from both Triton-solubilised and detergent-free lysates, and its immunofluorescent co-localization with intracellular pools of Cx32.

An interesting observation that arose from the detergent-free purification of mitochondria was that SFXN-1 was enriched in mitochondria, but also in the pure plasma membrane fraction that floated above the mitochondrial fractions following the sucrose gradient ultracentrifugation step. These fractionations clearly show that a significant amount of SFXN-1 protein is located in membranes containing the Na^+K^+ATPase, a result that was completely unexpected based on previous reports that SFXN-1 and other SFXN family members are mitochondrial proteins (Fleming et al., 2001; Miyake et al., 2002; Yoshikumi et al., 2005; Miotto et al., 2007). One possibility for the discrepancy in subcellular localization of SFXN family members between the current study and those of Fleming and Yoshikumi is that SFXN

localization was assessed in different tissue culture cell lines, and perhaps SFXN-1 has tissue-specific roles that rely on differential subcellular targeting. In these studies, SFXN-1 (in HEK293 cells) and SFXN-3 (in rat INS-1 cells) co-localized only with Mitotracker Red, however, neither of these cell types expressCx32 mRNA or protein (Vozzi et al., 1995; Charollais et al., 1999). Thus, Cx32 protein expression may be required for plasma membrane targeting of SFXN-1 in hepatocytes, and this dual targeting is likely an important mechanism of the yet undiscovered function(s) of SFXN-1. Our data clearly indicate that SFXN-1 localizes to mitochondria in HEK293A, cells but we have yet to examine whether ectopic expression of Cx32 alters this subcellular localization. We further intend to determine if SFXN-1 can target to the plasma membrane in the absence of Cx32 by probing the $Cx32^{Y/+}$ and $Cx32^{Y/-}$ mitochondria and plasma membrane fractions in Figure 3.5 for SFXN-1. Further, co-IF for SFXN-1 and a plasma membrane marker, along with Mitotracker Red staining in isolated hepatocytes will also help to determine if SFXN-1 localization is dependent upon the expression of Cx32.

4.5 Cx32 is enriched at the plasma membrane yet is present at low levels in liver mitochondria

The detergent-free purification of Cx32 from liver tissue provides the most convincing data that a small pool of Cx32 is targeted to the mitochondrion (Figure 3.5). While the majority of Cx32 is present in the

plasma membrane fractions, Cx32 is detected in all mitochondrial fractions, even those well separated from the plasma membrane fractions. Thus, as we have shown for SFXN-1, Cx32 also appears to experience dual targeting to both the plasma membrane and the mitochondrion.

Another indication that Cx32 may have functions in the mitochondria comes from the overwhelming contribution of mitochondrial proteins to the total number of Cx32 interactions. Of the nineteen proteins identified, eleven were mitochondrial (58%). While it is tempting to propose this novel subcellular localization for Cx32, we must also entertain the possibility that the high contribution of mitochondrial proteins to this list is due to the fact that mitochondria are protein-dense organelles, and the sheer concentration of proteins contained within fractions 4, 5, and 6 created a non-relevant abundance in the detection of mitochondrial proteins by MS. It is known that mitochondrial proteins often contaminate preparations of other organelles (Cox and Emili, 2006; Zheng et al., 2009), however, the spurious detection of mitochondrial proteins in our experiments is highly unlikely given our rigorous negative control purification from the same $Cx32^{Y/-}$ fractions.

In addition to suggesting that Cx32 can interact with mitochondrial proteins, these results highlight possible differences in the binding strength and kinetics of Cx32 interactions between plasma membrane and mitochondrial proteins. As shown in Chapter 2 and by numerous others, the majority of Cx32 is localized to the plasma membrane, where gap junction puncta clearly define the periphery of individual heptatocytes

(Paul, 1986; Rahman et al., 1993; Kojima et al., 1999; Kostin et al., 1999; Kojima et al., 2001; Duffy et al., 2007). We would therefore expect to find an abundance of plasma membrane or cytoplasmic proteins interacting with Cx32, especially given that the fractions were also enriched for the lipid raft markers Caveolin-1 and Flotillin-1. It is possible that Cx32 interactions with proteins at the plasma membrane are more transient, and therefore, weaker than interactions in the mitochondrion. If Cx32 is involved in the sequestration of intracellular signalling molecules at the plasma membrane, as has been suggested for Cx43, these interactions are likely transient and subject to constant remodelling in response to a variety of cues. Indeed, chemical cross-linking of protein homogenates prior to IP is often required for the detection of transient proteins interactions by MS (Kluger and Alagic, 2004), which could explain the lower occurrence of plasma membrane and cytoplasmic proteins in our screens.

Another line of evidence supporting the mitochondrial localization of Cx32 comes from the significant co-localization of its binding partner SFXN-1, and Mitotracker Red in HEK293A cells by IF. We have shown by tissue fractionation and co-IP studies that the interaction between Cx32 and SFXN-1 occurs at both the plasma membrane and at the mitochondrion, however, more detailed co-localization studies in primary hepatocytes and in isolated mitochondria are necessary to further corroborate this result.

The presence of a small pool of Cx32 in liver mitochondria is further substantiated given that Cx32 is predicted to target to the mitochondrion. Indeed, analysis of the N-terminal region of Cx32 reveals a high probability (P = 0.81) for the existence of a mitochondrial targeting motif (MitoProt, (Claros and Vincens, 1996). The ability of proteins to localize to mitochondria is encoded by N-terminal localization sequences, or by cryptic sites that are recognized by chaperone proteins and the mitochondrial import machinery (Claros and Vincens, 1996; Diekert et al., 1999; Stojanovski et al., 2003; Rodriguez-Sinovas et al., 2006). Although heterogeneous in nature, mitochondrial targeting sequences are often characterized by an enrichment of Arg, Leu, Ser and Ala, the presence of at least two positively charged residues, few acidic resides, and the ability to form alpha helical amphiphilic structures (von Heijne, 1986; von Heijne et al., 1989; Pak and Weiner, 1990; Claros and Vincens, 1996). Unlike Cx32, SFXN-1 is predominantly localized to mitochondria, yet does not contain an N-terminal mitochondrial targeting sequence, indicating its recognition by the mitochondrial import machinery is likely mediated by cryptic targeting pockets present in the tertiary structure of the protein, as has also been hypothesized is the case for mitochondrial Cx43 (Rodriguez-Sinovas et al., 2006).

Finally, the newly-discovered yet important roles of Cx43 in cardiac mitochondria also support a possible role for Cx32 at hepatocyte (and by inference to the fractionation data presented in Chapter two) CNS cell-derived mitochondria. IF and LC-MS have confirmed the presence of a

small fraction of cellular Cx43 localized to mitochondria (Rodriguez-Sinovas et al., 2006; Jorge et al., 2007), and this contribution increases following stress and as part of the normal ageing process (Boengler et al., 2007; Ruiz-Meana et al., 2008). Mitochondrial Cx43 is also involved in preconditioning to ischemic stress, for the maintenance of normal respiration control ratios, and for the regulation of mitochondrial matrix volume (Li et al., 2002; Boengler et al., 2006; Rodriguez-Sinovas et al., 2006; Ruiz-Meana et al., 2006; Boengler et al., 2007; Miro-Casas, 2007; Ruiz-Meana et al., 2007; Ruiz-Meana et al., 2008). Presumably, the homologous nature of the connexin family of proteins could indicate overlapping roles for both Cx43 and Cx32 in the mitochondria. We know from its interaction with SFXN-1 that Cx32 may be involved in mitochondrial iron acquisition, and from other mitochondrial interactions, can hypothesize its involvement in beta-oxidation of lipids, butanoate metabolism, and the urea cycle. However, this hypothesis remains speculative and will require direct assessment.

4.6 Mitochondria are involved in cell cycle regulation and differentiation

The overarching goal of my graduate work, both this M.Sc. and future Ph.D. studies, is to assess whether Cx32 functions independently of a canonical gap junction/hemichannel mechanism to regulate NPC fate. The significance of Cx32 interactions in the mitochondria in relation to

NPC fate specification indicate a departure from the traditional roles of mitochondria as the "powerhouses" of the cell, toward the emerging view that mitochondria are actually regulatory organelles, and represent an important source of biological signals that control cell fate (Coffman and Denegre, 2007; Van Blerkom, 2008). As such, the data presented in this thesis allow for possible speculation into how Cx32 could impact upon NPC fate. In general, the mitochondria of undifferentiated cells are few and small, with undeveloped cristae, however, upon differentiation, mitochondrial mass and number increase, representing a visual indicator for the importance of mitochondrial functions during fate determination (Cho et al., 2006). Corresponding with these changes in mitochondrial mass and number upon differentiation, mitochondria, through their ability to modulate the redox state of the intracellular environment, are involved in a number of redox-specific intracellular signalling pathways that appear to impact directly on the self-renewal and differentiation of progenitor cells (Irani et al., 1997; Kamata and Hirata, 1999; Smith et al., 2000; Dal-Pizzol et al., 2001; Connor et al., 2005; Ogasawara and Zhang, 2008). While the signalling cascades leading to alterations of such progenitor cell characteristics can vary, the ultimate outcomes can be simplified: it seems that an overall reduction of the cellular environment promotes progenitor self-renewal, while oxidation promotes differentiation (Smith et al., 2000). Smith and colleagues suggest that unlike specific effectors known to play a part in either proliferation or differentiation, such as p27, the redox state of progenitor populations is more of a central modulator of

these processes. Indeed, the intracellular redox state is both necessary and sufficient to modulate the balance between self-renewal and differentiation in dividing oligodendrocyte-type-2-astrocyte progenitor (O-2A) cells. In these experiments, the authors describe how cells with low oxidative loads (as measured by Rosamine fluorescence) exhibited a greater tendency to self-renew, while cells with higher oxidative loads rapidly differentiated. Treatment with the self-renewal factor neurotrophin 3 (NT-3) caused an overall reduction of the intracellular environment, and corresponded to an increase in the mitochondrial inner membrane potential ($\Delta\Psi$), which has been shown to induce a more reduced cell state. Conversely, treatment with thyroid hormone (TH), a promoter of oligodendrocyte differentiation, caused an oxidation of the intracellular environment and a decrease in $\Delta\Psi$ (Smith et al., 2000). These results clearly indicate that the intracellular redox state is a potent determinant of progenitor cell status, and that the mitochondrion is an important effecter of this process.

Iron, and the acquisition of iron to the mitochondrial respiratory proteins is also an important pathway that has been linked to the activation and differentiation of progenitor cells. Ishii and colleagues showed a marked increase in mitochondrial biogenesis during differentiation of pre-osteoclasts to mature osteoclasts, which reabsorb bone and mediate mineral homeostasis (Ishii et al., 2009). Furthermore, the upregulation of iron intake by corresponding increases in the iron transport machinery was

essential for the production of mature osteoclasts, while chelation of iron inhibited the differentiation of pre-osteoclasts. This line of research is particularly interesting to us, considering oligodendrocytes closely resemble octeoclasts in their requirement for a high-energy status, and also for iron. In fact, oligodendrocytes stain more prominently for iron than any other cell type in the brain (Zhang et al., 2005).

4.7 Role of Cx32/SFXN-1 interaction in the mitochondria

The examples above provide converging evidence for the involvement of both mitochondrial energetics and iron in cell differentiation programs, and can lead us to hypothesize that modulation of either of these pathways will induce changes in the proliferation or differentiation of progenitor cell populations. The Cx32 binding partner, SFXN-1, is predicted to localize to mitochondria, and due to the anemic phenotype of the (f/f) mouse, is thought to participate in mitochondrial iron utilization and heme biosysthesis. Unfortunately there is only a small body of literature concerning SFXN-1 and its family members (Capobianco et al., 1995; Fleming et al., 2001; Miyake et al., 2002; Yoshikumi et al., 2005; Miotto et al., 2007), however, given the importance of iron metabolism in cell differentiation, we hypothesize that SFXN-1 may be involved in this process in both regenerating hepatocytes, and in differentiating OPCs. Indeed, I have shown that SFXN-1 is highly expressed in liver, as is also the case for whole brain (Supplemental Fig 4.1).

As support for the hypothesis that SFXN-1 is involved in differentiation, Nakajima and colleagues have reported that heme biosynthesis and supply is necessary for the differentiation and iron metabolism of erythroid cells during hematopoeisis (Nakajima et al., 1999). Furthermore, transcription of SFXN-3 and other family members are significantly increased during pancreatic islet cell differentiation. These authors hypothesize that SFXN family members, through their function as channels or carrier molecules of the mitochondrion could be involved in regeneration of pancreatic endocrine cells (Yoshikumi et al., 2005).

If Cx32 also interacts with SFXN-1 in the mitochondria of progenitor cells in the brain, it is tempting to hypothesize that when Cx32 protein is first expressed in OPC populations, it is transported to either the outer or inner mitochondrial membrane where it activates or regulates the putative iron metabolism functions of SFXN-1. In turn, upregulation of iron utilization and associated mitochondrial signalling pathways could act as a molecular differentiation switch, allowing these progenitor cell populations to respond to environmental cues promoting either programmed cell death, or oligodendrogenesis (Melanson-Drapeau et al., 2003a). Given that only small fluctuations in the redox state of cells are sufficient to induce profound cellular changes, only a small amount of mitochondrial Cx32 would be necessary to initiate this differentiation cascade (Smith et al., 2000). In the absence of cues from Cx32, OPCs are less likely to embark upon such a differentiation pathway, as is seen by the dramatic

shift to the production of neuronal phenotypes by this subset of cells in the Cx32-null animal (Melanson-Drapeau et al., unpublished). Thus, the ability of OPCs to respond to extrinsic oligodendrocytic, neuronal, or death stimuli may be modulated by the intrinsic interactions of Cx32 with SFXN-1, or other mitochondrial proteins.

4.8 Possible roles of Cx32 in mitochondrial protein complexes

The mitochondrial localization of Cx32 in either liver or mature oligodendrocytes has never been investigated, and to our knowledge, there are no reported mitochondrial abnormalities in male $Cx32^{Y/-}$ or female $Cx32^{-/-}$ animals, nor in CMT patients presenting any number of Cx32 mutations: CMT results in mild peripheral neuropathy characterized by muscle weakness and fatigue (Niemann et al., 2006) while Cx32 null-mutant animals exhibit defective propagation from sympathetic nerves in the liver, yet do not show any morphology or conduction deficits of sciatic or facial nerves (Nelles et al., 1996). It is possible that ablation of Cx32 in mice or its mutation in humans results in subclinical mitochondrial abnormalities that are only evident upon significant challenge. We therefore propose two hypotheses to describe other possible roles of Cx32 in mitochondrial protein complexes: (1) Cx32 at the mitochondria renders cells more susceptible to oxidative stress, or (2) Cx32 at the mitochondria protects cells from oxidative stress. No matter the outcome of these two testable hypotheses, it is likely that alteration of the plasma

membrane:mitochondrial Cx32 ratio is involved in the cell's response to a variety of stressors.

Hypothesis 1 states that mitochondrial Cx32 renders cells more susceptible to oxidative stress. Similarly, pathological increase of normal levels of mitochondrial Cx32 may be detrimental, and may explain why a large proportion of NG2+ OPCs activated by the oxidative stressor kainic acid, show an induction of Cx32 and undergo apoptosis before differentiating to oligodendrocytes (Gluck et al., 2000). Furthermore, there are reports that Cx32 is able to interact with alpha-synuclein, the non-β-amyloid moiety of the ameloid precursor protein (Junn and Mouradian, 2002; Sung et al., 2007). Over-expression of alpha-synuclein is associated with increases in reactive oxygen species (ROS), which may be mediated by Cx32 translocation of alpha-synuclein aggregates to the mitochondria (Junn and Mouradian, 2002).

Here, mitochondrial overload of Cx32, especially in complex with alpha-synuclein aggregates, would likely result in increased susceptibility to ROS.

Support for a protective effect of mitochondrial Cx32 comes from the mounting evidence that mitochondrial Cx43 is responsible for the diazoxide-induced preconditioning of cardiomyocytes to oxidative stress (Rodriguez-Sinovas et al., 2006; Ruiz-Meana et al., 2006; Ruiz-Meana et al., 2007; Ruiz-Meana et al., 2008; Penna et al., 2009). These studies also represent an example of a how loss of mitochondrial Cx43 would result in subclinical mitochondrial pathologies, until a large enough stress

resulted in abnormal cardiomyocyte death due to a lack of preconditioning to ROS.

4.9 Role of Cx32/SFXN-1 interaction at the plasma membrane

In addition to probable roles of the Cx32/SFXN-1 interaction in mitochondria, the Cx32/SFXN-1 interaction at the plasma membrane is suggestive of a "sequestering" mechanism by Cx32, wherein Cx32 at the plasma membrane retains SFXN-1 and prevents its translocation to the mitochondrion. There have been several reports that connexins associate with known intracellular signalling proteins, thereby altering their ability to affect downstream targets. For example, the transcription factor, ZO-1-associated nucleic acid-binding protein (ZONAB) binds to ZO-1, a scaffolding protein that has been localized to both oligodendrocyte and astrocyte gap junctions (Penes et al., 2005). ZONAB is known to repress expression of the tyrosine kinase receptor ErbB2, and thus it has been hypothesized that sequestering of ZONAB by ZO-1 de-represses ErbB2 expression (Balda and Matter, 2000). ErbB2 is the receptor for neuregulin, and neuregulin-ErbB2 signalling pathways control oligodendrocyte survival, differentiation and myelination (Park et al., 2001; Kim et al., 2003). Another example of protein sequestration by connexins occurs in hepatocytes wherein Cx32 maintains the tumor-supressor protein Dlgh1 at the plasma membrane, where it is known to regulate growth by blocking the cell cycle in the G0/G1 phase (Funke et al., 2005;

Duffy et al., 2007). Following the loss of Cx32, Dlgh1 translocates to the nucleus where it has been shown to increase cell proliferation (Funke et al., 2005).

The sequestration of SFXN-1 by Cx32 at the plasma membrane could serve to regulate the amount of mitochondrial SFXN-1 available to participate in its supposed carrier protein functions. Dynamic regulation of mitochondrial SFXN-1 could be implicated in various mitochondrial processes. For example, if SFXN-1 is indeed responsible for the import of pyridoxine to the mitochondrial matrix to act as a cofactor for ALAS2, the levels of mitochondrial SFXN-1 could directly affect the amount of heme that is synthesized, which in turn results in the chelation of mitochondrial iron. The upregulation of heme biosynthesis is associated with numerous cellular processes, including the differentiation of N2a cells (Shinjyo and Kita, 2006), while the chelation of mitochondrial iron prevents iron-mediated hydroxyl radical formation which can lead to significant mitochondrial damage (Santos et al., 2001; Shinjyo and Kita, 2006).

An alternate hypothesis is that SFXN-1 has function at the plasma membrane, and requires plasma membrane-associated Cx32 to traffic there. Support for this hypothesis comes from the observation that SFXN-1 localizes primarily to mitochondria in HEK293 and INS-1 cell lines that do not express Cx32, however, SFXN-1 appears to be distributed fairly evenly between mitochondria and the plasma membrane in liver tissue that expresses Cx32. It is possible that SFXN-1 functions at the plasma membrane as a transport molecule for tricarboxylates such as citrate,

since the liver readily uptakes citrate from the blood through the NaCT tricarboxylate transporter (Mycielska et al., 2009) despite controversial literature (Azzi et al., 1993; Fleming et al., 2001). The NaCT transporter, along with the other main plasma membrane Na+/dicarboxylate/tricarboxylate co-transporters, NaDC1 and NaDC3, have varying specificities for the valency of the species transported, and efficiency of transport is differentially affected by pH_o, leading one to hypothesize that other citrate transporters with different specificities could exist (Pajor, 2000). Furthermore, Mycielska and colleagues report that especially for outward transport of di-and tricarboxylates, the transport mechanisms are unknown. SFXN-1 could mediate the outward transport of citrate and other citric acid cycle intermediates, wherein neighboring Cx32 and/or Cx26 could buffer the exchange of charged species to maintain membrane potential, as has been proposed for the Cx43 and Aquaporin4 association in astrocytes (Nicchia et al., 2005).

5.0 General Conclusions

In conclusion, we have developed techniques and identified appropriate reagents to specifically detect Cx32 in liver and brain by IF, IB and IP. Using these techniques, I have successfully immunopurified Cx32 from liver fractions enriched for Cx32, and identified nineteen protein interactions, most of which were novel and consisted of mitochondrial proteins. This surprising contribution of mitochondrial interactions led us to further validate Cx32 interaction with SFXN-1, a relatively new protein

with unclear functions related to iron metabolism. Given our original hypothesis that protein-protein interactions with Cx32 were responsible for the Cx32-mediated inhibition of neurogenesis of a subset of NG2+ OPCs in the hippocampus, we discuss the possible function of Cx32/SFXN-1 interactions in the mitochondria in relation to modulation of progenitor cell fate, and suggest possible roles of Cx32 in mitochondrial protein complexes. We hypothesize that a tightly regulated proportion of cellular Cx32 is localized to the mitochondria, and that alterations in this balance can be detrimental under certain conditions of stress. Furthermore, small contributions of mitochondrial Cx32 may mediate critical molecular events during the differentiation of NG2+ OPC progenitor cell populations. In addition, we have discovered that in liver tissue, a portion of the mitochondrial protein SFXN-1 is localized at the plasma membrane, and interacts with Cx32. We suggest that this dual localization could be mediated by Cx32, in that binding to this connexin either sequesters SFXN-1 from the mitochondria, or actually facilitates the traffic of SFXN-1 to the plasma membrane where it fulfils functions of its own.

My Ph.D. work will continue with this research to fully characterize the novel finding that Cx32 can localize to mitochondria, and that protein interactions in this organelle may have profound effects on the fate of progenitor cell populations. Future work will also describe the precise protein interaction domains and trafficking mechanisms involved in the Cx32/SFNX-1 interaction, and validate additional proteins identified in these original screens by co-IP and co-IF. Finally, using the techniques

developed in Chapter 2, we will perform Cx32 immunopurifications from myelinating glia and NPC populations with the ultimate goal of generating brain-specific interaction profiles for Cx32. Investigating the channel-independent functions of Cx32 by the generation of protein interaction networks will be an important step in determining how Cx32 is involved in NPC fate determination, and how we can modulate this process to regenerate functional neuronal networks in degenerative disease states, or following traumatic brain or spinal cord injury.

References:

Ai Z, Fischer A, Spray DC, Brown AM, Fishman GI (2000) Wnt-1 regulation of connexin43 in cardiac myocytes. J Clin Invest 105:161-171.

Alexander DB, Goldberg GS (2003) Transfer of biologically important molecules between cells through gap junction channels. Curr Med Chem 10:2045-2058.

Balda MS, Matter K (2000) The tight junction protein ZO-1 and an interacting transcription factor regulate ErbB-2 expression. EMBO J 19:2024-2033.

Belliveau DJ, Kidder GM, Naus CC (1991) Expression of gap junction genes during postnatal neural development. Dev Genet 12:308-317.

Boengler K, Gres P, Cabestrero A, Ruiz-Meana M, Garcia-Dorado D, Heusch G, Schulz R (2006) Prevention of the ischemia-induced decrease in mitochondrial Tom20 content by ischemic preconditioning. J Mol Cell Cardiol 41:426-430.

Boengler K, Gres P, Dodoni G, Konietzka I, Di Lisa F, Heusch G, Schulz R (2007) Mitochondrial respiration and membrane potential after low-flow ischemia are not affected by ischemic preconditioning. J Mol Cell Cardiol 43:610-615.

Bruzzone R, White TW, Paul DL (1996) Connections with connexins: the molecular basis of direct intercellular signalling. Eur J Biochem 238:1-27.

Capobianco L, Bisaccia F, Michel A, Sluse FE, Palmieri F (1995) The N- and C-termini of the tricarboxylate carrier are exposed to the cytoplasmic side of the inner mitochondrial membrane. FEBS Lett 357:297-300.

Charollais A, Serre V, Mock C, Cogne F, Bosco D, Meda P (1999) Loss of alpha 1 connexin does not alter the prenatal differentiation of pancreatic beta cells and leads to the identification of another islet cell connexin. Dev Genet 24:13-26.

Cho YM, Kwon S, Pak YK, Seol HW, Choi YM, Park do J, Park KS, Lee HK (2006) Dynamic changes in mitochondrial biogenesis and antioxidant enzymes during the spontaneous differentiation of human embryonic stem cells. Biochem Biophys Res Commun 348:1472-1478.

Claros MG, Vincens P (1996) Computational method to predict mitochondrially imported proteins and their targeting sequences. Eur J Biochem 241:779-786.

Coffman JA, Denegre JM (2007) Mitochondria, redox signalling and axis specification in metazoan embryos. Dev Biol 308:266-280.

Connor KM, Subbaram S, Regan KJ, Nelson KK, Mazurkiewicz JE, Bartholomew PJ, Aplin AE, Tai YT, Aguirre-Ghiso J, Flores SC,

Melendez JA (2005) Mitochondrial H2O2 regulates the angiogenic phenotype via PTEN oxidation. J Biol Chem 280:16916-16924.

Cox B, Emili A (2006) Tissue subcellular fractionation and protein extraction for use in mass-spectrometry-based proteomics. Nat Protoc 1:1872-1878.

Dal-Pizzol F, Klamt F, Dalmolin RJ, Bernard EA, Moreira JC (2001) Mitogenic signalling mediated by oxidants in retinol treated Sertoli cells. Free Radic Res 35:749-755.

Dermietzel R, Farooq M, Kessler JA, Althaus H, Hertzberg EL, Spray DC (1997) Oligodendrocytes express gap junction protein connexin32 and connexin45. Glia 20:101-114.

Dermietzel R, Traub O, Hwang TK, Beyer E, Bennett MV, Spray DC, Willecke K (1989) Differential expression of three gap junction proteins in developing and mature brain tissues. Proc Natl Acad Sci U S A 86:10148-10152.

Diekert K, Kispal G, Guiard B, Lill R (1999) An internal targeting signal directing proteins into the mitochondrial intermembrane space. Proc Natl Acad Sci U S A 96:11752-11757.

Duffy HS, Iacobas I, Hotchkiss K, Hirst-Jensen BJ, Bosco A, Dandachi N, Dermietzel R, Sorgen PL, Spray DC (2007) The gap junction protein connexin32 interacts with the Src homology 3/hook domain of discs large homolog 1. J Biol Chem 282:9789-9796.

Elias LA, Kriegstein AR (2008) Gap junctions: multifaceted regulators of embryonic cortical development. Trends Neurosci 31:243-250.

Fleming MD, Campagna DR, Haslett JN, Trenor CC, 3rd, Andrews NC (2001) A mutation in a mitochondrial transmembrane protein is responsible for the pleiotropic hematological and skeletal phenotype of flexed-tail (f/f) mice. Genes Dev 15:652-657.

Fulton BP (1995) Gap junctions in the developing nervous system. Perspect Dev Neurobiol 2:327-334.

Funke L, Dakoji S, Bredt DS (2005) Membrane-associated guanylate kinases regulate adhesion and plasticity at cell junctions. Annu Rev Biochem 74:219-245.

Giepmans BN (2004) Gap junctions and connexin-interacting proteins. Cardiovasc Res 62:233-245.

Giepmans BN (2006) Role of connexin43-interacting proteins at gap junctions. Adv Cardiol 42:41-56.

Gluck MR, Jayatilleke E, Shaw S, Rowan AJ, Haroutunian V (2000) CNS oxidative stress associated with the kainic acid rodent model of experimental epilepsy. Epilepsy Res 39:63-71.

Herve JC, Bourmeyster N, Sarrouilhe D (2004) Diversity in protein-protein interactions of connexins: emerging roles. Biochim Biophys Acta 1662:22-41.

Herve JC, Bourmeyster N, Sarrouilhe D, Duffy HS (2007) Gap junctional complexes: from partners to functions. Prog Biophys Mol Biol 94:29-65.

Irani K, Xia Y, Zweier JL, Sollott SJ, Der CJ, Fearon ER, Sundaresan M, Finkel T, Goldschmidt-Clermont PJ (1997) Mitogenic signalling

mediated by oxidants in Ras-transformed fibroblasts. Science 275:1649-1652.

Ishii KA, Fumoto T, Iwai K, Takeshita S, Ito M, Shimohata N, Aburatani H, Taketani S, Lelliott CJ, Vidal-Puig A, Ikeda K (2009) Coordination of PGC-1beta and iron uptake in mitochondrial biogenesis and osteoclast activation. Nat Med 15:259-266.

Jorge I, Casas EM, Villar M, Ortega-Perez I, Lopez-Ferrer D, Martinez-Ruiz A, Carrera M, Marina A, Martinez P, Serrano H, Canas B, Were F, Gallardo JM, Lamas S, Redondo JM, Garcia-Dorado D, Vazquez J (2007) High-sensitivity analysis of specific peptides in complex samples by selected MS/MS ion monitoring and linear ion trap mass spectrometry: application to biological studies. J Mass Spectrom 42:1391-1403.

Junn E, Mouradian MM (2002) Human alpha-synuclein over-expression increases intracellular reactive oxygen species levels and susceptibility to dopamine. Neurosci Lett 320:146-150.

Kamata H, Hirata H (1999) Redox regulation of cellular signalling. Cell Signal 11:1-14.

Kim JY, Sun Q, Oglesbee M, Yoon SO (2003) The role of ErbB2 signalling in the onset of terminal differentiation of oligodendrocytes in vivo. J Neurosci 23:5561-5571.

Kluger R, Alagic A (2004) Chemical cross-linking and protein-protein interactions-a review with illustrative protocols. Bioorg Chem 32:451-472.

Kojima T, Kokai Y, Chiba H, Yamamoto M, Mochizuki Y, Sawada N (2001) Cx32 but not Cx26 is associated with tight junctions in primary cultures of rat hepatocytes. Exp Cell Res 263:193-201.

Kojima T, Sawada N, Chiba H, Kokai Y, Yamamoto M, Urban M, Lee GH, Hertzberg EL, Mochizuki Y, Spray DC (1999) Induction of tight junctions in human connexin 32 (hCx32)-transfected mouse hepatocytes: connexin 32 interacts with occludin. Biochem Biophys Res Commun 266:222-229.

Kostin S, Hein S, Bauer EP, Schaper J (1999) Spatiotemporal development and distribution of intercellular junctions in adult rat cardiomyocytes in culture. Circ Res 85:154-167.

Kumar A, Agarwal S, Heyman JA, Matson S, Heidtman M, Piccirillo S, Umansky L, Drawid A, Jansen R, Liu Y, Cheung KH, Miller P, Gerstein M, Roeder GS, Snyder M (2002) Subcellular localization of the yeast proteome. Genes Dev 16:707-719.

Laird DW, Jordan K, Thomas T, Qin H, Fistouris P, Shao Q (2001) Comparative analysis and application of fluorescent protein-tagged connexins. Microsc Res Tech 52:263-272.

Li H, Brodsky S, Kumari S, Valiunas V, Brink P, Kaide J, Nasjletti A, Goligorsky MS (2002) Paradoxical overexpression and translocation of connexin43 in homocysteine-treated endothelial cells. Am J Physiol Heart Circ Physiol 282:H2124-2133.

Li J, Hertzberg EL, Nagy JI (1997) Connexin32 in oliogdendrocytes and association with myelinated fibers in mouse and rat brain. JCompNeurol 379:571-591.

Martin G, Sewell RB, Yeomans ND, Smallwood RA (1992) Ageing has no effect on the volume density of hepatocytes, reticulo-endothelial cells or the extracellular space in livers of female Sprague-Dawley rats. Clin Exp Pharmacol Physiol 19:537-539.

Melanson-Drapeau L, Beyko S, Dave S, Hebb AL, Franks DJ, Sellitto C, Paul DL, Bennett SA (2003a) Oligodendrocyte progenitor enrichment in the connexin32 null-mutant mouse. J Neurosci 23:1759-1768.

Melanson-Drapeau L, Beyko S, Davé S, Hebb ALO, Franks DJ, Sellito C, Paul DL, Bennett SAL (2003b) Oligodendrocyte progenitor enrichment in the connexin32 null-mutant mouse. J Neurosci 23:1759-1768.

Miotto G, Tessaro S, Rotta GA, Bonatto D (2007) In silico analyses of Fsf1 sequences, a new group of fungal proteins orthologous to the metazoan sideroblastic anemia-related sideroflexin family. Fungal Genet Biol 44:740-753.

Miro-Casas E, Ruiz-Meana, M., Agulló, E., Torre, I., Cabestrero, A., Rodríguez-Sinovas, A., Morente, M., Boengler, K., Schulz, R., Heusch G., Garcia-Dorado, D. (2007) Mitochondrial connexin 43 hemichannels. J Mol Cell Cardiol 42:S120.

Miyake S, Yamashita T, Taniguchi M, Tamatani M, Sato K, Tohyama M (2002) Identification and characterization of a novel mitochondrial tricarboxylate carrier. Biochem Biophys Res Commun 295:463-468.

Mycielska ME, Patel A, Rizaner N, Mazurek MP, Keun H, Ganapathy V, Djamgoz MB (2009) Citrate transport and metabolism in mammalian cells: prostate epithelial cells and prostate cancer. Bioessays 31:10-20.

Nagy JI, Ionescu AV, Lynn BD, Rash JE (2003a) Connexin29 and connexin32 at oligodendrocyte and astrocyte gap junctions and in myelin of the mouse central nervous system. J Comp Neurol 464:356-370.

Nagy JI, Ionescu AV, Lynn BD, Rash JE (2003b) Coupling of astrocyte connexins Cx26, Cx30, Cx43 to oligodendrocyte Cx29, Cx32, Cx47: Implications from normal and connexin32 knockout mice. Glia 44:205-218.

Nakajima O, Takahashi S, Harigae H, Furuyama K, Hayashi N, Sassa S, Yamamoto M (1999) Heme deficiency in erythroid lineage causes differentiation arrest and cytoplasmic iron overload. EMBO J 18:6282-6289.

Nakase T, Naus CC (2004) Gap junctions and neurological disorders of the central nervous system. Biochim Biophys Acta 1662:149-158.

Nelles E, Buetzler C, Jung D, Temme A, Gabriel HD, Dahl U, Traub O, Stuempel F, Jungermann K, Zielasek J, Toyka KV, Dermietzel R, Willecke K (1996) Defective propagation of signals generated by

sympathetic nerve stimulation in the liver of connexin32-deficient mice. Proc Natl Acad Sci USA 93:9565-9570.

Nicchia GP, Srinivas M, Li W, Brosnan CF, Frigeri A, Spray DC (2005) New possible roles for aquaporin-4 in astrocytes: cell cytoskeleton and functional relationship with connexin43. FASEB J 19:1674-1676.

Niemann A, Berger P, Suter U (2006) Pathomechanisms of mutant proteins in Charcot-Marie-Tooth disease. Neuromolecular Med 8:217-242.

Ogasawara MA, Zhang H (2008) Redox Regulation and its Emerging Roles in Stem Cells and Stem-Like Cancer Cells. Antioxid Redox Signal.

Pajor AM (2000) Molecular properties of sodium/dicarboxylate cotransporters. J Membr Biol 175:1-8.

Pak YK, Weiner H (1990) Import of chemically synthesized signal peptides into rat liver mitochondria. J Biol Chem 265:14298-14307.

Park SK, Miller R, Krane I, Vartanian T (2001) The erbB2 gene is required for the development of terminally differentiated spinal cord oligodendrocytes. J Cell Biol 154:1245-1258.

Paul DL (1986) Molecular cloning of cDNA for rat liver gap junction protein. JCellBiol 103:123-134.

Penes MC, Li X, Nagy JI (2005) Expression of zonula occludens-1 (ZO-1) and the transcription factor ZO-1-associated nucleic acid-binding protein (ZONAB)-MsY3 in glial cells and colocalization at

oligodendrocyte and astrocyte gap junctions in mouse brain. Eur J Neurosci 22:404-418.

Penna C, Perrelli MG, Raimondo S, Tullio F, Merlino A, Moro F, Geuna S, Mancardi D, Pagliaro P (2009) Postconditioning induces an anti-apoptotic effect and preserves mitochondrial integrity in isolated rat hearts. Biochim Biophys Acta.

Rahman S, Carlile G, Evans WH (1993) Assembly of hepatic gap junctions. Topography and distribution of connexin 32 in intracellular and plasma membranes determined using sequence-specific antibodies. J Biol Chem 268:1260-1265.

Rash JE, Yasumura T, Dudek FE, Nagy JI (2001) Cell-specific expression of connexins and evidence of restricted gap junctional coupling between glial cells and between neurons. J Neurosci 21:1983-2000.

Rodriguez-Sinovas A, Boengler K, Cabestrero A, Gres P, Morente M, Ruiz-Meana M, Konietzka I, Miro E, Totzeck A, Heusch G, Schulz R, Garcia-Dorado D (2006) Translocation of connexin 43 to the inner mitochondrial membrane of cardiomyocytes through the heat shock protein 90-dependent TOM pathway and its importance for cardioprotection. Circ Res 99:93-101.

Rouach N, Avignone E, Meme W, Koulakoff A, Venance L, Blomstrand F, Giaume C (2002) Gap junctions and connexin expression in the normal and pathological central nervous system. Biol Cell 94:457-475.

Ruiz-Meana M, Abellan A, Miro-Casas E, Garcia-Dorado D (2007) Opening of mitochondrial permeability transition pore induces hypercontracture in Ca2+ overloaded cardiac myocytes. Basic Res Cardiol 102:542-552.

Ruiz-Meana M, Garcia-Dorado D, Miro-Casas E, Abellan A, Soler-Soler J (2006) Mitochondrial Ca2+ uptake during simulated ischemia does not affect permeability transition pore opening upon simulated reperfusion. Cardiovasc Res 71:715-724.

Ruiz-Meana M, Rodriguez-Sinovas A, Cabestrero A, Boengler K, Heusch G, Garcia-Dorado D (2008) Mitochondrial connexin43 as a new player in the pathophysiology of myocardial ischaemia-reperfusion injury. Cardiovasc Res 77:325-333.

Santos NC, Castilho RF, Meinicke AR, Hermes-Lima M (2001) The iron chelator pyridoxal isonicotinoyl hydrazone inhibits mitochondrial lipid peroxidation induced by Fe(II)-citrate. Eur J Pharmacol 428:37-44.

Shinjyo N, Kita K (2006) Up-regulation of heme biosynthesis during differentiation of Neuro2a cells. J Biochem 139:373-381.

Smith J, Ladi E, Mayer-Proschel M, Noble M (2000) Redox state is a central modulator of the balance between self-renewal and differentiation in a dividing glial precursor cell. Proc Natl Acad Sci U S A 97:10032-10037.

Sohl G, Maxeiner S, Willecke K (2005) Expression and functions of neuronal gap junctions. Nat Rev Neurosci 6:191-200.

Stojanovski D, Johnston AJ, Streimann I, Hoogenraad NJ, Ryan MT (2003) Import of nuclear-encoded proteins into mitochondria. Exp Physiol 88:57-64.

Sung JY, Lee HJ, Jeong EI, Oh Y, Park J, Kang KS, Chung KC (2007) Alpha-synuclein overexpression reduces gap junctional intercellular communication in dopaminergic neuroblastoma cells. Neurosci Lett 416:289-293.

Torok K, Stauffer K, Evans WH (1997) Connexin 32 of gap junctions contains two cytoplasmic calmodulin-binding domains. Biochem J 326 (Pt 2):479-483.

Toyofuku T, Akamatsu Y, Zhang H, Kuzuya T, Tada M, Hori M (2001) c-Src regulates the interaction between connexin-43 and ZO-1 in cardiac myocytes. J Biol Chem 276:1780-1788.

Van Blerkom J (2008) Mitochondria as regulatory forces in oocytes, preimplantation embryos and stem cells. Reprod Biomed Online 16:553-569.

von Heijne G (1986) Mitochondrial targeting sequences may form amphiphilic helices. EMBO J 5:1335-1342.

von Heijne G, Steppuhn J, Herrmann RG (1989) Domain structure of mitochondrial and chloroplast targeting peptides. Eur J Biochem 180:535-545.

Vozzi C, Ullrich S, Charollais A, Philippe J, Orci L, Meda P (1995) Adequate connexin-mediated coupling is required for proper insulin production. J Cell Biol 131:1561-1572.

Yoshikumi Y, Mashima H, Ueda N, Ohno H, Suzuki J, Tanaka S, Hayashi M, Sekine N, Ohnishi H, Yasuda H, Iiri T, Omata M, Fujita T, Kojima I (2005) Roles of CTPL/Sfxn3 and Sfxn family members in pancreatic islet. J Cell Biochem 95:1157-1168.

Zhang X, Haaf M, Todorich B, Grosstephan E, Schieremberg H, Surguladze N, Connor JR (2005) Cytokine toxicity to oligodendrocyte precursors is mediated by iron. Glia 52:199-208.

Zheng YZ, Berg KB, Foster LJ (2009) Mitochondria do not contain lipid rafts, and lipid rafts do not contain mitochondrial proteins. J Lipid Res 50:988-998.

Zhu H, Bilgin M, Snyder M (2003) Proteomics. Annu Rev Biochem 72:783-812.

Supplemental Figure 4.1: SFXN-1 is expressed in brain and co-IPs with Cx32.

(A) Expression of SFXN-1 from 5 ug liver protein and 20 ug brain protein. (B) is Cx32 IP blotted for SFXN-1, showing that SFXN-1 likely associates with Cx32 in the brain as well as the liver. Methods are as described in Chapter 3.

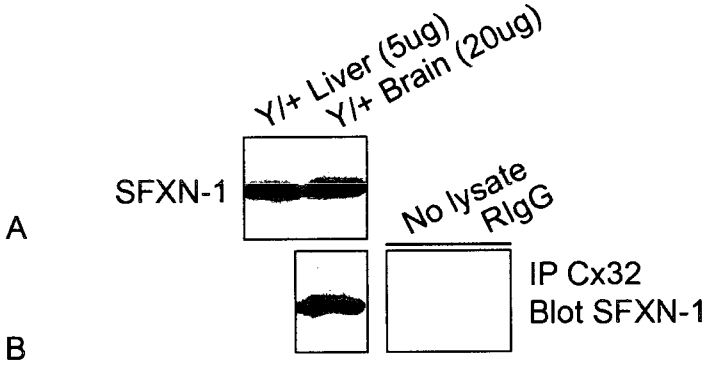

Supplemental Figure 4.1

Appendix I: Supplemental Methodology

Three potential antigenic sequences were detected within the IL of Cx32 (Fig 2.2A-E, Table 2.2). Two of these sequences were present in the peptide used to generate AB1. All three sequences were present in AB2 and AB3. Because AB1, AB2, and AB3 are monoclonal antibodies and generated identical banding patterns (Fig 2.2A-C), it is likely that they recognize the same epitope, either the EEVKRHKV or EGHGDPLH/GDPLHLEE antigenic sequences, located towards the CT of the IL encompassed by the peptides used to generate AB1 (Table 2.2). Although the exact peptide sequence used to generate AB4 and AB5 was not disclosed by the manufacturer, both antibodies were distinguished from AB1-3 by a species variation in the doublet detected in human samples (Fig 2.2D). Based on this difference, we hypothesized that they likely detect one of the two potential epitope variants (EGHGDPLH/GDPLHLEE) (Table 2.2). Only polyclonal AB5 demonstrated specificity and thus we hypothesized recognizes the only antigenic sequence that does not overlap with AB1 (i.e., QQHIEKKM) located towards the N-terminus of the IL (Table 2.2). This analysis predicted that the cross-reactive protein would contain contiguous amino acid sequences, exposed under denaturing/reducing conditions that share the EEVKRHKV and EGHGDPLH/GDPLHLEE but not the QQHIEKKM epitopes with Cx32.

In the CT of Cx32, five potentially antigenic sequences were

detected (Fig 2.3A-E, Table 2.2). Polyclonal AB6 (Fig 2.3A) was directed against a known sequence that encompassed the most distal CT antigen (GLAEKSDR, Table 2.2). Polyclonal AB7 generated a pattern distinct from all of the other reagents and thus likely recognizes epitope(s) distinct from AB6 (Fig 2.3B). AB8 and AB9 detected a doublet in human brain samples and thus likely recognize the same species-specific antigenic sequences (Fig 2.3C,D). AB10 was Cx32-specific and, as a monoclonal antibody, is raised against a single epitope (Fig 2.3E). Based on this pattern, we predicted that the cross-reactive protein would contain, in addition to the epitopes recognized by the IL antibodies, contiguous sequences in primary sequence homologous to at least three and likely four of the Cx32 CT epitopes but no significant homology with the fifth predicted antigenic sequences (recognized by Cx32-specific AB10).

Only Cx30 met these criteria. The IL EEVKRHKV epitope exhibited a significant alignment score of 62% whereas alignment of the EGHGDPLH/GDPLHLEE antigenic sequences met the minimum number of adjacent amino acids required to raise an antigenic response (contiguous alignment score of 25). Further, as predicated, the QQHIEKKM epitope was not found in the Cx30 primary sequence (alignment score of 12%). Four of the five Cx32 CT epitopes produced significant alignment scores of 25-62. The fifth epitope NPPSRKGS did not exhibit any significant alignment in contiguous sequence (≤12%). Despite this potential homology, stringent testing with null-mutant controls provided conclusive evidence that Cx32 antibodies do not cross-react with

Cx30 (Fig 2.8).

Appendix II: Curriculum Vitae

TEACHING EXPERIENCE

Teachers' Science and Technology Outreach Program (TSTOP), Ottawa, ON **2007 - 2008**

Ministry of Research and Innovation pilot program
Supplementing the Grade seven Science curriculum with lecture-style teaching, hands-on laboratory experiments, visits to science laboratories, and educational field trips

University of Ottawa, Ottawa, ON **2007 - 2009**

Laboratory Teaching Assistant
Courses: Molecular Biology Laboratory (BCH3356)
Introduction to Biochemistry (BCH2333)

Mount Allison University, Sackville, NB **2004 - 2006**

Laboratory Teaching Assistant
Courses: Animal Physiology (BIOL 3201), Animal Cell Physiology (BIOL 3211)

Assignment Evaluation
Course: Introduction to Physics I (PHYS 1051)

VOLUNTEER & EXTRACURRICULAR INVOLVEMENT

- Volunteer Ford Ironman Triathlon, Lake Placid, USA **2008**
- Running Room clinic member **2008-Present**
- Volunteer for Team Parkinson, supporting the Ottawa Parkinson Research Consortium **2007-Present**
- Ottawa Regional Youth Choir **2007-Present**
- Volunteer – "Progress in Systems Biology" (Conference, Ottawa, ON) **2007, 2009**
- Volunteer - "Rendez-vous Biosciences" (Atlantic Biotech Conference) **2006**
- Organizing Committee - Shinerama (fundraiser for Cystic Fibrosis research) **2002 - 2006**
- Organizing Committee - Canadian Cancer Society's Relay for Life **2002 - 2006**
- Colchester Regional Hospital Volunteer **2004-2005**

PUBLICATIONS

- **Fowler, S***., McLean, A.M*., Bennett, S.A.L. Tissue-specific cross-reactivity of Connexin32 antibodies: Problems and solutions unique to the central nervous system. Cell Communication and Adhesion, *in press*. *Both authors contributed equally.
- **Fowler, S.**, Hamilton, D., Currie, S. (2009) A comparison of the heat shock response in juvenile and adult rainbow trout (*Oncorhynchus mykiss*) – implications for increased thermal sensitivity with age. Canadian Journal of Fisheries and Aquatic Sciences, 66:91–100.
- Rendell, J., **Fowler, S.**, Cockshutt, A., Currie, S. (2006) Development–dependent differences in intracellular localization of stress proteins (hsps) in rainbow trout (*Oncorhynchus mykiss)* following heat shock. Comparative Biochemistry and Physiology, Part D, 1:238-252.

PRESENTATIONS

- "Identifying binding partners of Cx32 involved in channel-independent signaling pathways". Poster presentation at the Ottawa Institute of Systems Biology: Brain and Mind Symposium, Ottawa, ON, April 2009.
- "Brain-specific cross-reactivity of connexin32 antibodies: problems and solutions". Poster presentation at the Society for Neuroscience Meeting, Washington DC, November 2008.
- "Connexin32 expression is under hormonal control in the adult female hippocampus". Poster presentation at the International Gap Junction Conference, Copenhagen, Denmark, August 2007.
- "The use of salmonid heat shock protein antibodies to detect tissue-specific cellular stress in rainbow trout (*Oncorhynchus mykiss*). First prize oral presentation at the Atlantic Universities Aquaculture Conference, Charlottetown PEI, March 2006; first prize oral presentation at Mount Allison University's Honours Day, Sackville NB, April 2006; poster presentation at the Canadian Society of Zoologists Annual Meeting, Edmonton AB, May 2006.
- "Stress and social status: stress protein induction and dominance hierarchies in rainbow trout (*Oncorhynchus mykiss*). First prize poster presentation at the Science Undergraduate Research Fair, Mount Allison University, September 2005.

REFERENCES

Available upon request